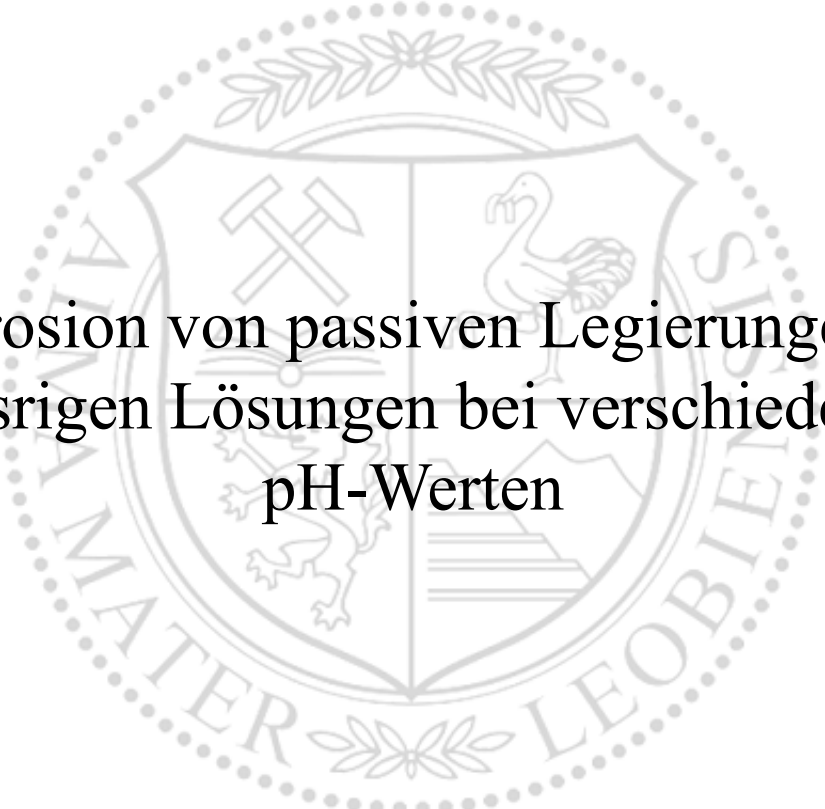




Lehrstuhl für Allgemeine und Analytische Chemie

Masterarbeit



Korrosion von passiven Legierungen in
wässrigen Lösungen bei verschiedenen
pH-Werten

Federico Todeschi

Oktober 2023

UNIVERSITÀ DEGLI STUDI DI TRENTO

Dipartimento di Ingegneria Industriale

and

MONTANUNIVERSITÄT LEOBEN

International Master in Sustainable Materials



EIT Raw Materials

Corrosion of passive alloys in aqueous solutions at different pH values

Relatore:

Prof. Gregor Mori

Prof. Michele Fedel

Laureando:

Todeschi Federico

Academic year 2021 - 2022

Todeschi Federico
8th November 2023

Abstract

Now a day with the problems of the climate change and the high price of the fossil materials, it is very important found new more eco-friendly way to produce plastic and fuel in addition to improve circularly economy.

ReOil is a process developed by OMV (Österreichische Mineraölverwaltung) that want to solve this problem by the production of synthetic crude oil from the plastic wast by pyrolysis process.

The products exit from the pyrolysis process couldn't be directly distilled to produce the refinery products, but they need a series of washing steps to remove unreacted materials and the unwanted products. In the washing steps are use aggressive solutions at the different pH.

In this thesis are analyzed nine different materials two nickel alloys (2.4605, 2.4819) and seven stainless steel (1.4404, 1.4539, 1.4562, 1.4462, 1.4410, Sanicro 35, Böhler P569) in the washing solution from the OMV ReOil plant, to select the most correct material for each washing step.

Acidic wash, neutral wash, alkaline wash are the name of the ReOil washing solutions delivered from OMV sampled from the working line in the three washing steps and that are use as electrolyte.

In this thesis the investigate materials are valuated by potentiodynamic measurements at 50 and 90°C, immersion test and autoclave test, and also to have a more meaningful results the materials are also tested in artificial electrolytes, at different pH from 1 to 4, similar to the OMV acidic wash solution, because this solution is the most critical electrolyte from the delivered from OMV.

In the conclusion of the thesis are shown the results of all that tests and the material recommended for each steps, that can be summarized in: Sanicro 35 for acidic wash, 1.4410 for neutral wash and 1.4404 for the alkaline wash.

Abstract

Al giorno d'oggi, con i problemi del cambiamento climatico e il prezzo elevato dei materiali fossili, è molto importante trovare nuovi modi più ecologici per produrre plastica e carburante, al fine di migliorare l'economia circolare.

ReOil è un processo sviluppato da OMV (Österreichische Mineraölverwaltung) che vuole risolvere questo problema con la produzione di petrolio grezzo sintetico dai rifiuti plastici attraverso il processo di pirolisi.

I prodotti che escono dal processo di pirolisi non possono essere distillati direttamente per produrre i prodotti di raffineria, ma necessitano di una serie di fasi di lavaggio per rimuovere i materiali non reagiti e i prodotti indesiderati.

Nelle fasi di lavaggio vengono utilizzate soluzioni aggressive a diverso pH.

In questa tesi sono stati analizzati nove diversi materiali, due leghe di nichel (2.4605, 2.4819) e sette acciai inossidabili (1.4404, 1.4539, 1.4562, 1.4462, 1.4410, Sanicro 35, Böhler P569) nella soluzione di lavaggio dell'impianto OMV ReOil, per selezionare il materiale più corretto per ogni fase di lavaggio. Lavaggio acido, lavaggio neutro e lavaggio alcalino sono i nomi delle soluzioni di lavaggio ReOil fornite da OMV, prelevate dalla linea di lavoro nelle tre fasi di lavaggio e utilizzate come elettrolita.

In questa tesi i materiali in esame sono stati valutati mediante misure potenziodinamiche a 50 e 90°C, test di immersione e test in autoclave; inoltre, per avere risultati più significativi, i materiali sono stati testati anche in elettroliti artificiali, a diversi pH da 1 a 4, simili alla soluzione di lavaggio acida OMV, in quanto questa soluzione è l'elettrolita più critico tra quelli forniti da OMV.

Nella conclusione della tesi sono riportati i risultati di tutti i test e il materiale consigliato per ogni fase, che possono essere riassunti in: Sanicro 35 per il lavaggio acido, 1,4410 per il lavaggio neutro e 1,4404 per il lavaggio alcalino.

Contents

1	Introduction	1
2	Corrosion behavior of passive alloys	3
2.1	Acid solutions	3
2.1.1	Iron alloys	3
2.1.1.1	Effect of Chromium	3
2.1.1.2	Effect of Molybdenum	5
2.1.1.3	Effect of Nickel	8
2.1.1.4	Effect of Nitrogen	9
2.1.1.5	Effect of Copper	10
2.1.1.6	Effect of Carbon	11
2.1.1.7	Effect of Sulphur	12
2.1.2	Nickel base alloys	12
2.1.2.1	Effect of Chromium	13
2.1.2.2	Effect of Molybdenum	14
2.1.2.3	Effect of Copper	15
2.1.2.4	Effect of Iron	15
2.2	Neutral solutions	16
2.2.1	Iron alloys	16
2.2.1.1	Effect of Chromium	16
2.2.1.2	Effect of Molybdenum	16
2.2.1.3	Effect of Nickel	17
2.2.1.4	Effect of Nitrogen	18
2.2.1.5	Effect of Copper	19
2.2.1.6	Effect of Carbon	20

2.2.1.7	Effect of Sulphur	21
2.2.2	Nickel alloys	22
2.2.2.1	Effect of Chromium	22
2.2.2.2	Effect of Molybdenum	22
2.2.2.3	Effect of Copper	23
2.2.2.4	Effect of Iron	23
2.3	Alkaline solutions	24
2.3.1	Iron alloys	24
2.3.1.1	Effect of Chromium	25
2.3.1.2	Effect of Molybdenum	25
2.3.1.3	Effect of Nickel	25
2.3.1.4	Effect of Nitrogen	26
2.3.1.5	Effect of Copper	27
2.3.1.6	Effect of Carbon	27
2.3.1.7	Effect of Sulphur	28
2.3.2	Nickel alloys	28
2.3.2.1	Effect of Chromium	28
2.3.2.2	Effect of Molybdenum	29
2.3.2.3	Effect of Copper	30
2.3.2.4	Effect of Iron	30
3	Experimental	32
3.1	Materials	32
3.2	Corrosion test	42
3.2.1	Potentiodynamic measurement	42
3.2.2	Immersion test	44
3.2.3	Autoclave test	46
4	Results	48
4.1	Potentiodynamic measurement	48

4.2	Immersion test	63
4.3	Autoclave test	66
5	Discussion	69
5.1	Impact of Inhibitor and Chloride content	69
5.2	Impact of Temperature	70
5.3	Impact of pH	71
6	Conclusion	73
	References	75
A	Solutions Composition	79

List of Figures

1.1	ReOil chemical recycling process[2]	1
1.2	ReOil pilot plant [2]	2
2.1	Pourbaix diagram of chromium. [8]	4
2.2	Polarization curves of stainless steels with different chromium quantity in Ar-saturated $0.5 \text{ mol/dm}^3 \text{ H}_2\text{SO}_4$ electrolyte. [5]	5
2.3	Pourbaix diagram of molybdenum in acidic environments. [8]	6
2.4	Effect of Mo addition to 17%Cr on the Passive current density in 1 M HCl at 29.6°C. [10]	7
2.5	Cyclic potentiodynamic polarization curves of steel 304 with addition of 0Mo,1Mo,2Mo in 4 M NaCl. [11]	8
2.6	Anodic polarisation curves for 18% Cr-8% Ni stainless steels containing various amounts of nitrogen, tested in a hydrogen-purged 1N $\text{H}_2\text{SO}_4 + 0.5 \text{ M NaCl}$ solution at ambient temperature. [16]	9
2.7	Pourbaix diagram of copper in acid. [8]	10
2.8	Cyclic polarization curve of steel ASTM A890 with the addition of 0%Cu 3%Cu in 0.3 M H_2SO_4 . [17]	11
2.9	Cyclic polarization curve of Steel ASTM S32750 with addition of 0, 0.03, 0.1% sulphur (S) in deaerated solution of 0.5 N HCl + 1 N NaCl at 50°C[19]	12
2.10	Pourbaix diagram of nickel.[8]	13
2.11	Polarization curves of nickel alloys with different chromium quantity in Ar-saturated 20 mol/l H_2SO_4 electrolyte. [21]	14
2.12	Potentiodynamic polarization curves of Ni-20Cr, Ni-11Cr-7Mo, Ni-11Cr-13Mo in 1 M NaCl at pH 3.09 and 90°C. [22]	15
2.13	Comparison of pitting potential for different FeCrMo alloys in deaerated synthetic seawater at 98°C. [10]	17
2.14	Copson Curve. [14]	18

2.15	Cyclic polarization curve of steel ASTM A890 with the addition of 0%Cu 3%Cu in 0.6 M NaCl. [17]	20
2.16	Cyclic polarization curve of Steel ASTM S32750 with addition of 0, 0.03, 0.1% sulphur (S) in deaerated solution of 22% of NaCl at 70°C[19]	21
2.17	Potentiodynamic polarization curves of Ni-20Cr, Ni-11Cr-7Mo, Ni-11Cr-13Mo in 1 M NaCl at pH 7.78 and 90°C. [22]	23
2.18	Potentiodynamic polarization curves nickel-iron alloys in neutral (pH 7) Na ₂ SO ₄ electrolyte at 25°C. [27]	24
2.19	Polarization curves of carbon steel and nickel-bearing steel in calcium hydroxide (Ca(OH) ₂) saturate solution with 3.5 % NaCl and 7 % NaHCO ₃ (pH 11.5). [28]	26
2.20	Potentiodynamic curves of Ni and Ni-15Cr alloy in borate buffer solution. [24]	29
2.21	Potentiodynamic polarization curves of Ni-20Cr, Ni-11Cr-7Mo, Ni-11Cr-13Mo in 1 M NaCl at pH 12.48 and 90°C. [22]	30
2.22	Potentiodynamic curves of Ni, Ni-15Cr and Ni-15Cr-8Fe alloys in borate buffer solution. [24]	31
3.1	Microstructure of material N. 1.4404 (X2CrNiMo17-12-2)	35
3.2	Microstructure of material N. 1.4410 (X2CrNiMoN25-7-4)	36
3.3	Microstructure of material N. 1.4462 (X2CrNiMoN22-5-3)	37
3.4	Microstructure of material N. 1.4539 (X1NiCrMoCu25-20-5)	38
3.5	Microstructure of material N. 2.4819 (NiMo16Cr15W)	39
3.6	Microstructure of material Sanicro35	40
3.7	Microstructure of material N. 2.4605 (Alloy59)	41
3.8	Microstructure of material N. 1.4562 (Alloy31)	41
3.9	Microstructure of material P569	42
3.10	Experimental setup and corrosion cell used to perform potentiodynamic tests	44
3.11	Testing cell and flask with specimen for immersion test	45
3.12	Small tensile specimen with spring and nuts for constant load test (CLT)	46
3.13	Autoclave testing equipment	46
3.14	Autoclave mounted on the rotating shafts within a heated chamber	47

4.1	Type of result after potentiodynamic tests	49
4.2	Results in the solution 1000 mg/l $\text{Cl}^- + \text{H}_2\text{SO}_4$ at 90°C and pH 1	50
4.3	Specimens after testing in 1000 mg/l $\text{Cl}^- + \text{H}_2\text{SO}_4$ at 90°C and pH 1	51
4.4	Results in the solution 1000 mg/l $\text{Cl}^- + \text{H}_2\text{SO}_4$ at 90°C and pH 2	52
4.5	Specimens after testing in 1000 mg/l $\text{Cl}^- + \text{H}_2\text{SO}_4$ at 90°C and pH 2	53
4.6	Results in the solution 1000 mg/l $\text{Cl}^- + \text{H}_2\text{SO}_4$ at 90°C and pH 3	54
4.7	Specimens after testing in 1000 mg/l $\text{Cl}^- + \text{H}_2\text{SO}_4$ at 90°C and pH 3	55
4.8	Results in the solution 1000 mg/l $\text{Cl}^- + \text{H}_2\text{SO}_4$ at 90°C and pH 4	56
4.9	Specimens after testing in 1000 mg/l $\text{Cl}^- + \text{H}_2\text{SO}_4$ at 90°C and pH 4	57
4.10	Results in the solution Acidic Wash at 90°C and pH 4	58
4.11	Results in the solution Acidic Wash at 50°C and pH 4	59
4.12	Results in the solution Neutral Wash at 90°C and pH 5,5	60
4.13	Results in the solution Neutral Wash at 50°C and pH 5,5	61
4.14	Results in the solution Caustic Wash at 90°C and pH 10	62
4.15	Specimens after testing in Caustic Wash at 90°C	63
4.16	Mass lost immersion test	64
4.17	Samples 1.4404 63x magnification after the immersion test at 50°C	65
4.18	Samples 1.4404 63x magnification after the immersion test at 90°C	66
4.19	Total results of the autoclave test	67
4.20	Visual appearance of some specimens after the autoclave test	68
5.1	Different behavior of the specimens 1.4410 at 90°C at pH 2 between the OMV Acidic Wash and Artificial solution 1000 mg/l $\text{Cl}^- + \text{H}_2\text{SO}_4$	69
5.2	Different behavior of the specimens 1.4462 at 90°C at pH 4 between the OMV Acidic Wash and Artificial solution 1000 mg/l $\text{Cl}^- + \text{H}_2\text{SO}_4$	70
5.3	Behavior of the specimens 1.4404 at pH 1 at the variation of the temperature	71
5.4	Behavior of material 1.4410 at 90°C at different pH values	72

List of Tables

- 3.1 Chemical composition of the tested alloys 33
- 3.2 Mechanical properties of the tested alloys 34
- 3.3 Parameters and solutions for the potentiodynamic measurements 43
- 3.4 Parameters and solutions for the immersion test 45
- 3.5 Parameters and solutions for the autoclave test 47

- 4.1 Total results of the autoclave test 67

- 6.1 Recommendation for choice of material during washing steps in a ReOil process . . . 74

- A.1 Total composition of pH 2 solution for the autoclave test 79
- A.2 Total composition of pH 13 solution for the autoclave test 80

1. Introduction

Nowadays, the climate change is one of the most relevant topics worldwide. At the last international meeting organised by UNO, the “26th World Climate Conference” (COP 26) in Glasgow in 2021, it was decided that every country must reduce their carbon footprint by 45 % by 2030 and reach the net zero by 2050. [1]

At the same time, however, Europe faces a very strong energetic crisis for a lot of reasons, both inside and outside the European control.

All these conditions force countries and their companies to find new methods to produce more energy and fuel for the market but at the same time to reduce their carbon footprint.

OMV (Österreichische Mineralölverwaltung), the largest Austrian petrochemical company, decided to produce crude oil from plastic waste in order to obtain fuels and plastics. [2] The OMV’s new project is called ReOil. It aims at converting post-consumer plastics from urban waste and post-industrial plastics into synthetic crude oil (Syncrude). This will subsequently be refined to obtain fuels and new monomers for plastics production.

The recycling process is shown schematically in Fig. 1.1. [2]

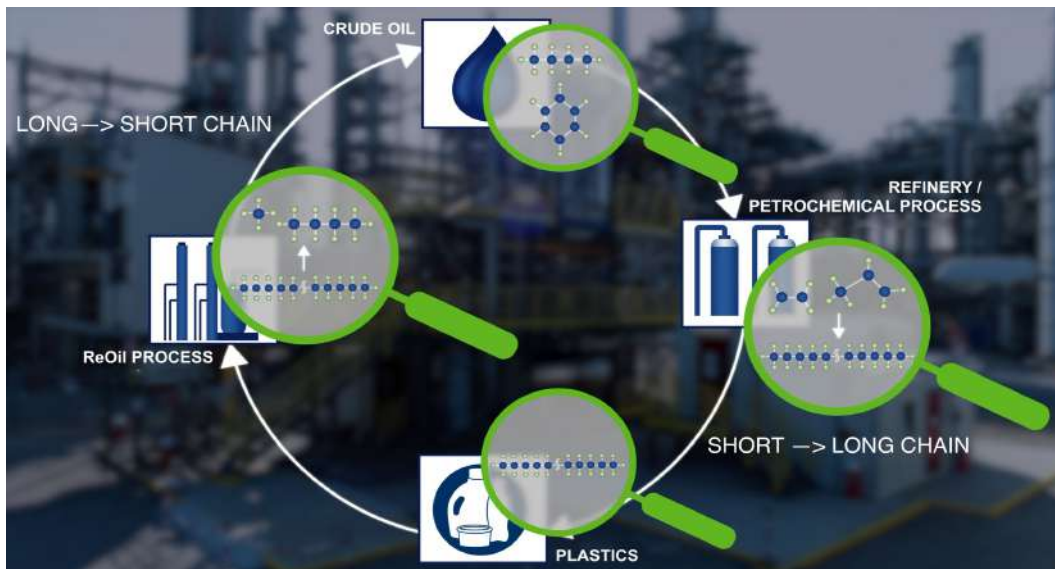


Figure 1.1: ReOil chemical recycling process[2]

The crude oil is a of a pyrolysis process at 400 °C. After the pyrolysis reaction the products must be

washed to eliminate the solid part and other undesired components. The washing process is divided in 3 phases. This operation uses corrosive solutions, which cause severe corrosive environments inside the reactors, and where the fluids flow. Therefore, these components should be made of materials with high corrosion resistance. [2]

The three washing steps are:

1. Caustic wash.
2. Acidic wash.
3. Water wash.

After the washing process the products go to a desiccator to remove the remaining water from the hydrocarbon products. The washing waste goes to evaporators to strip fresh water that can be reused later for the washing process, from the concentrated sour water that is stored in a tank and treated like toxic waste.

Currently, there is only one pilot plant at the Schwechat refinery, shown in Fig. 1.2. This plant is able to convert 100 kg of plastic per hour into an average of 100 l of crude oil per hour, but currently a 2000 kg/h plant is built. For this reason it is very important to know which is the behaviour in the operative environments of different alloys to choose the best option in terms of cost and performance for every part of the plant.



Figure 1.2: ReOil pilot plant [2]

2. Corrosion behavior of passive alloys

2.1 Acid solutions

2.1.1 Iron alloys

Low-alloy steels have a very low corrosion resistance in acidic environments. The corrosion rate depends on temperature, pressure, fluid velocity, and also the presence of small quantities of contaminants increasing the corrosion rate rapidly. [3]

Stainless steels generally have a good corrosion resistance in acidic environments. Especially in an oxidizing acid, like HNO₃, corrosion resistance is higher because it promotes the formation of stable oxides on the surface of steel. On the contrary, stainless steels cannot be used in hydrochloric acid (HCl) since the high quantity of chloride ions can result in a higher uniform corrosion rate, pitting corrosion and stress corrosion cracking (SCC).[3, 4]

2.1.1.1 Effect of Chromium

Chromium is one of the most important alloying elements for stainless steels. It is added to steel in order to achieve formation of an oxide passive layer of Cr₂O₃ on the steel surface. [5, 6]

The minimum quantity of chromium necessary to have the formation of passive layer is 10,5%. [3, 7].

The Pourbaix diagram shows the stability of the passive layer as a function of the pH variation. Fig. 2.1 shows a Pourbaix diagram for chromium.

Chromium is not able to produce a stable passive layer at the pH lower than 4 or at high potentials.

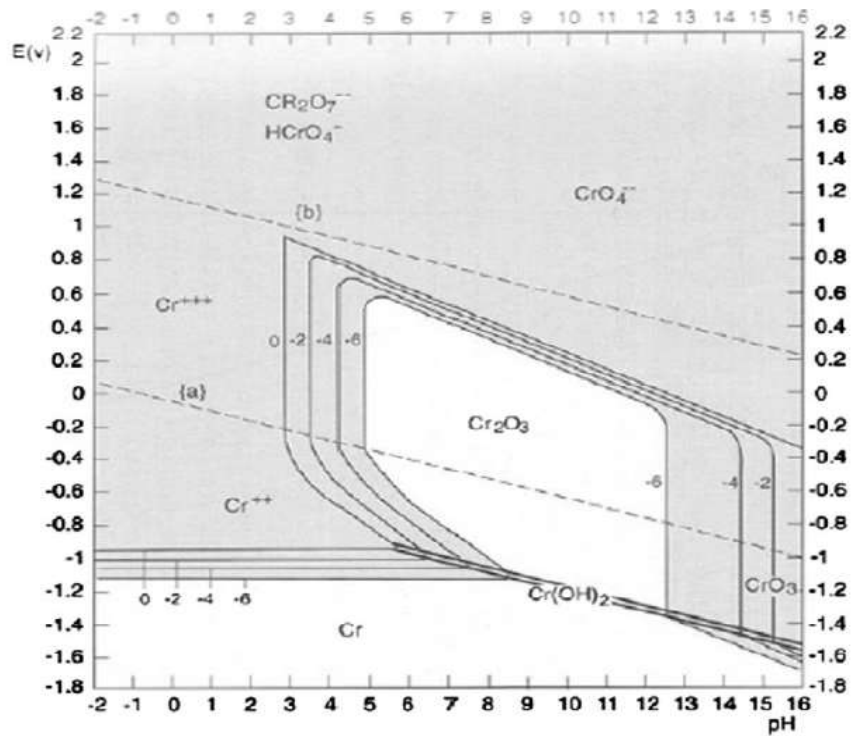


Figure 2.1: Pourbaix diagram of chromium. [8]

Increasing the quantity of chromium increases the corrosion resistance of the steel. [5, 6]

The following figure (Fig. 2.2) shows the results of an electrochemical analysis and the relation between the quantity of chromium and the corrosion resistance of steels.

An increasing chromium content in steels leads to the reduction of current density, which better yields under a corrosion resistance. [5]

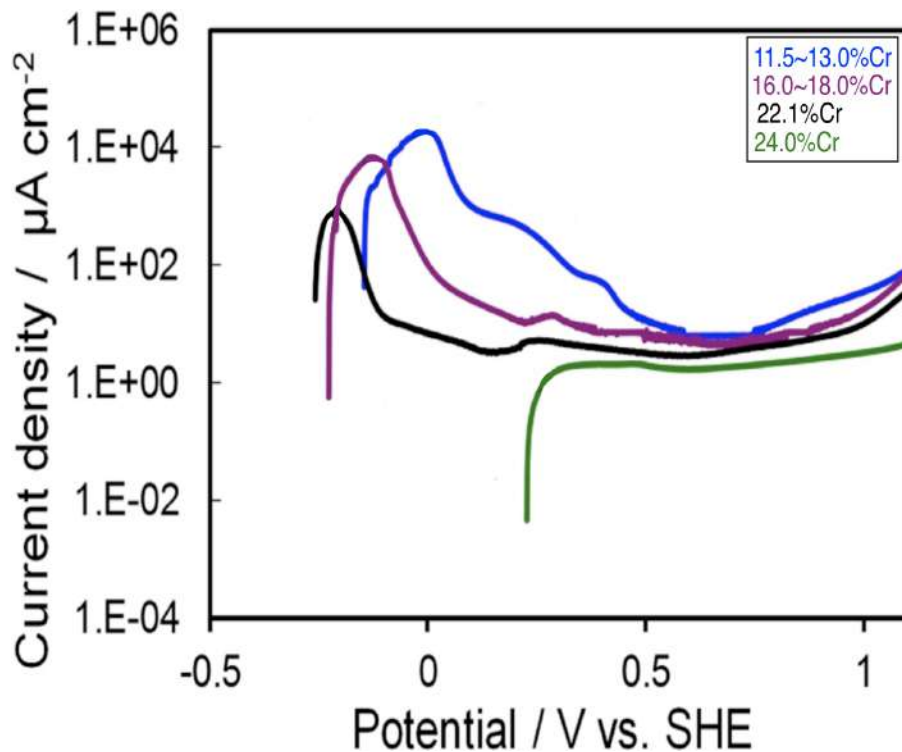


Figure 2.2: Polarization curves of stainless steels with different chromium quantity in Ar-saturated $0.5 \text{ mol/dm}^3 \text{ H}_2\text{SO}_4$ electrolyte. [5]

2.1.1.2 Effect of Molybdenum

Molybdenum is the second most important alloying element used to prevent the corrosion of stainless steels. As shown in the Pourbaix diagram (Fig. 2.3) molybdenum does not form a passive layer in acidic environments. The presence of molybdenum as an alloying element can have a negative impact on a strongly oxidizing environment, such as in concentrated nitric acid. [9] Nevertheless, it has a positive effect in chloride containing environments since it improves the pitting resistance and the properties of the passive layer.

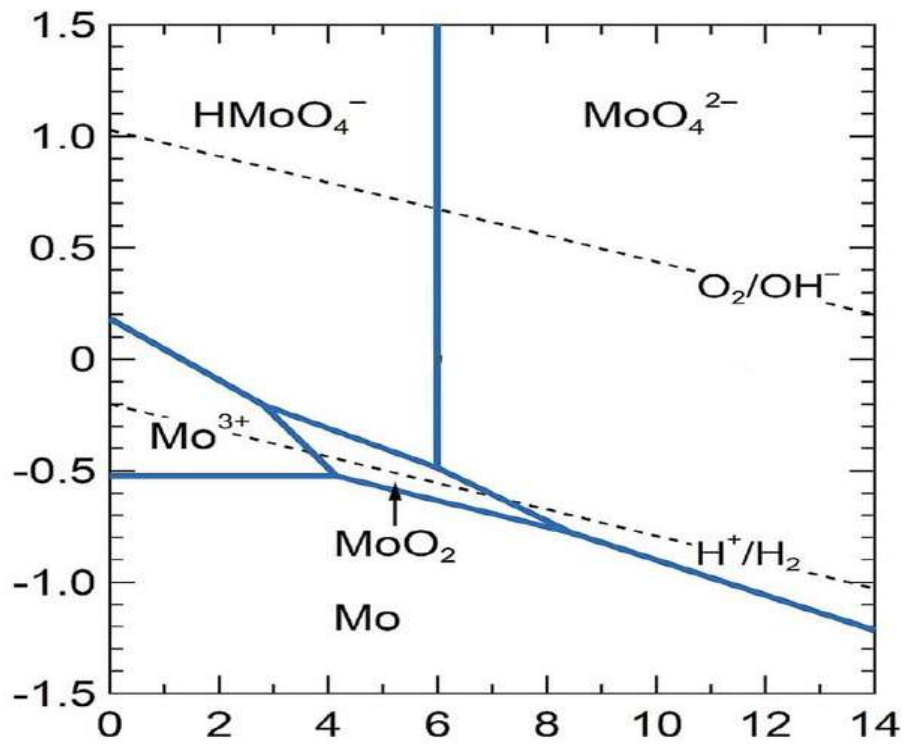


Figure 2.3: Pourbaix diagram of molybdenum in acidic environments. [8]

The effect of introducing molybdenum into the system can be seen in Fig. 2.4.

An increase of the quantity of molybdenum results in a decrease of current density. In addition, it increases the pitting potential. [10]

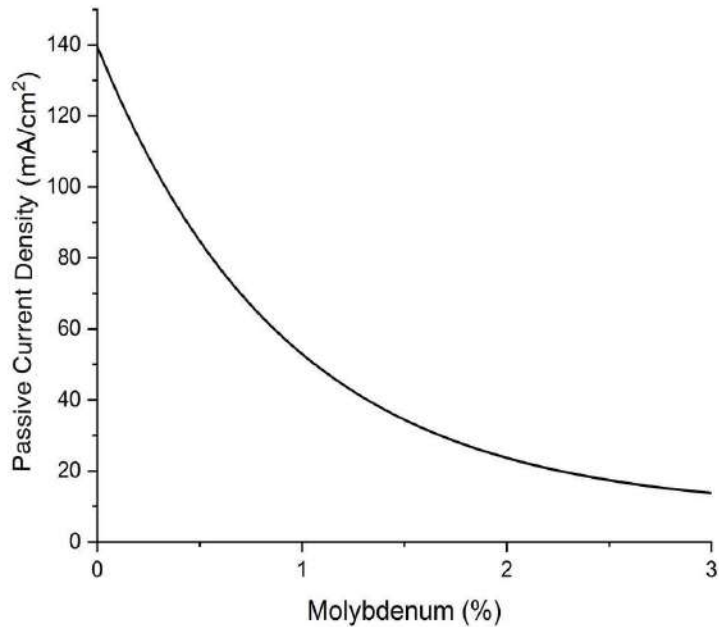


Figure 2.4: Effect of Mo addition to 17%Cr on the Passive current density in 1 M HCl at 29.6°C. [10]

There is also a connection between the molybdenum content in the alloy and the critical pitting temperature (CPT). This phenomenon was studied by Brigham and Tozer. CPT increases linearly with higher content of molybdenum. [10]

Several researchers who studied the effect of molybdenum concluded that the beneficial effect is caused by a passive layer improvidently and by a lower dissolution kinetics of steel. [10, 11]

During their research Sun and Jiang found molybdenum in the passive film changes its structure. It increases the thickness of the passive film and reduces the active sites on the surface of the passive film, hindering the penetration of chloride ions through the passive layer. The presence of molybdenum can also decrease the concentration of metallic ions in the solutions by precipitation of insoluble compounds. However, molybdenum is useless in presence of other halogen acids (HBr, HI, HF) where the effect of molybdenum is negligible. [11]

In the following figure (Fig. 2.5) the polarization curve of three alloys with different quantity of molybdenum is presented.

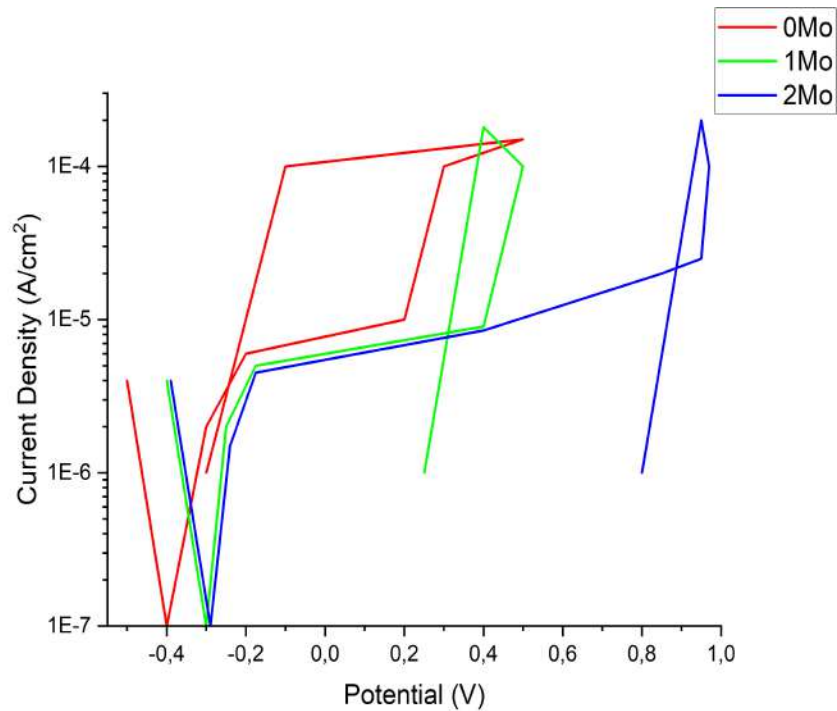


Figure 2.5: Cyclic potentiodynamic polarization curves of steel 304 with addition of 0Mo,1Mo,2Mo in 4 M NaCl. [11]

2.1.1.3 Effect of Nickel

Nickel is an important alloying element because it is an austenite former, and it increases the corrosion resistance of stainless steels. Nickel is the most noble alloying element in stainless steels. To an extent, it improves the resistance to acids due to its noble behavior.

In acid environments, the main reason to add nickel to stainless steels is to stabilize the austenitic lattice.

Two researchers Condit [12] and Alharthid [13] investigated the behaviour of iron-nickel alloys in sulfuric acid (H_2SO_4) and hydrochloric acid (HCl).

The addition of nickel is important for stress corrosion cracking resistance because increasing nickel in stainless steels decreases the minimum time required for cracking, as shown in the Copson Curve. [14]

2.1.1.4 Effect of Nitrogen

Nitrogen is present in many stainless steels.

Nitrogen is an important alloying element because it is economically feasible, it is an austenite former, like nickel, and it increases the pitting resistance of steel. The effect on the higher pitting resistance is even more pronounced in case nitrogen is used together with molybdenum. [9]

Levey [15] studied the effect of nitrogen in different acidic solutions and he deduced that nitrogen increases the pitting corrosion resistance of molybdenum-free stainless steels (H_2SO_4) environments. [15]

For instance, the potentiodynamic curves for stainless steels containing different amounts of nitrogen are presented in Fig. 2.6.

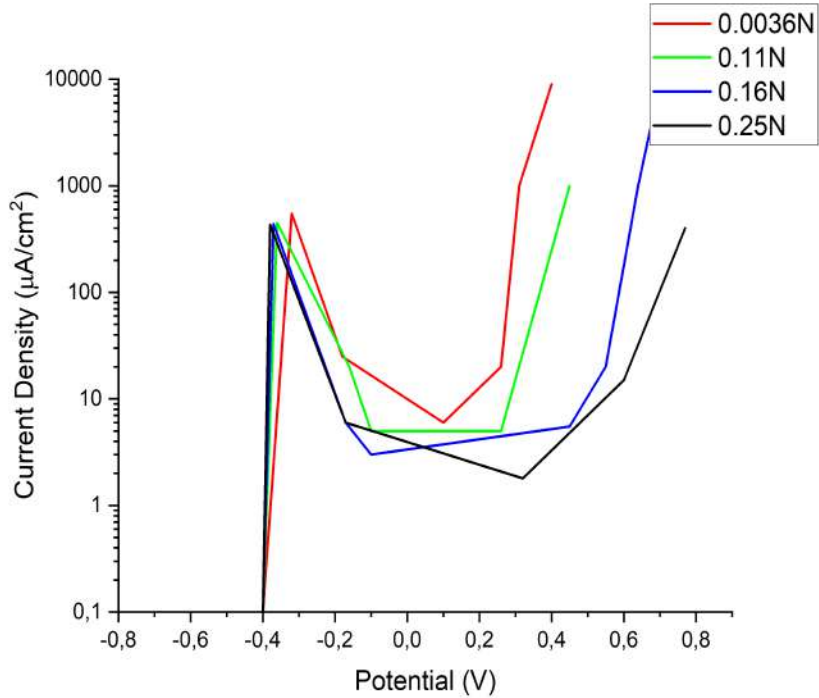


Figure 2.6: Anodic polarisation curves for 18% Cr-8% Ni stainless steels containing various amounts of nitrogen, tested in a hydrogen-purged 1N H_2SO_4 + 0.5 M NaCl solution at ambient temperature. [16]

2.1.1.5 Effect of Copper

Copper can be added to stainless steels to increase the strength of steel by precipitation hardening. In low concentrations (0.5-1%) it can increase the corrosion resistance in non-oxidizing agents like sulfuric acid (H_2SO_4), but it can also decrease resistance to localization corrosion attack when copper is precipitated. Copper is always present in recycled steels because it is impossible to remove during the secondary metallurgy. It can only be diluted by adding new iron to steel. [17]

As is shown on the Pourbaix diagram (Fig. 2.7) copper is not able to create a passive layer in acidic solutions.

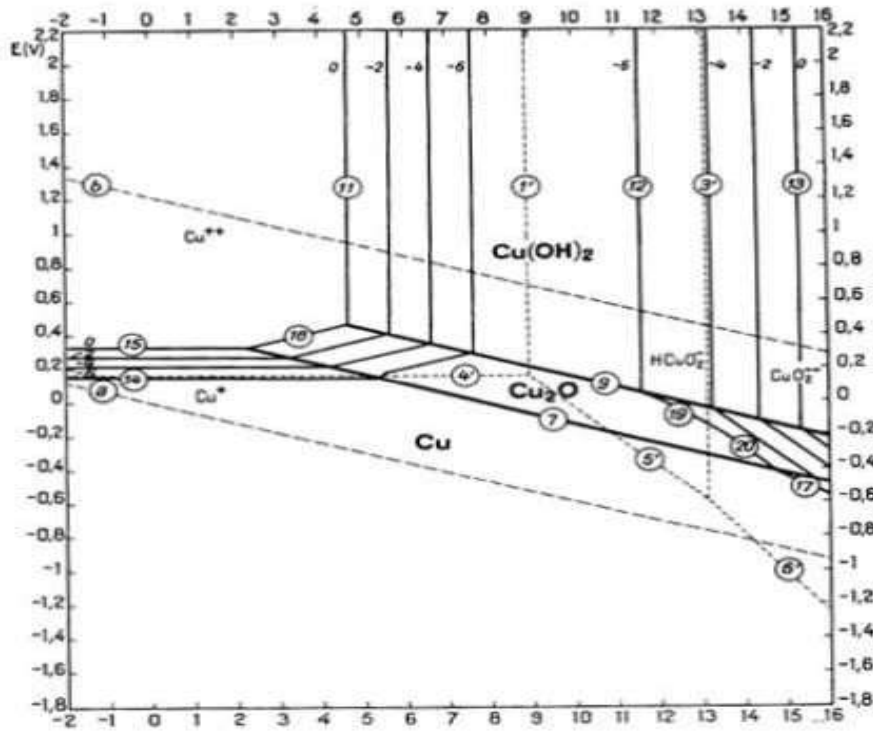


Figure 2.7: Pourbaix diagram of copper in acid. [8]

Martins et al. [17] conducted research about the effect of copper on stainless steels in acidic environments.

Fig. 2.15 shows the results of their investigation about cyclic polarization in acidic environments. The presence of copper decreases the passivation current and obtains a more noble open circuit potential. [17]

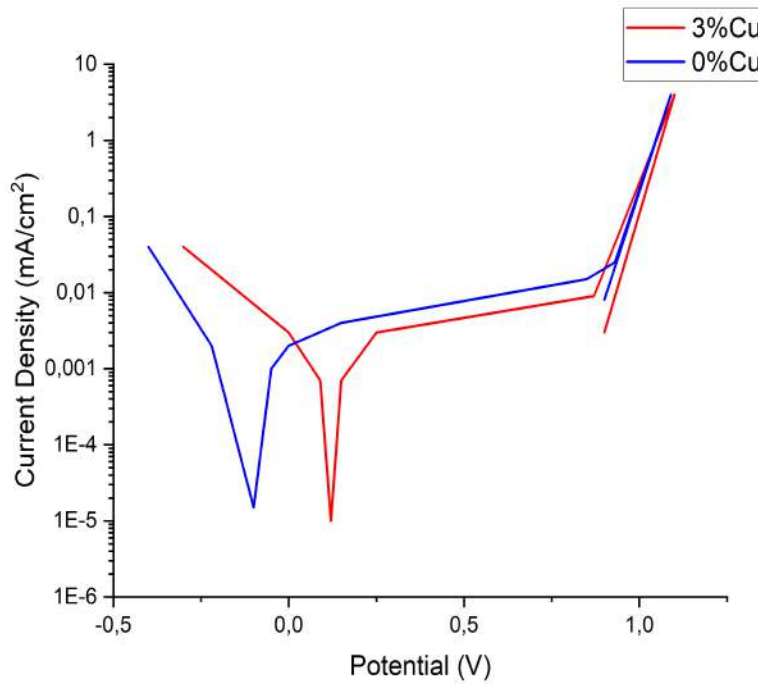


Figure 2.8: Cyclic polarization curve of steel ASTM A890 with the addition of 0%Cu 3%Cu in 0.3 M H₂SO₄. [17]

They also found out that the presence of copper decreases the critical pitting temperature (CPT). For instance, in the solution 0.6 M NaCl + 0.3 M H₂SO₄ the sample with 3% copper has a lower CPT in comparison to the sample without copper. [17]

2.1.1.6 Effect of Carbon

Carbon is the fundamental alloying element for the steel. In stainless steels there is a maximum content of carbon of 2,1%. Normally the content of carbon in the stainless steel is very low (<0.2%). [18]

Increasing the quantity of carbon results in an increase of the hardness of steel but it can simultaneously enhance the brittleness of steel and can cause chromium carbide precipitation (Cr₂₃C₆). [3]

2.1.1.7 Effect of Sulphur

Sulphur is generally considered a contaminant and for this reason it is often removed during the secondary metallurgy. In some cases, sulphur is added to improve the machinability of steel. The presence of sulphur causes a reduction of corrosion properties of the steel.

Jeon et al. investigated the effect of sulphur on the critical pitting temperature (CPT) in acidic environments. As shown in Fig. 2.9, an increase of sulphur increases of the passive current density. [19]

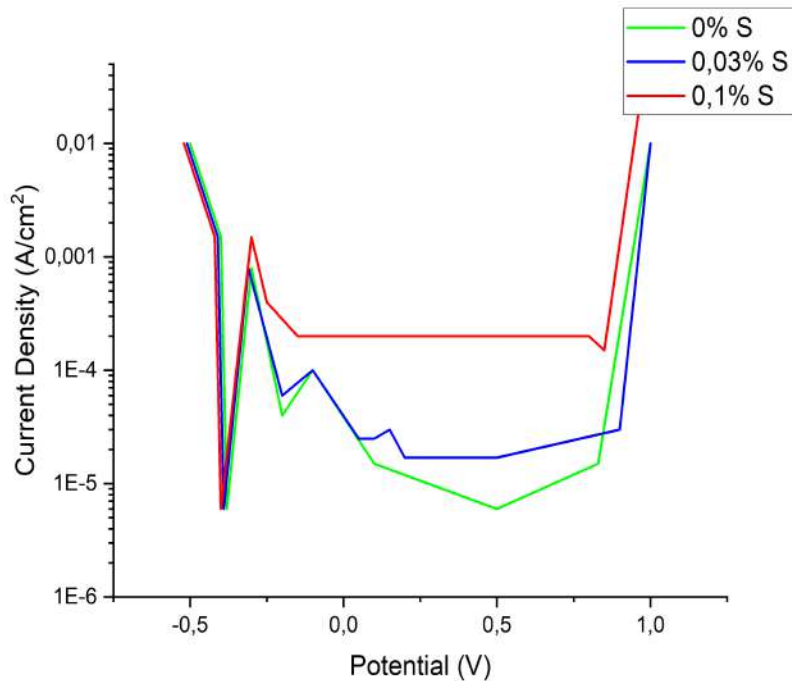


Figure 2.9: Cyclic polarization curve of Steel ASTM S32750 with addition of 0, 0.03, 0.1% sulphur (S) in deaerated solution of 0.5 N HCl + 1 N NaCl at 50°C[19]

They also found that an increasing quantity of sulphur in stainless steels causes a reduction of CPT in acidic environments. [19]

2.1.2 Nickel base alloys

In the acid environment, nickel is able to form a passive layer only at the high potential values, as it is shown in the Pourbaix diagram in Fig. 2.10.

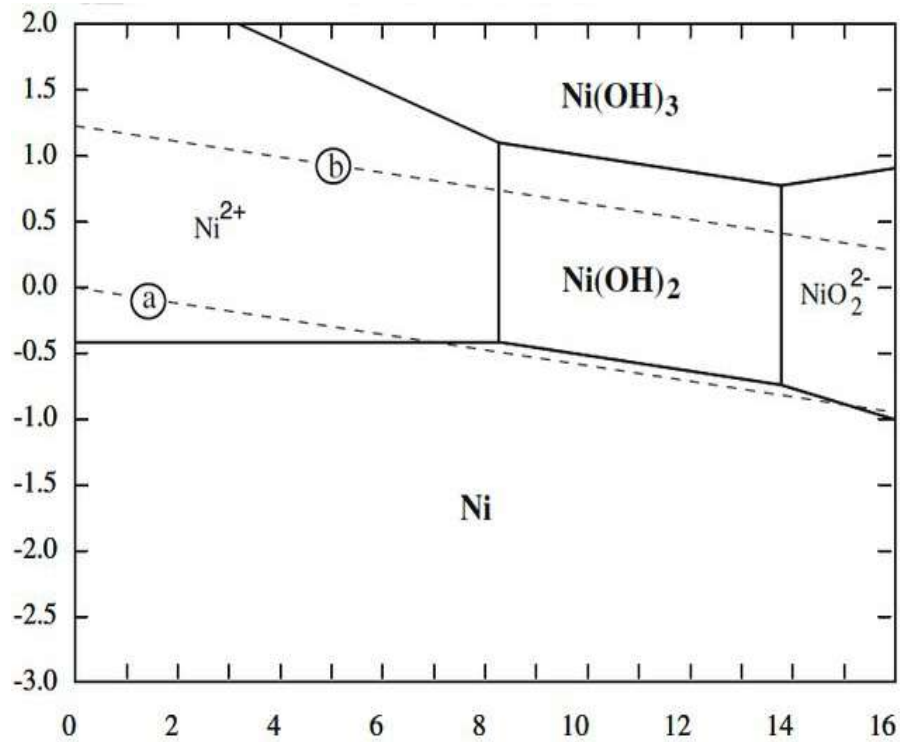


Figure 2.10: Pourbaix diagram of nickel.[8]

2.1.2.1 Effect of Chromium

Chromium is useful in the presence of oxidizing agents like HNO₃, because it enables the formation of a stable passive layer of chromium oxide (Cr₂O₃). [20]

In case of nickel alloys in acidic environments the presence of chromium increases the stability of the passive layer. By increasing the quantity of chromium in the alloy there is a shift to lower values of passivation potential and a decreasing passive current density (Fig. 2.11). [21]

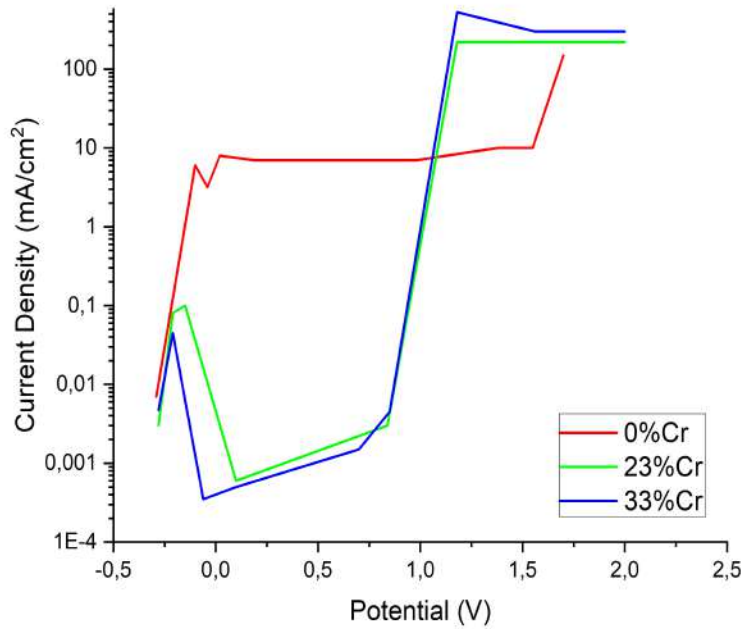


Figure 2.11: Polarization curves of nickel alloys with different chromium quantity in Ar-saturated 20 mol/l H_2SO_4 electrolyte. [21]

2.1.2.2 Effect of Molybdenum

Molybdenum is beneficial in the presence of reducing agents like HCl, thus increasing the quantity of molybdenum in nickel alloys decreases the corrosion rate. [20] The nickel-molybdenum alloys suffer from sensitization during welding but this phenomenon can be reduced by adding a small amount of iron as an alloying element.

Increasing the quantity of molybdenum results in a better pitting corrosion resistance and repassivation behavior. Fig. 2.12 shows that by increasing the quantity of molybdenum alloys increase the pitting resistance. In addition, repassivation potentials become sloppy with increasing Mo content. [3, 22]

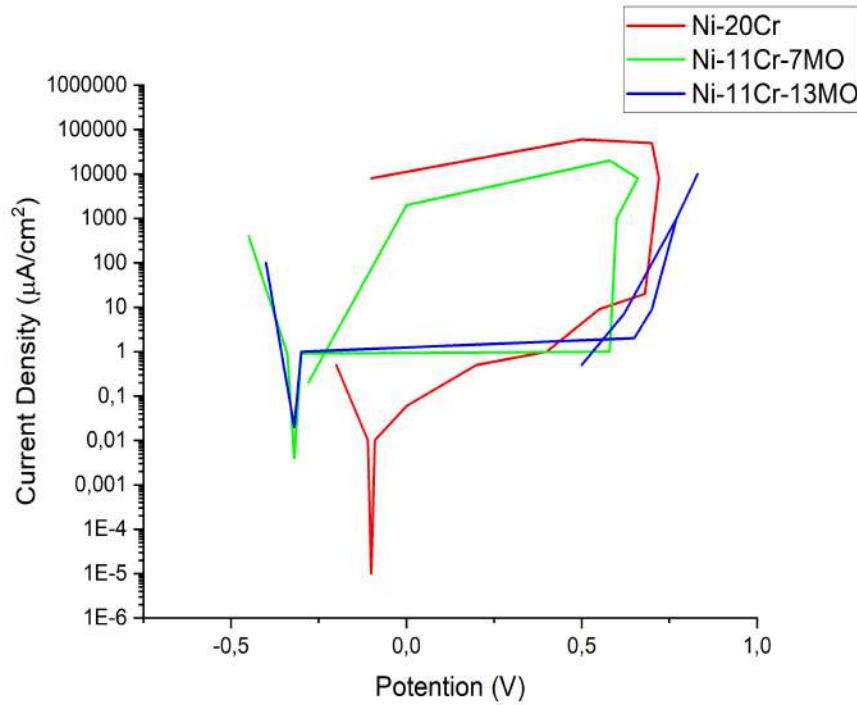


Figure 2.12: Potentiodynamic polarization curves of Ni-20Cr, Ni-11Cr-7Mo, Ni-11Cr-13Mo in 1 M NaCl at pH 3.09 and 90°C. [22]

2.1.2.3 Effect of Copper

The effect of copper in nickel alloys depends on the environment. In strong acid the presence of copper increases the corrosion resistance but, on the contrary, corrosion resistance in the presence of oxidize agent (HNO_3) is a little bit lower than pure nickel. Another important property is the very good resistance of nickel-copper alloys to localized corrosion. [23]

2.1.2.4 Effect of Iron

Iron is usually added as an alloying element with the principal goal to decrease the cost of the produced alloy. [24]

But in the acidic environment the presence of iron decreases the corrosion properties of nickel alloys, it causes a reduction of the corrosion resistances. Reason behind this is that iron is less noble than nickel and it is also not able to form a passive corrosion product in the acidic pH. Condit [12] investigated the effect of iron on the behavior of nickel alloys in sulfuric acid (H_2SO_4) and he

concluded that greater quantities of iron increase corrosion current density. [12]

2.2 Neutral solutions

2.2.1 Iron alloys

Stainless steels have a very good corrosion resistance in neutral environments, but the presence of halogen ions can cause pitting corrosion and stress corrosion cracking (SCC). [3]

2.2.1.1 Effect of Chromium

Chromium is the most important alloying element in stainless steel, it is principally responsible for the formation of the passive layer in neutral environment. As shown in the Pourbaix diagram (Fig. 2.1) chromium can form an insoluble and protective layer at the pH between pH 6-8.

In order to have the formation of the passive layer, minimum required content of chromium in steel is 10.5%. In neutral environments the formation of three different chromium compounds takes place, $\text{Cr}(\text{OH})_3$, Cr_2O_3 and $\text{Cr}(\text{OH})_3 \cdot n\text{H}_2\text{O}$. [8] Increasing the quantity of chromium decreases the corrosion rate but steel remains sensible to a uniform type of corrosion at high potential and from pitting corrosion in the presence of halogen ions which can attack the passive layer. [4]

2.2.1.2 Effect of Molybdenum

Molybdenum is one of the most important alloying elements for the stainless steel but, as shown in the Pourbaix diagram (Fig. 2.3) the effect of the formation of the passive layer is very moderate. Nevertheless, the presence of molybdenum can modify the resistance to uniform corrosion resistance and increase the pitting resistance.

The principal effect of molybdenum is the increase of pitting resistance because it modifies the passive layer on the way to become more stable against breakdown by chloride ions. Moreover, its addition improves the repassivation behaviour of steel. However, molybdenum is useless in the presence of other halogen ions (Br^- , I^- , F^-) where the effect of molybdenum is negligible.

Molybdenum can also increase corrosion resistance because increasing the quantity of molybdenum increases the corrosion potential. [25]

The following figure (Fig. 2.13) depicts the variation of pitting potential in case of different commercial stainless steels with the increase of molybdenum content.

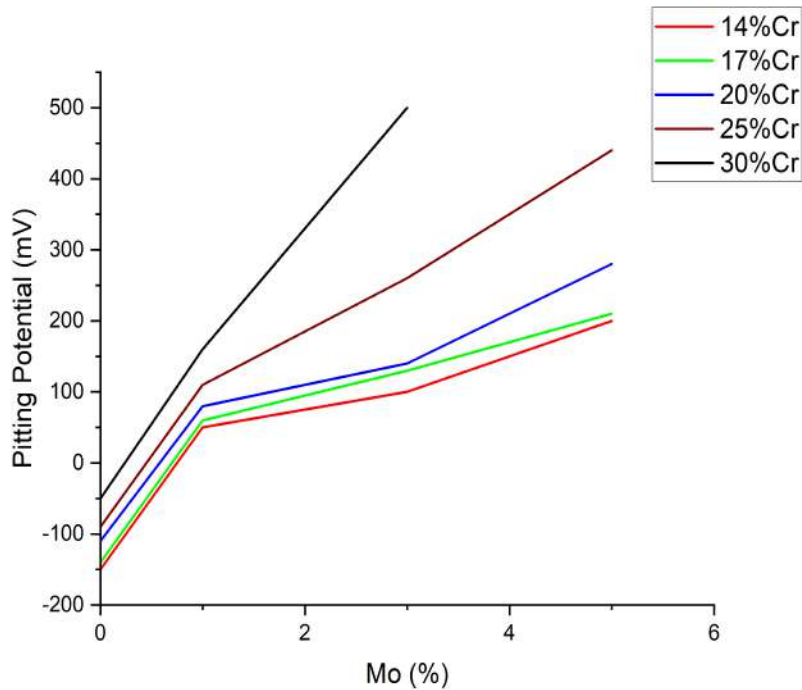


Figure 2.13: Comparison of pitting potential for different FeCrMo alloys in deaerated synthetic seawater at 98°C. [10]

2.2.1.3 Effect of Nickel

In neutral environments nickel is able to create a passive layer only at high potentials. The latter is shown in the Pourbaix diagram in Fig. 2.10. This is the reason behind constant use of the stainless steel together with the chromium.

The use of nickel in neutral environments aims at forming and stabilizing the austenitic phase in stainless steels. However, the presence of nickel has some negative effects in neutral environments. Nickel decreases the solubility of nitrogen in stainless steel[16],and can increase the possibility of stress corrosion cracking (SCC). SCC phenomenon is caused by increasing the quantity of nickel in steel, which consequently decreases the breaking time for SCC. In Fig. 2.14 the Copson curve is shown. This curve shows the variation of the minimum time required for cracking with respect to the increase of the nickel quantity. It is observable that increasing the quantity of nickel from 0 to 10% decreases the minimum time for cracking. After that there is a steady increase until 45%, after that concentration of nickel required for the minimum cracking time becomes so high that SCC is not considered anymore. [14]

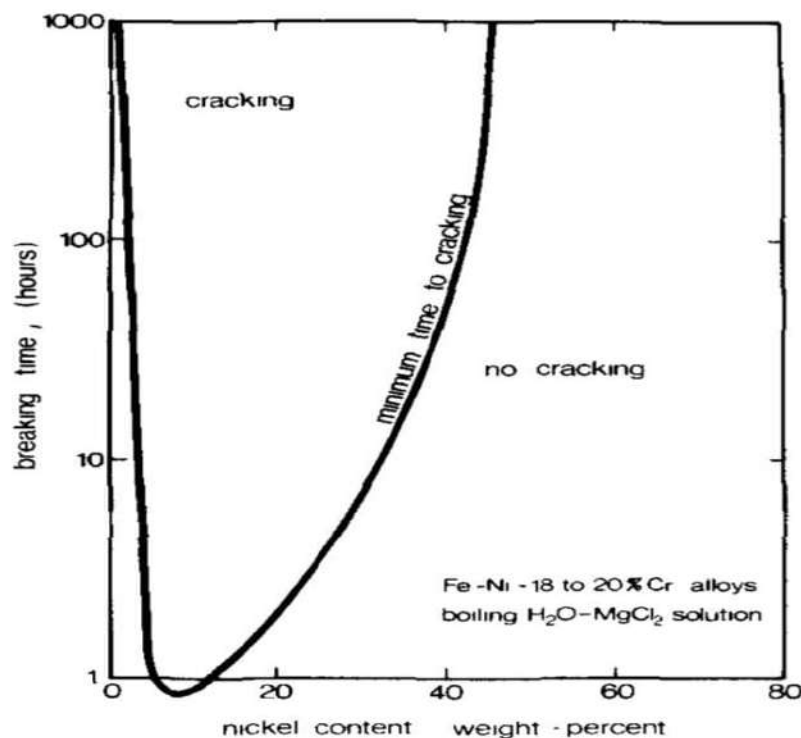


Figure 2.14: Copson Curve. [14]

2.2.1.4 Effect of Nitrogen

Nitrogen is a very useful alloying element and its use has been increased over the past few years. There are several reasons why: it is a very cheap alloying element, it is an austenite former such as nickel, it increases corrosion and pitting resistance and the effect on pitting resistance is more exaggerated if it is combined with molybdenum. [9]

Nitrogen is always present, in low quantity, in all stainless steels because of its spontaneous absorption from melting metal during manufacturing. Nevertheless, this low quantity is not sufficient to have an influence on steel, therefore the quantity of nitrogen has to be increased. [7]

It is very important to control nitrogen because if the amount overpasses the solute limit, a formation of gas bobbles occurs inside steel and/or the formation of compounds with other alloying elements (chromium, molybdenum,...). The reduction of quantity of alloying elements causes the increase of the corrosion rate and the possibility to have sensitization of some zones as well as the pitting corrosion and intergranular corrosion. [16]

The presence of molybdenum and manganese increases the solubility of nitrogen while it decreases in the presence of nickel, carbon, silicon and copper solubility.

2.2.1.5 Effect of Copper

Copper can be added to the stainless steel in order to increase the strength of the steel by precipitation hardening and it can be used to produce the weathering steel(Cor-Ter). [3] Weathering steel is special type of steel with a very good corrosion resistance in the atmospheric environment. In general, the presence of copper as an alloying element decreases resistance to the localization corrosion attack.

Copper is always present as a contaminant in recycled steel because it is impossible to remove during the second metallurgical working since it is still more noble than iron in every temperature. It is impossible to remove it without oxidizing all iron and it can be only diluted by adding new iron to the furnace. [17]

As shown on the Pourbaix diagram (Fig. 2.7), copper is able to create a passive layer in neutral environment only over the pH 7.

Martins et al. [17] investigated the effect of copper on the stainless steel in neutral environment. The result of their research of corrosion behaviour of copper is shown in Fig. 2.15. It is noticeable that the polarization curve in both case, with copper and without copper, are almost same. [17]

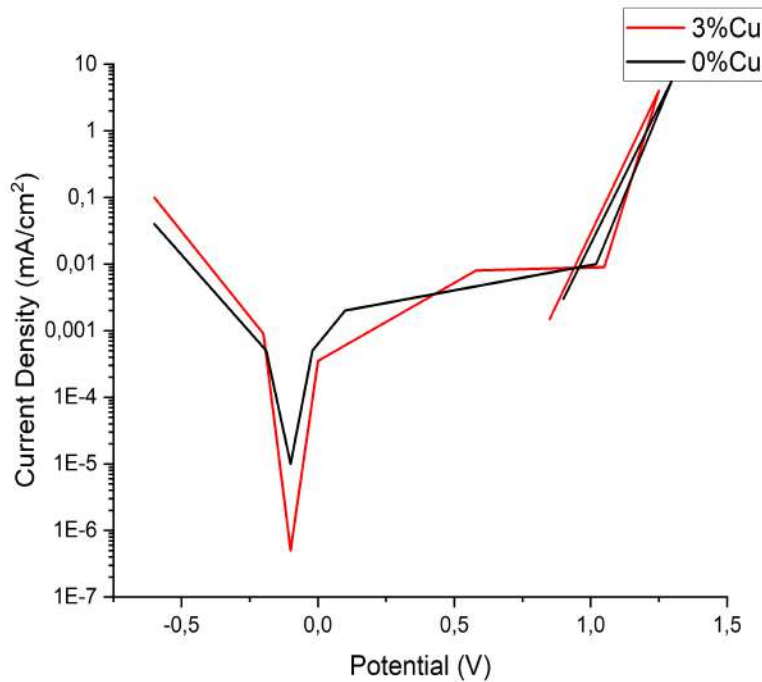


Figure 2.15: Cyclic polarization curve of steel ASTM A890 with the addition of 0%Cu 3%Cu in 0.6 M NaCl. [17]

They also concluded that the presence of copper decreases the critical pitting temperature (CPT). For instance, during their experiments they noticed that in the solution of 0.6 M NaCl the sample without copper has a higher CPT than the sample with the quantity of 3% of copper. [17]

2.2.1.6 Effect of Carbon

Carbon is the basic alloying element in steel. Steel is a binary compound of iron and carbon. In steels carbon content can reach 2,1% but in stainless steel it is usually very low (0.1-0.2%). [18]

Increasing the quantity of carbon increases the hardness of steel but at the same time it increases the brittleness of steel as well. Most importantly, it can cause a reduction of the quantity of chromium. Carbon reduces the quantity of chromium by the formation of chromium carbide (Cr_3C_2) and that phenomenon is provoked by the presence of high quantity of carbon or by the welding process. The effect of carbon is very important in a neutral environment because, as shown in Fig. 2.1 chromium is responsible for the formation of the passive layer at that range of pH 6-8. [3]

2.2.1.7 Effect of Sulphur

Sulphur is normally considered a contaminant and for this reason it is usually removed during the second metallurgical process. But in some cases sulphur is added as an alloying element to improve the machinability of steel. The presence of sulphur causes the reduction of the corrosion properties of steel.

Jeon et al. investigated the effect of sulphur on corrosion resistance and on the critical pitting temperature (CPT) in a neutral environment.

As shown in 2.16 , by increasing the content of sulphur the breakdown potential decreases; this is caused by the reduction of pitting resistance. [19]

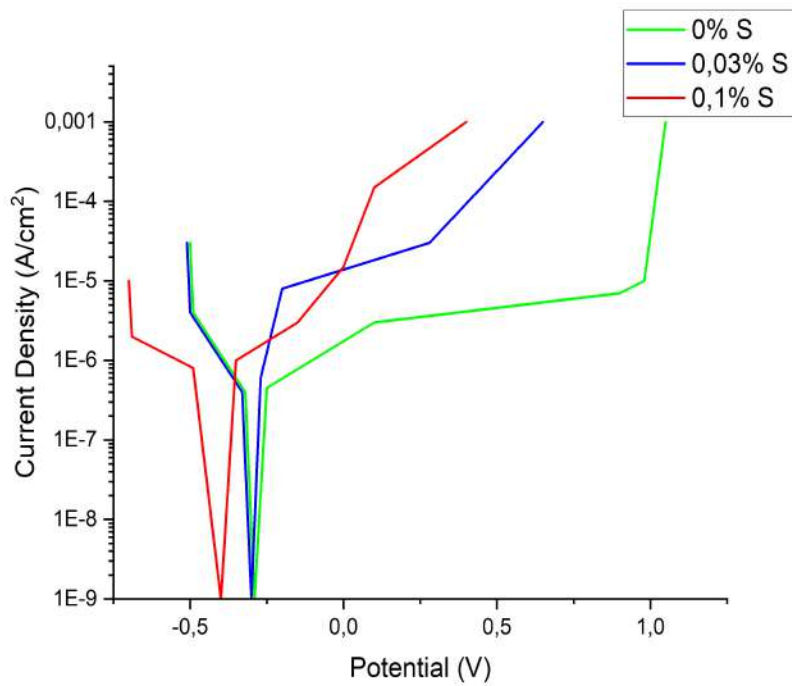


Figure 2.16: Cyclic polarization curve of Steel ASTM S32750 with addition of 0, 0.03, 0.1% sulphur (S) in deaerated solution of 22% of NaCl at 70°C[19]

They also discovered that increasing the quantity of sulphur in stainless steel causes the reduction of the CPT in a neutral environment. [19]

2.2.2 Nickel alloys

Nickel alloys have a good corrosion resistance in a neutral solution and they also have a good resistance in sea water with high velocity. [3] The presence of low velocity sea water or high quantity of halogens ions can cause pitting corrosion and stress corrosion cracking (SCC). This problem can be solved by adding alloying elements to nickel. [3, 26]

2.2.2.1 Effect of Chromium

Chromium permits the increase of nickel alloy corrosion resistance when oxidizing ions are present in the environment, due to the formation of passive layers in an oxidizing environment. The minimum quantity of chromium necessary to have the formation of the passive layer is 11 %. Increasing the quantity of chromium decreases the corrosion rate and increases the passive behavior of the alloy in an oxidizing environment. [3, 22]

2.2.2.2 Effect of Molybdenum

Molybdenum is a very important alloying element because the formation of molybdenum oxide film can disable further dissolution of the pit and increase the repassivation behavior.

Nickel-molybdenum alloys cannot be used when welding is necessary because they can suffer from sensitization.

Another problem of the addition of molybdenum in nickel alloys is that the existence of oxidizing ions such as Cu^{2+} and Fe^{3+} cause an increase of the alloy corrosion rate. [3, 22]

Haves et al. [22] pointed out in their research that by adding higher amount of molybdenum to nickel alloys the pitting resistance of the material is higher and the occurring hysteresis phenomenon in a neutral environment is eliminated. Potentiodynamic polarization curves of various nickel alloys with different molybdenum content can be seen in Fig. 2.17.

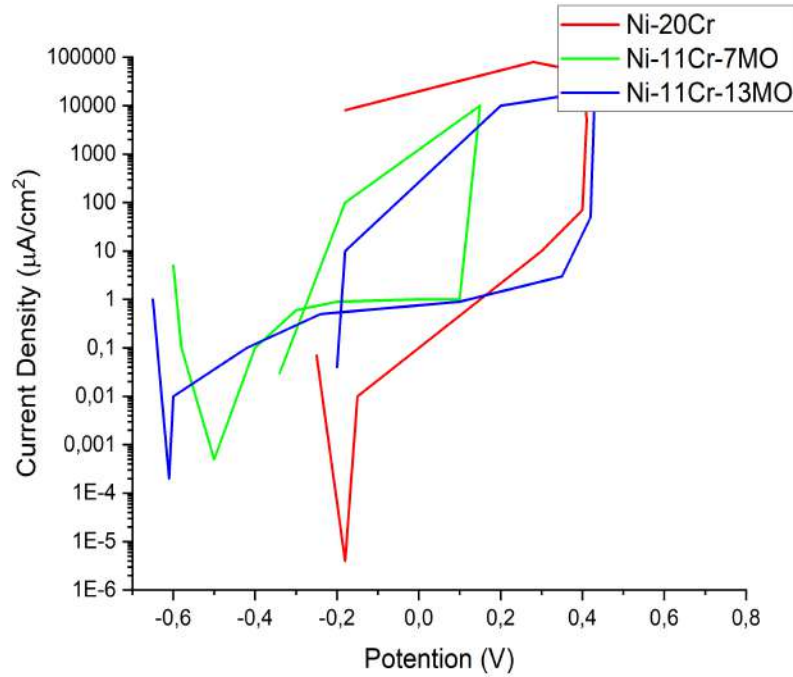


Figure 2.17: Potentiodynamic polarization curves of Ni-20Cr, Ni-11Cr-7Mo, Ni-11Cr-13Mo in 1 M NaCl at pH 7.78 and 90°C. [22]

2.2.2.3 Effect of Copper

Minerals nickel is extracted from generally contain also copper and the process to eliminate copper from nickel is very expensive. For this reason, in some cases it can be decided to leave part of copper inside the alloy to reduce the cost of production.

The effect of copper in the corrosion resistance of nickel alloys depends on the environmental contaminants presence. In the presence of oxidizing agents (Fe^{3+} , NO_3^-) corrosion resistance is a little bit lower than pure nickel but the most important property is the capacity of copper to reduce the formation of the passive layer in nickel-copper alloys. Therefore, this forbids the starting of the local corrosion but permits only the uniform corrosion. [23]

2.2.2.4 Effect of Iron

In a neutral environment the presence of iron as an alloying element does not have any significant effect on the corrosion resistance. The purpose of adding iron in this case is to obtain cheaper nickel

alloys.

Sabatini et al [27] showed in their work the polarization curve of nickel and nickel-iron alloys in a neutral environment. From potentiodynamic polarization curve in Fig. 2.18 no apparent alteration of the curve can be seen by increasing the iron content. [27]

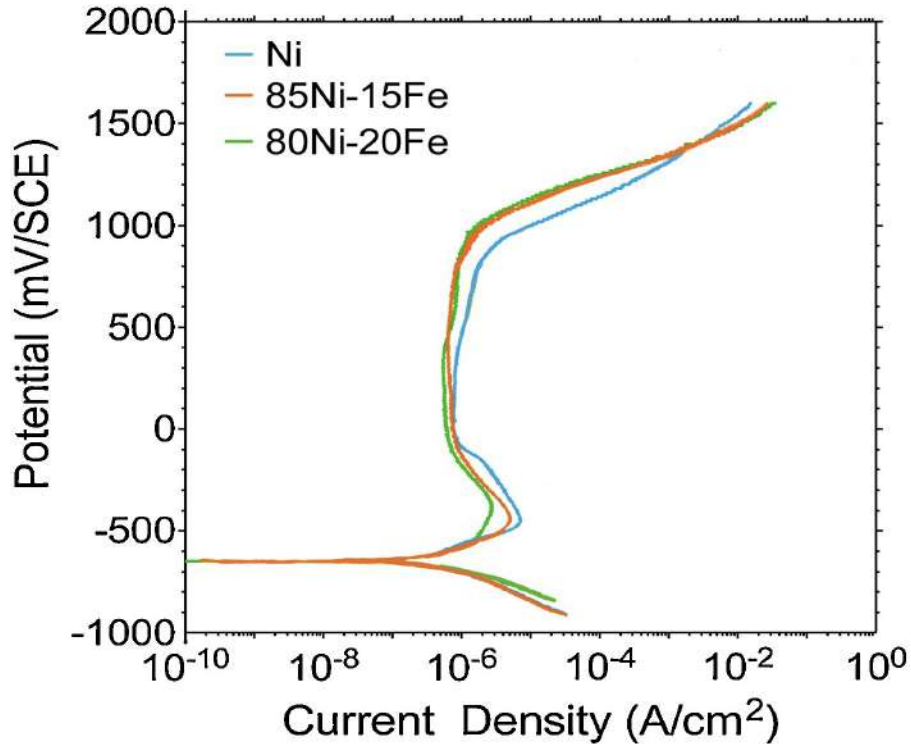


Figure 2.18: Potentiodynamic polarization curves nickel-iron alloys in neutral (pH 7) Na_2SO_4 electrolyte at 25°C. [27]

2.3 Alkaline solutions

2.3.1 Iron alloys

Low-alloys steels are subject to corrosion in every alkaline solution. [3] Stainless steels have a good general corrosion resistance to sodium hydroxide (NaOH) solution below 65°C. [3, 4] They also have a good corrosion resistance for every temperature and concentration in ammonium (NH_3) and ammonium hydroxide (NH_3OH) solution. [3]

2.3.1.1 Effect of Chromium

Chromium is the most important alloying element in stainless steels but it is not very important in an alkaline environment. In the Pourbaix diagram (Fig. 2.1), the stability range of the chromium passive layer is shown. As shown, chromium forms a passive layer through complete alkaline range but after exceeding the pH 9 it becomes useless because the passive range of chromium is overlapping or becomes overcome by the passive range of iron. For this reason, in an alkaline condition the presence of chromium is not necessary to have the formation of a passive layer. [8]

2.3.1.2 Effect of Molybdenum

The presence of molybdenum is useless for the formation of passive layers because it is not able to form passive layers in an alkaline environment at a pH higher than 9. The behavior of molybdenum to form passive layers in alkaline solutions is shown in the Pourbaix diagram (Fig. 2.3). In an alkaline environment the presence of molybdenum as an alloying element can also be negative because it decreases the corrosion resistance of stainless steels. [9]

At the same time the presence of molybdenum as an alloying element is crucial when chloride is present in the environment. This increases the pitting resistance and the repassivation behavior of stainless steel in an alkaline environment.

2.3.1.3 Effect of Nickel

The presence of nickel as an alloying element is very important in an alkaline environment. Nickel increases the corrosion resistance of steel, and it permits the formation of a passive layer. [28]

As shown in the Pourbaix diagram (Fig. 2.10), nickel forms an insoluble passive layer in an alkaline environment and it is also stable at very high potential. There is only the solubilization of the film in low potential with a pH lower than 9 and higher than 12 but this is not a major issue since in these zones the iron passive layer is stable.

The comparison between the polarization curve for carbon steel and nickel-bearing steel in saturate calcium hydroxide ($\text{Ca}(\text{OH})_2$) solution with pH of 11.5 can be seen in Fig. 2.19.

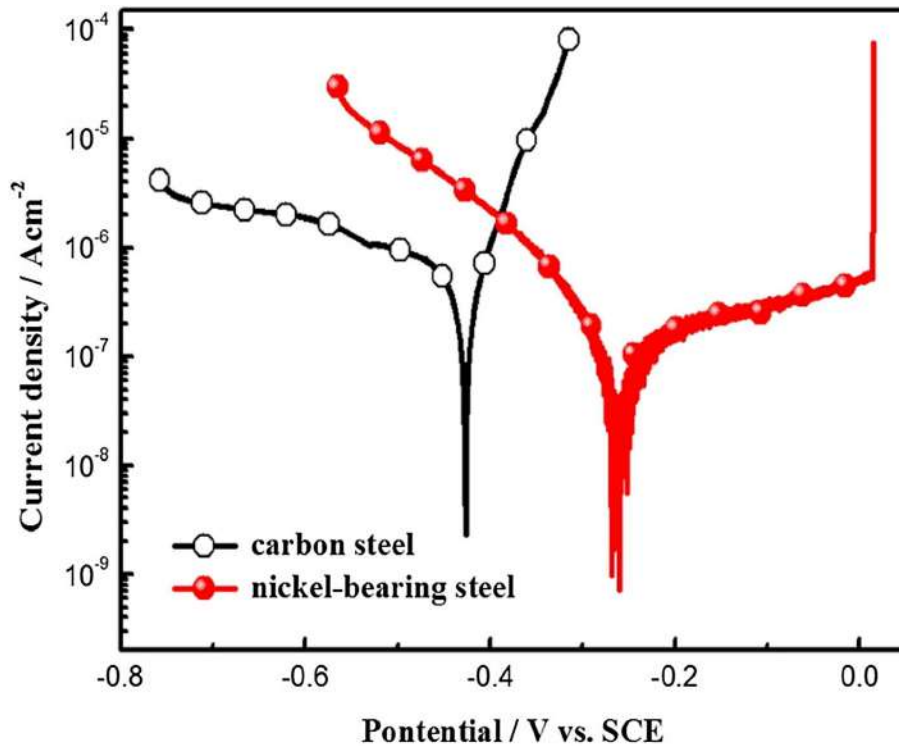


Figure 2.19: Polarization curves of carbon steel and nickel-bearing steel in calcium hydroxide ($\text{Ca}(\text{OH})_2$) saturate solution with 3.5 % NaCl and 7 % NaHCO_3 (pH 11.5). [28]

In Fig. 2.19 shows that the presence of nickel shifts the polarization curve towards lower current density and higher potential, in addition to the formation of a passive layer, as mentioned beforehand. Furthermore, nickel decreases the defect density and the whole thickness of the iron oxide film. In addition, it increases the $\text{Fe}^{2+}/\text{Fe}^{3+}$ ratio and the inner barrier layer thickness. All these effect influences have an effect on the formation of the protective passive layer. [28]

Increasing the nickel quantity decreases the corrosion rate but, on the other hand, it also decreases the minimum breaking time required for stress corrosion cracking to take place. [4, 29]

2.3.1.4 Effect of Nitrogen

The use of nitrogen as an alloying element has expanded in the last few years because it is a very cheap alloying element, it is an austenite former as nickel and it increases the pitting resistance. [9] In low quantity nitrogen is always present in stainless steels because it is absorbed spontaneously from the atmosphere by melting metal during the manufacturing. However, at this low quantity it does not show any significant effect on the steel properties. For this reason, the quantity of nitrogen

is increased by a special operation during manufacturing. [7]

The solubility of nitrogen in stainless steel depends on the presence of the other alloy element. The presence of nickel, carbon, silicon and copper decreases the presence of molybdenum and manganese increases the solubility of nitrogen while the presence of molybdenum and manganese increases its solubility. If the quantity of nitrogen overpasses the solute limit, there is the formation of gas bobbles inside steel and/or the formation of compounds with other alloying elements. This reduction of quantity of alloying elements causes the increase of the corrosion rate and the possibility to have sensitization of some zones as well as the pitting corrosion and intergranular corrosion. [16] This phenomenon is very important in an alkaline environment where the quantity of nickel in stainless steels is generally higher. For all these reasons nitrogen in an alkaline environment is useful for nickel-free alloys because it is able to substitute nickel for the formation of austenite in all the situations where the use of nickel is forbidden like for medical applications. [30]

2.3.1.5 Effect of Copper

Copper can be introduced to stainless steel in order to increase the strength of steel by precipitation hardening but the presence of copper as an alloying element generally decreases the resistance to the local corrosion attack. Copper is always present as a contaminant in recycled steel because it is impossible to remove during the second metallurgical manufacture since it is more noble than iron at every temperature. It is impossible to remove it by the oxidation process but it can be only diluted by adding new iron in the furnace. [17]

As is shown on the Pourbaix diagram (Fig. 2.7), copper is able to create a passive layer in an alkaline environment until the pH 12,5, after that pH the passive layer is stable only at low potential.

G. Pena et al. [31] investigated the possibility to use copper to increase the corrosion resistance of stainless steel in alkaline corrosion and the possibility to substitute nickel as an alloying element. They concluded that stainless steel with copper has a corrosion behaviour comparable with nickel stainless steel in an alkaline environment. But high nickel stainless steel still have the best quality of corrosion resistance in alkaline solutions, for this reason copper can be used to reduce the quantity of nickel in low alkaline pH but it can be used to substitute nickel. [31]

2.3.1.6 Effect of Carbon

Carbon is the essential alloying element in steel. Steel is a binary compound of iron and carbon; in carbon steel the content of carbon can amount to 2,1%, after which content becomes cast iron. The

content of carbon in stainless steel is usually very low (0.1-0.2%). [18]

Increasing the quantity of carbon increases the hardness of steel but it also increases the brittleness of steel and can cause a reduction of chromium quantity in a solid solution.

In an alkaline environment the presence of carbon is not a problem since the presence of chromium in a solid solution to form a passive layer is not necessary. This is due to the fact that at the pH higher than 9 steels are able to form a passive layer only by the formation of iron oxides (Fe_2O_3 , Fe_3O_4) and iron hydroxides ($\text{Fe}(\text{OH})_3$, $\text{Fe}(\text{OH})_2$). [3, 8]

2.3.1.7 Effect of Sulphur

Sulphur is generally considered a contaminant and for this reason it is often removed during the second metallurgical process. However, in some cases it is necessary to add some sulphur as an alloying element to improve the machinability of steel but its presence also causes a reduction of the corrosion properties of steel.

2.3.2 Nickel alloys

Nickel alloys are commonly used for applications in an alkaline environment because nickel has a very good corrosion resistance to all alkaline solutions except for ammonium hydroxide (NH_4OH). [3] With greater content of nickel in the alloy, general corrosion resistance and stress corrosion resistance are higher. [3, 26] In case of high concentration of sodium hydroxide (NaOH) and potassium hydroxide (KOH) at elevated temperatures, there is the possibility to have selective molybdenum dealloying in Ni-Mo and Ni-Cr-Mo alloys. [3, 32]

2.3.2.1 Effect of Chromium

In an alkaline environment the presence of chromium as an alloying element shifts the passive zone to lower potential but it also causes the increase of current density in a transpassive zone. [24]

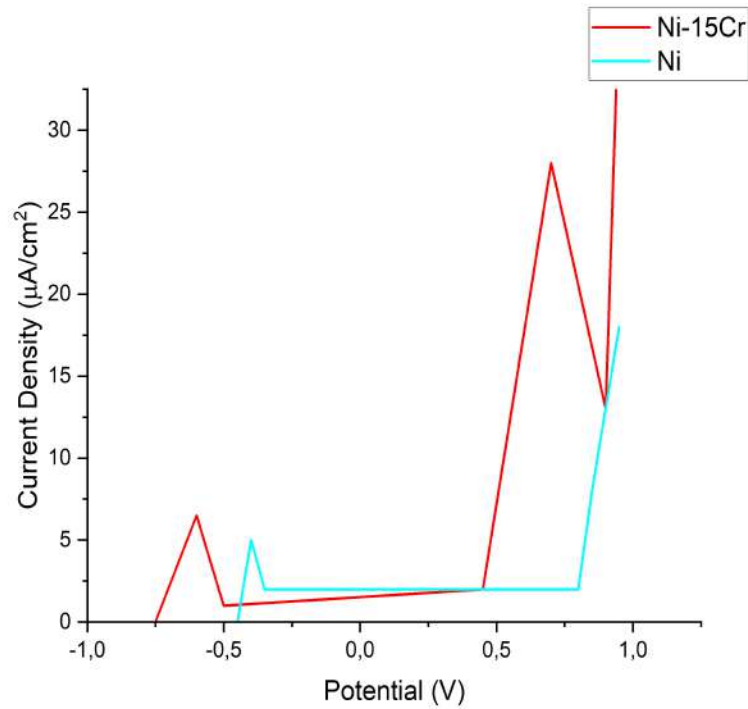


Figure 2.20: Potentiodynamic curves of Ni and Ni-15Cr alloy in borate buffer solution. [24]

2.3.2.2 Effect of Molybdenum

Molybdenum is one of the most common alloying elements in nickel alloys. The main effect of molybdenum is the improvement of the repassivation behavior in alkaline environments. However, the presence of molybdenum can cause the sensitization of the alloy during the welding process.

In the Fig. 2.21 the result of a study of Myres and Fontana [22] about the effect of molybdenum are shown. This test shows that a low quantity of molybdenum is sufficient to prevent pitting corrosion in an alkaline environment. [3, 22]

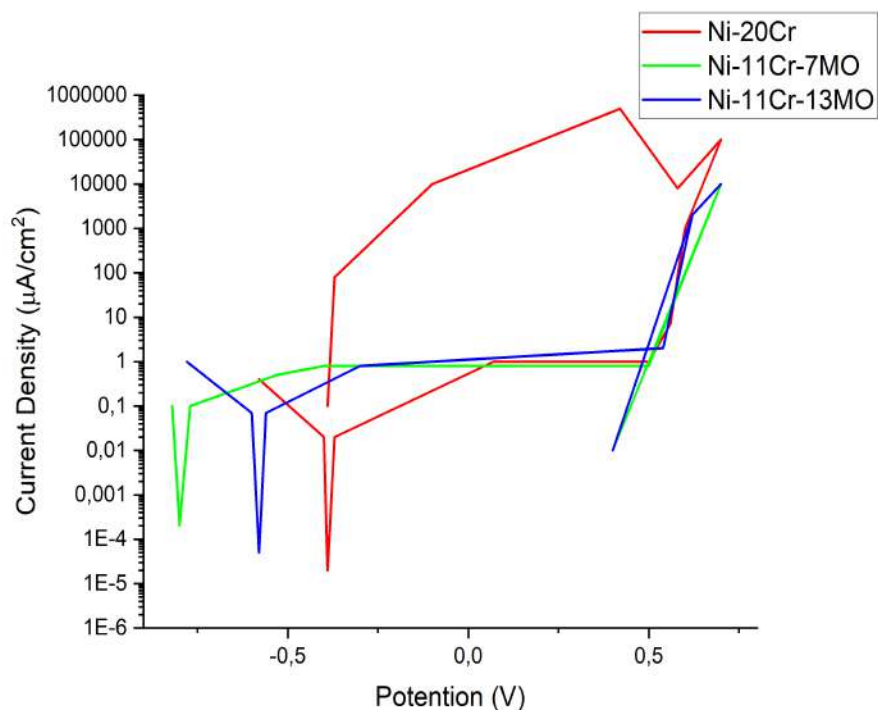


Figure 2.21: Potentiodynamic polarization curves of Ni-20Cr, Ni-11Cr-7Mo, Ni-11Cr-13Mo in 1 M NaCl at pH 12.48 and 90°C. [22]

2.3.2.3 Effect of Copper

Copper can usually be found in the same minerals that contain nickel. The process of extracting copper is not economically feasible, thus in some cases certain percentage of copper is left in the alloy. In this way the costs of production are reduced.

In an alkaline environment, copper does not modify the corrosion resistance of nickel but it reduces the probability of passive layer formation and, therefore, material is less susceptible to pitting corrosion. [23]

2.3.2.4 Effect of Iron

The presence of iron as an alloying element decreases the cost of alloys. Nevertheless, it can also cause an increase of current density at low potentials where iron has an active behavior. The presence of iron is convenient in alkaline environments if it is added to nickel-chromium alloys. In such cases iron can form a passive layer at high potential in opposition to the transpassive zone caused by

chromium. [24] This effect can be seen in the following figure (Fig. 2.22).

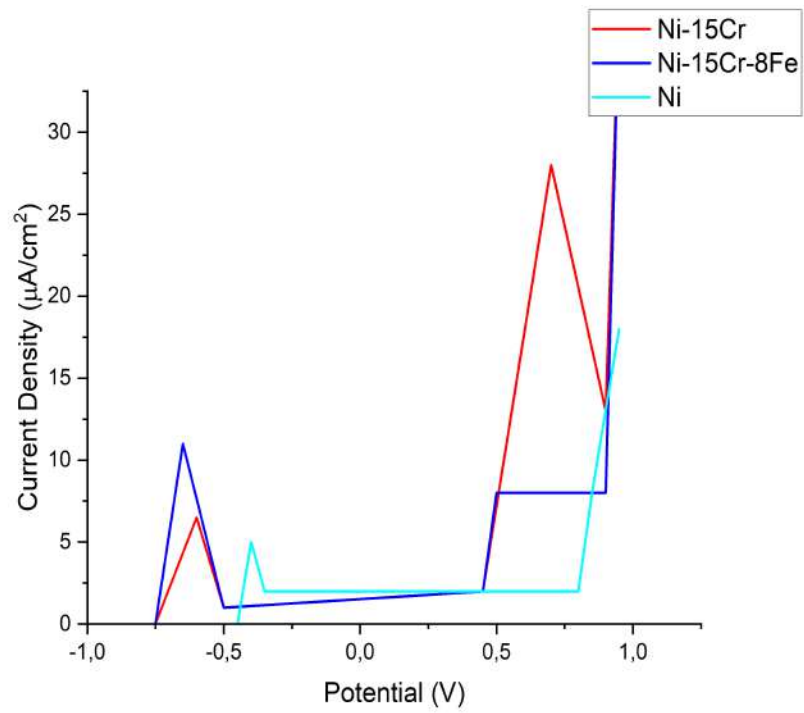


Figure 2.22: Potentiodynamic curves of Ni, Ni-15Cr and Ni-15Cr-8Fe alloys in borate buffer solution. [24]

3. Experimental

The aim of this thesis is to investigate the behavior of five alloys with different composition in various pH solutions (acidic, neutral and alkaline) to use them in the washing units of ReOil plant and for the storage of toxic waste. To ascertain the effect of varying alloy composition and pH, autoclave tests together with electrochemical techniques were carried out jointly. The results from autoclave tests will point out the resistance of certain alloys to stress corrosion cracking. On the other hand, comparative cyclic polarization measurements should imply the behavior of material at different polarization potentials. In addition, the results of electrochemical measurements will reveal the susceptibility of each material to form passive layers and its stability. In order to simulate real conditions present in ReOil plant, solutions have been taken directly from the site. Excluding the on-site solution, artificial solutions have also been used. Finally, the collected results altogether should facilitate the most appropriate material for application under certain conditions present in the plant.

3.1 Materials

The investigated alloys are two types of duplex stainless steels (X2CrNiMoN25-7-4, X2CrNiMoN22-5-3), an austenitic stainless steel (X2CrNiMo17-12-2), a super austenitic stainless steel (X1NiCrMoCu25-20-5), a Sanicro alloy (Sanicro 35), an hastalloy (NiMo16Cr15W), and three special alloy from Böhler (Alloy59, Alloy31, Böhler P569).

The chemical composition in wt% of the alloys examined is presented in Table 3.1.

Table 3.1: Chemical composition of the tested alloys

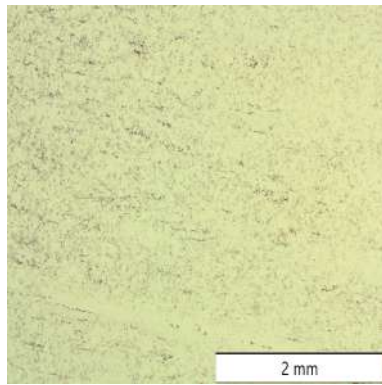
Material N.	Name	C	Si	Mn	P	S	Cr	Mo	Ni
		%	%	%	%	%	%	%	%
1.4404	X2CrNiMo17-12-2	0.02	<1.0	<2	<0.05	<0.030	17	2	12
1.4410	X2CrNiMoN25-7-4	0.02	<1.0	<2	<0.03	<0.015	25	4	7
1.4462	X2CrNiMoN22-5-3	0.02	<1.0	<2	<0.03	<0.020	22	3	5
1.4539	X1NiCrMoCu25-20-5	0.01	<0.7	<2	<0.03	<0.010	20	5	25
2.4819	NiMo16Cr15W	<0.01	<0.1	<1	<0.02	<0.015	15	16	bal
	Sanicro 35	<0.03	<0.5	0,8	<0.03	<0.020	27	6.5	35
2.4605	Alloy59	<0.01	<0.1	<0.5	<0.02	<0.015	23	16	bal
1.4562	Alloy31	0.015	<0.3	<2	-	-	27	6.5	31
	Böhler P569	<0.05	-	5.5	-	-	27	3.5	14
		V	Nb	Ti	N	Cu	Co	Fe	W
		%	%	%	%	%	%	%	%
1.4404	X2CrNiMo17-12-2	-	-	-	<0.11	-	-	bal	-
1.4410	X2CrNiMoN25-7-4	-	-	-	0.30	-	-	bal	-
1.4462	X2CrNiMoN22-5-3	-	-	-	0.16	-	-	bal	-
1.4539	X1NiCrMoCu25-20-5	-	-	-	<0.15	1.60	-	bal	-
2.4819	NiMo16Cr15W	<0.35	-	-	-	<0.50	<2.50	5.50	3.75
	Sanicro35	-	-	-	0.3	0.2	-	bal	-
2.4605	Alloy59	-	-	-	-	<0.50	<0.3	<1.50	-
1.4562	Alloy31	-	-	-	0.2	1.2	-	bal	-
	Böhler P569	-	-	-	0.7	-	-	bal	-

The mechanical properties of the alloys tested: yield strength (YS), ultimate tensile strength (UTS), fracture elongation (A) and Young modulus (E) at 20°C are shown in Table 3.2

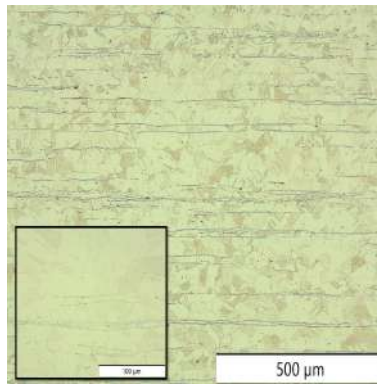
Table 3.2: Mechanical properties of the tested alloys

Material N.	Name	YS	UTS	A	E
		MPa	MPa	%	GPa
1.4404	X2CrNiMo17-12-2	200	500-700	40	193
1.4410	X2CrNiMoN25-7-4	280	580-800	40	200
1.4462	X2CrNiMoN22-5-3	450	650-800	25	200
1.4539	X1NiCrMoCu25-20-5	230	530-730	35	195
2.4819	NiMo16Cr15W	310	750	30	208
	Sanicro35	425	750	35	190
2.4605	Alloy59	340	690	40	210
1.4562	Alloy31	280	850	40	198
	Böhler P569	500-700	950	40	200

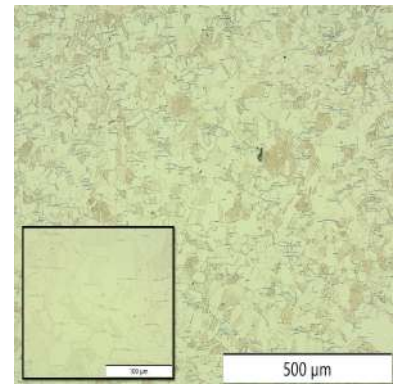
The microstructure of the different materials investigated are examined by the optical microscope "Olympus AX70" with the camera "Olympus DP50" and the metallographic preparation for each sample was done by the Austrian Casting Institute of Leoben (Österreichisches Gießerei-Institut).



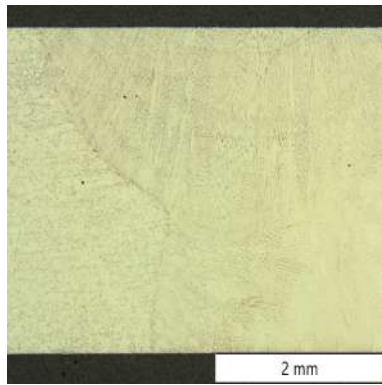
(a) Top view 25x magnification



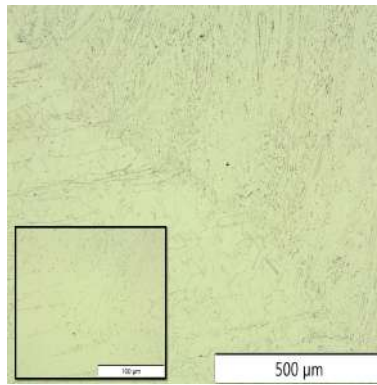
(b) Front view 100x and 500x magnification



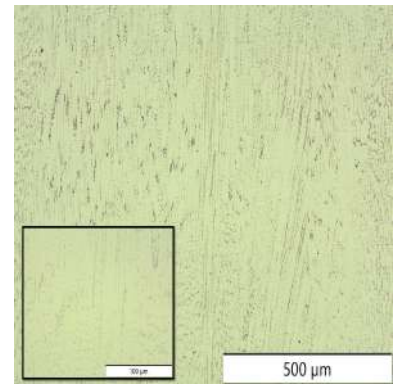
(c) Side view 100x and 500x magnification



(d) Front view of welding 25x magnification



(e) Front view of welding 100x and 500x magnification

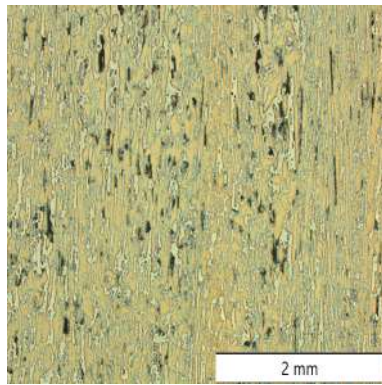


(f) Front view of weld 100x and 500x magnification

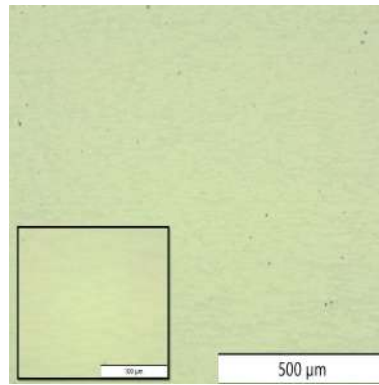
Figure 3.1: Microstructure of material N. 1.4404 (X2CrNiMo17-12-2)

However, Fig. 3.1a displays the microstructure of the material N 1.4404 from the top view at 25x magnification while the Fig. 3.1b, 3.1c shows the microstructure from the other two views at 100x and 500x magnifications. It has a microstructure of equiaxed austenitic grain and annealing twins. In addition, there is some δ ferrite in the rolling direction.

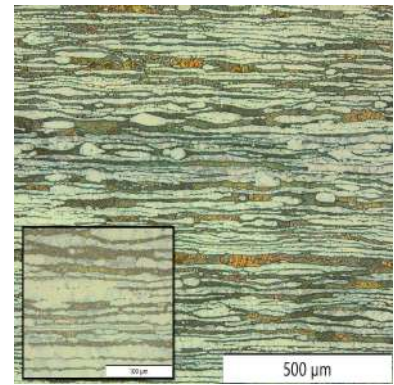
Besides, Fig. 3.1d, 3.1f, 3.1e show the microstructure of the same material but in the presence of weld zone at 25x, 100x and 500x magnifications. The microstructure of the welding zone is composed of bigger austenitic grains and a lot of CrC precipitations uniformly distributed.



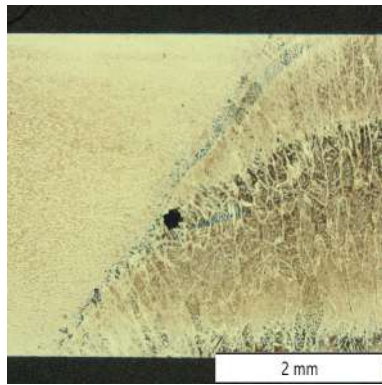
(a) Top view 25x magnification



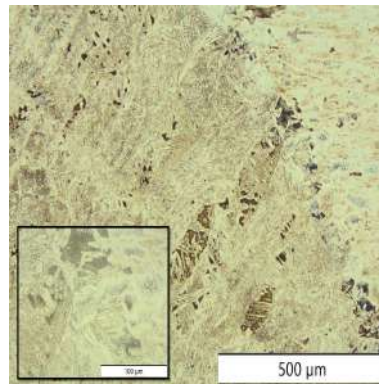
(b) Front view 100x and 500x magnification



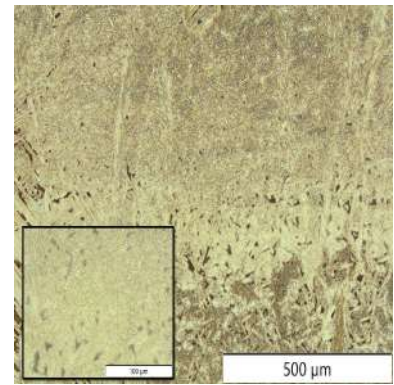
(c) Side view 100x and 500x magnification



(d) Front view of welding 25x magnification



(e) Front view of welding 100x and 500x magnification



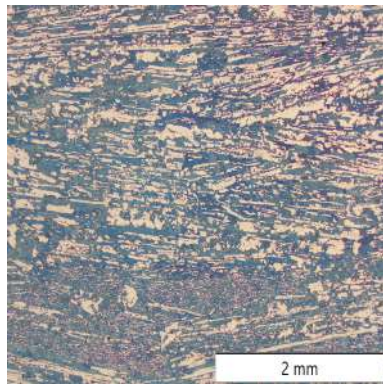
(f) Front view of weld 100x and 500x magnification

Figure 3.2: Microstructure of material N. 1.4410 (X2CrNiMoN25-7-4)

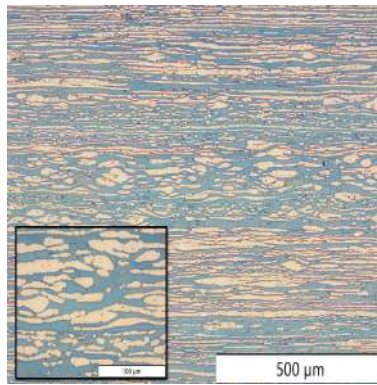
However, Fig. 3.2a exhibits the microstructure of the material N 1.4410 from the top view at 25x magnification while the Fig. 3.2b, 3.2c show the microstructure from the other two views at 100x and 500x magnifications. It has a microstructure composed of ferritic elongated grains (colored one) in the rolling direction, in an austenitic matrix.

Besides, Fig. 3.2d, 3.2f, 3.2e display the microstructure of the same material but in the presence of weld zone at 25x, 100x and 500x magnifications.

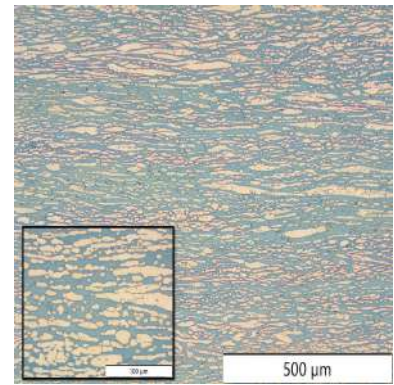
The microstructure of the welding zone is composed of martensitic and bainitic grains in a retained austenitic matrix.



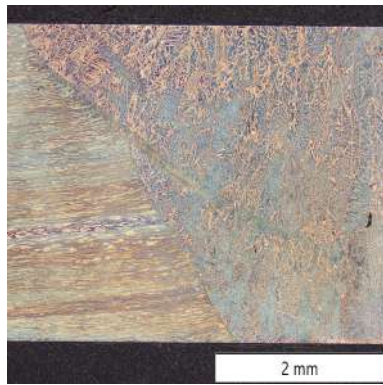
(a) Top view 25x magnification



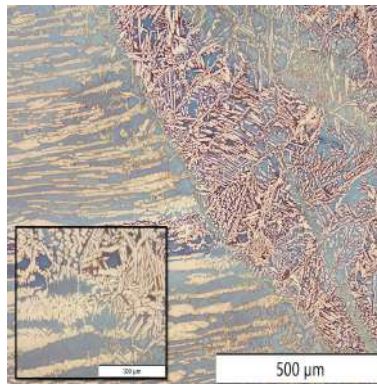
(b) Front view 100x and 500x magnification



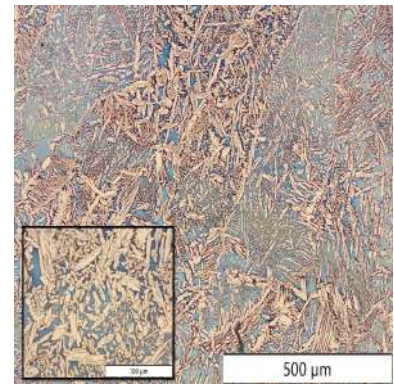
(c) Side view 100x and 500x magnification



(d) Front view of welding 25x magnification



(e) Front view of welding 100x and 500x magnification



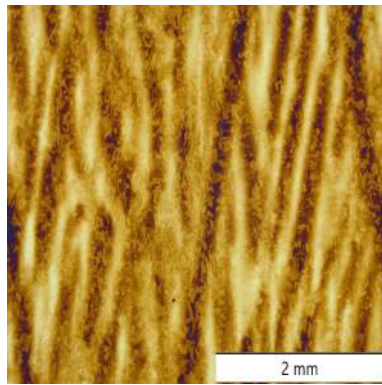
(f) Front view of weld 100x and 500x magnification

Figure 3.3: Microstructure of material N. 1.4462 (X2CrNiMoN22-5-3)

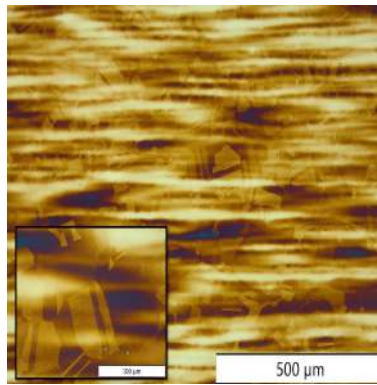
However, Fig. 3.3a shows the microstructure of the material N. 1.4462 from the top view at 25x magnification while the Fig. 3.3b, 3.3c display the microstructure from the other two views at 100x and 500x magnifications. It has a microstructure composed of austenitic elongate grains in the rolling direction, in an ferritic matrix (colored one).

Besides, Fig. 3.3d, 3.3f, 3.3e show the microstructure of the same material but in the presence of weld zone at 25x, 100x and 500x magnifications.

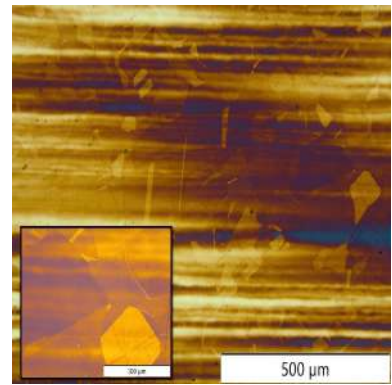
The microstructure of the welding zone is composed of bainitic grains in a retain austenitic matrix.



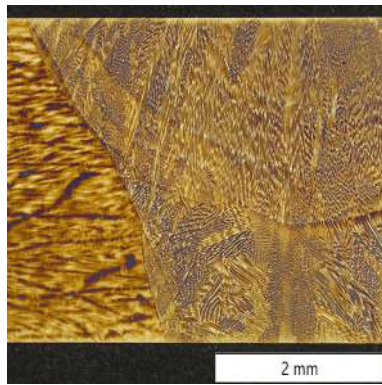
(a) Top view 25x magnification



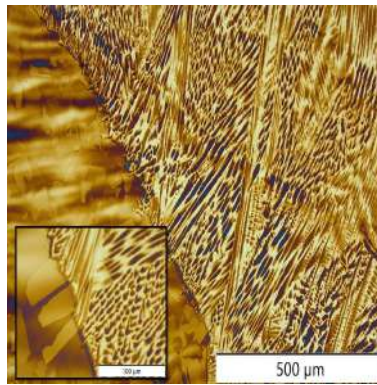
(b) Front view 100x and 500x magnification



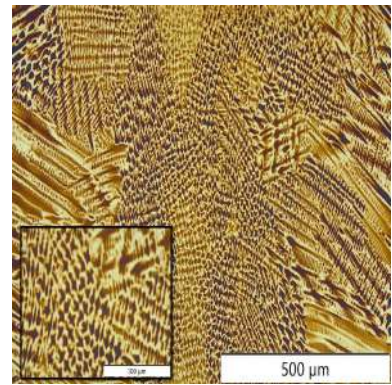
(c) Side view 100x and 500x magnification



(d) Front view of welding 25x magnification



(e) Front view of welding 100x and 500x magnification

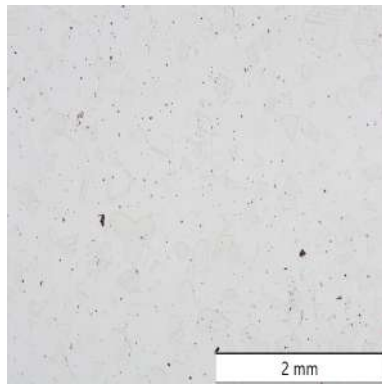


(f) Front view of weld 100x and 500x magnification

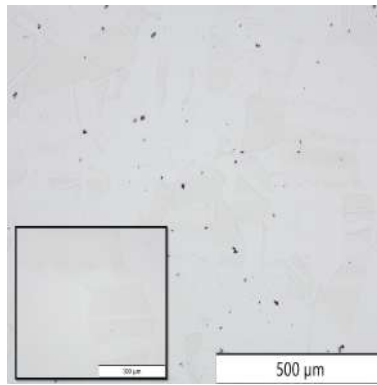
Figure 3.4: Microstructure of material N. 1.4539 (X1NiCrMoCu25-20-5)

However, Fig. 3.4a shows the microstructure of material N. 1.4539 from the top view at 25x magnification while Fig. 3.4b, 3.4c display the microstructure from the other two views at 100x and 500x magnifications. It shows austenitic grains with segregation in rolling direction.

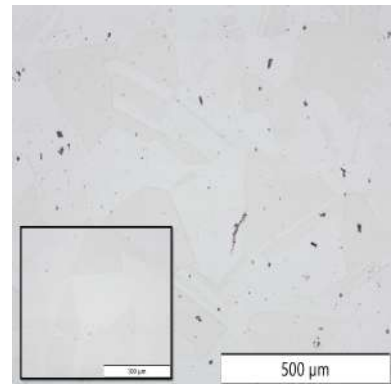
Besides, Fig. 3.4d, 3.4f, 3.4e show the microstructure of the same material but in the presence of weld zone at 25x, 100x and 500x magnifications



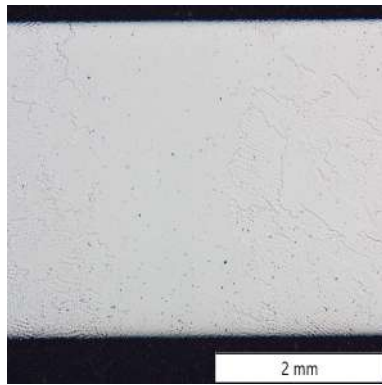
(a) Top view 25x magnification



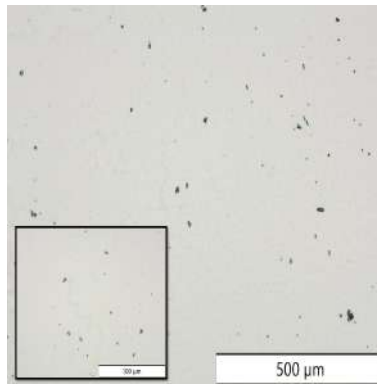
(b) Front view 100x and 500x magnification



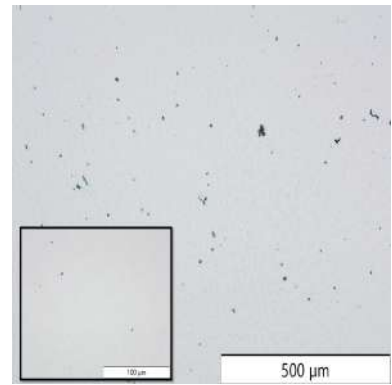
(c) Side view 100x and 500x magnification



(d) Front view of welding 25x magnification



(e) Front view of welding 100x and 500x magnification



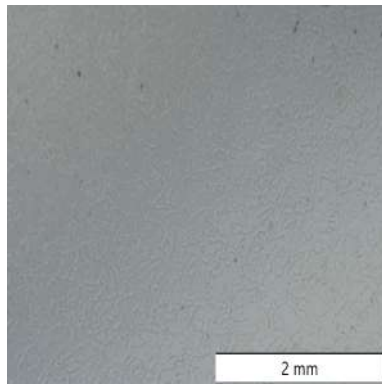
(f) Front view of weld 100x and 500x magnification

Figure 3.5: Microstructure of material N. 2.4819 (NiMo16Cr15W)

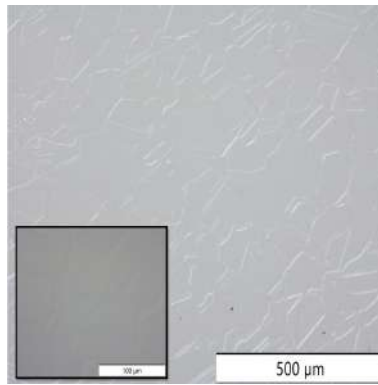
Fig. 3.5a displays the microstructure of material N 2.4819 from the top view at 25x magnification while Fig. 3.5b, 3.5c show the microstructure from the other two views at 100x and 500x magnifications. Its microstructure is composed of austenitic nickel grains and annealing twins.

Besides, Fig. 3.5d, 3.5f, 3.5e show the microstructure of the same material but in the presence of weld zone at 25x, 100x and 500x magnifications.

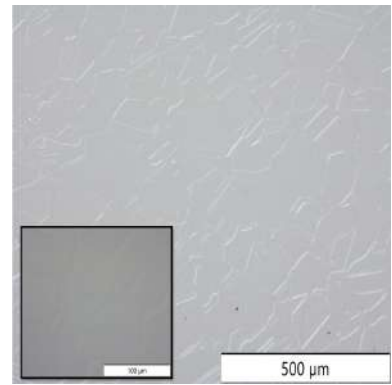
The microstructure of the welding zone is composed of fine equiaxial austenitic nickel grains.



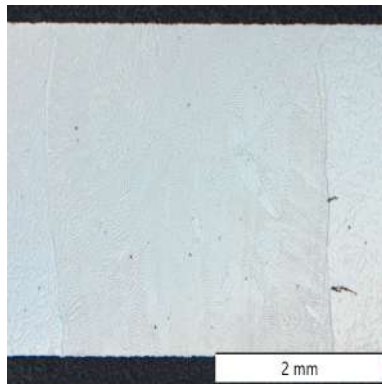
(a) Top view 25x magnification



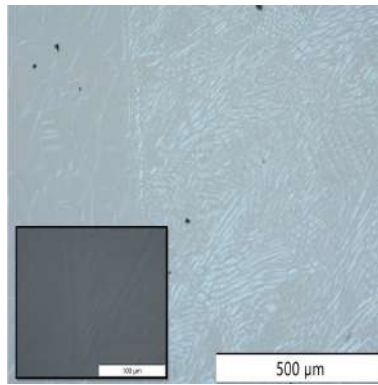
(b) Front view 100x and 500x magnification



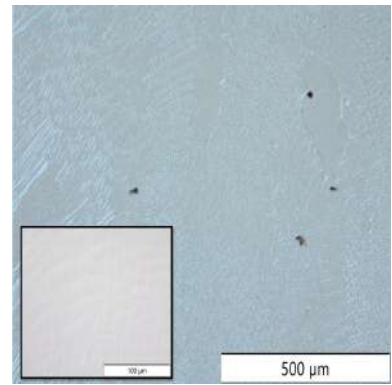
(c) Side view 100x and 500x magnification



(d) Front view of welding 25x magnification



(e) Front view of welding 100x and 500x magnification



(f) Front view of weld 100x and 500x magnification

Figure 3.6: Microstructure of material Sanicro35

Fig. 3.6a shows the microstructure of the material Sanicro35 from the top view at 25x magnification while Fig. 3.6b, 3.6c display the microstructure from the other two views at 100x and 500x magnifications. Its microstructure is composed of austenitic grains.

Besides, Fig. 3.6d, 3.6f, 3.6e display the microstructure of the same material but in the presence of weld zone at 25x, 100x and 500x magnifications.

The microstructure of the welding zone is composed of fine equiaxial austenitic nickel grains.

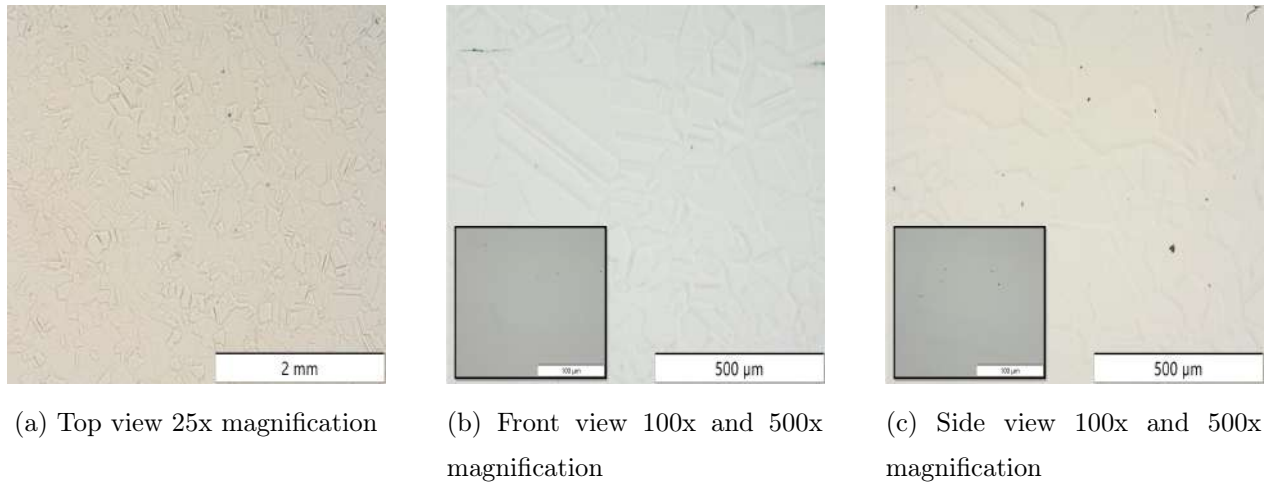


Figure 3.7: Microstructure of material N. 2.4605 (Alloy59)

Fig. 3.7a shows the microstructure of the material N 2.4605 from the top view at 25x magnification while Fig. 3.7b, 3.7c display the microstructure from the other two views at 100x and 500x magnifications. Its microstructure is composed of austenitic nickel grains and annealing twins.

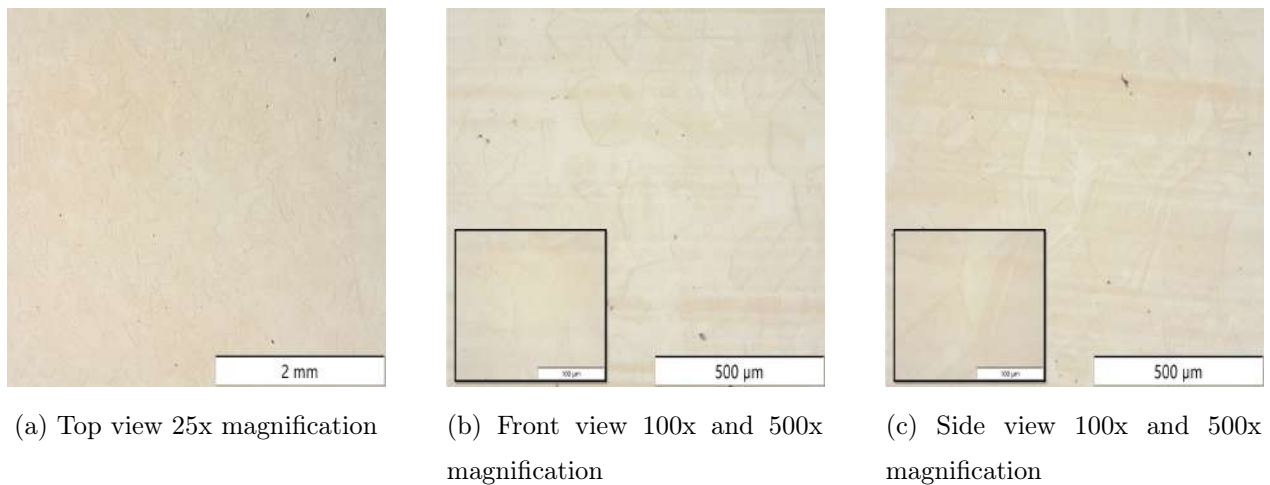


Figure 3.8: Microstructure of material N. 1.4562 (Alloy31)

Fig. 3.8a shows the microstructure of the material N 1.4562 from the top view at 25x magnification while Fig. 3.8b, 3.8c display the microstructure from the other two views at 100x and 500x magnifications. It shows austenitic grains.

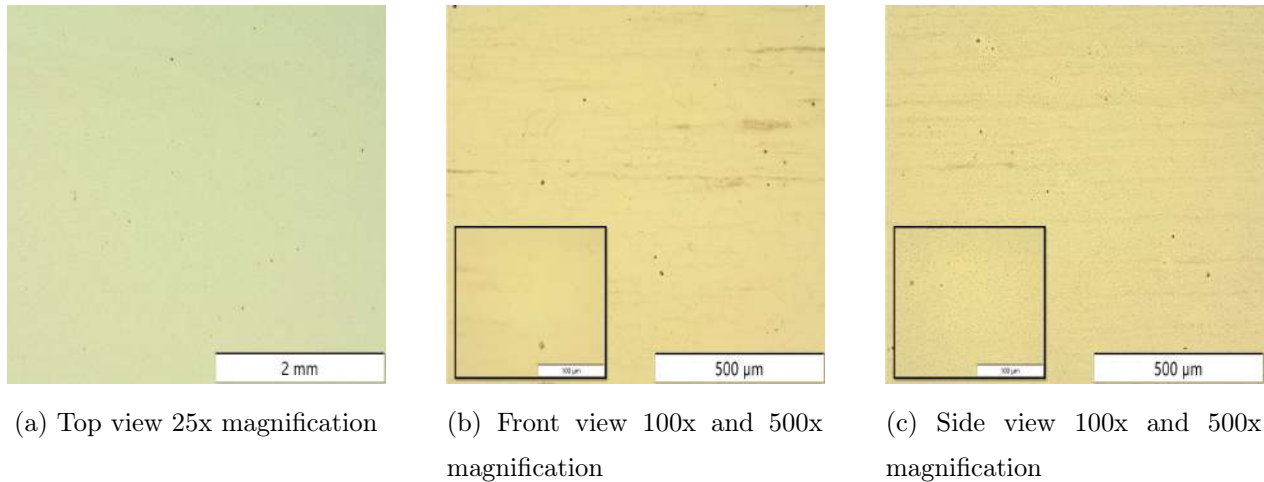


Figure 3.9: Microstructure of material P569

Fig. 3.9a shows the microstructure of the material P569 from the top view at 25x magnification while Fig. 3.9b, 3.9c display the microstructure from the other two views at 100x and 500x magnifications. It shows fine austenitic grains.

3.2 Corrosion test

To determine the behavior of the alloys examined at various pH values present at ReOil plant, potentiodynamic measurements and autoclave tests were conducted for each investigated material at different set conditions.

3.2.1 Potentiodynamic measurement

Potentiodynamic tests are performed on parallelepiped specimens (size: 40mm x 15mm x 3mm) with rounded edges in a corrosion cell (Fig. 3.10). The specimens are fully immersed in the solution along with the contact area (Pt contact).

The solutions performed for the test are shown in Table 3.3.

Table 3.3: Parameters and solutions for the potentiodynamic measurements

Main Composition	Temperature	pH
Acidic Wash	50°C	4
Acidic Wash	90°C	4
Acidic Wash + H ₂ SO ₄	90°C	2
1000 mg/l Cl ⁻ + H ₂ SO ₄	90°C	4
1000 mg/l Cl ⁻ + H ₂ SO ₄	90°C	3
1000 mg/l Cl ⁻ + H ₂ SO ₄	90°C	2
1000 mg/l Cl ⁻ + H ₂ SO ₄	90°C	1
1000 mg/l Cl ⁻ + H ₂ SO ₄	50°C	3
1000 mg/l Cl ⁻ + H ₂ SO ₄	50°C	2
1000 mg/l Cl ⁻ + H ₂ SO ₄	50°C	1
Neutral Wash	50°C	5.5
Neutral Wash	90°C	5.5
Caustic Wash	90°C	10

Before starting the experiment, the samples were ground with abrasive SiC paper ranging from #80 to #500, washed with water and ethanol. After grinding and cleaning procedure, the samples were stored for at least one day in a desiccator to achieve repassivation on the material surface.

Electrochemical measurements were conducted by using a Garmy Reference 600 potentiostat.

A three electrode cell was the implemented to provide the results of the electrochemical tests. In these three electrode system working electrode was the investigated material, saturated calomel electrode (SCE) at a potential of 241 mV_{SHE} was used as a reference electrode, and a Pt sheet severed as a counter electrode.



Figure 3.10: Experimental setup and corrosion cell used to perform potentiodynamic tests

The solution was purged with CO_2 before the test in order to remove free oxygen from the solution. The purging was continued during the whole time of the measurement. To accomplish the desired testing temperature, the solution was heated for 35 minutes before starting the measurement. In addition, heating the solution is used to eliminate the volatile organic compounds and to generate a homogenic composition of the solution. The temperature was kept constant in the system by using the Lauda E4G thermostat. The open circuit potential (OCP) was measured for one hour before starting the potentiodynamic test to investigate the potential equilibrium between the solution and the sample. For the potentiodynamic measurements, the starting potential was set to 100 mV below OCP, the scan rate was 200 mV/h. After reaching the potential of 2 V_{SCE} or the current density of 1 mA/cm^2 , the scan was reversed. Finally, the test finished when the behaviour of the sample came back to the cathodic polarization regime.

3.2.2 Immersion test

Immersion test we are performed with specimen size 10 x 7 x 3mm in a flask inside of a testing cell (Fig. 3.11). The solutions performed for the test are shown in the Table 3.4.

Table 3.4: Parameters and solutions for the immersion test

Main Composition	Temperature	pH
1000 mg/l $\text{Cl}^- + \text{H}_2\text{SO}_4$	90°C	4
1000 mg/l $\text{Cl}^- + \text{H}_2\text{SO}_4$	90°C	3
1000 mg/l $\text{Cl}^- + \text{H}_2\text{SO}_4$	90°C	2
1000 mg/l $\text{Cl}^- + \text{H}_2\text{SO}_4$	90°C	1
1000 mg/l $\text{Cl}^- + \text{H}_2\text{SO}_4$	50°C	4
1000 mg/l $\text{Cl}^- + \text{H}_2\text{SO}_4$	50°C	3
1000 mg/l $\text{Cl}^- + \text{H}_2\text{SO}_4$	50°C	2
1000 mg/l $\text{Cl}^- + \text{H}_2\text{SO}_4$	50°C	1

Before starting the experiment, the samples were ground with #240 abrasive SiC paper, washed with water and ethanol. After the grinding and cleaning procedures, the sample were stored for at least one day in a desiccator to achieve repassivation on the material surface. The specimens were weighed and fully immersed in 50 ml of the solution and the flasks were put in the testing cell at a constant temperature for 72 hours. The temperature was maintained constant by the Lauda E4G thermostat.



Figure 3.11: Testing cell and flask with specimen for immersion test

At the end of the 72 hours, the samples were taken out of the solution, dried, weighed to calculate the mass lost, and checked with the stereoscope "Olympus SZX12" with the camera "Olympus DP50" to search the presence of pits on the surface.

3.2.3 Autoclave test

The autoclave tests we are performed with small tensile specimens (Fig. 3.12) constantly loaded with a cobalt-base alloy spring and ceramic nuts.



Figure 3.12: Small tensile specimen with spring and nuts for constant load test (CLT)

The test are made in an autoclave made of UNS N06625 (Alloy 625) (Fig. 3.13) with the testing solution inside.



Figure 3.13: Autoclave testing equipment

The solutions performed for the test are shown in the Table 3.5.

Table 3.5: Parameters and solutions for the autoclave test

Main composition	Temperature	pH	Pressure
Acidic Wash	90°C	4	5 Bar
Neutral Wash	90°C	5.5	5 Bar
Caustic Wash	90°C	10	5 Bar
H ₂ SO ₄ ^a	90°C	2	5 Bar
NaOH ^b	170°C	13	5 Bar

^aTotal composition in the Table A.1

^bTotal composition in the Table A.2

Before starting the test, the samples were ground with the #400 abrasive SiC paper to have a good surface finished and washed with ethanol. After the grinding and cleaning procedures, the samples were stored for at least some days in a desiccator to achieve repassivation on the material surface. The samples were loaded with the spring and the nuts at 90% of their yield stress and put into the autoclave. Afterwards, the vessels were evacuated and purged with argon several times to obtain a very low partial pressure of oxygen. After that, the autoclaves were filled with the test solution and, finally, the autoclaves were mounted on the rotating shafts in a heated chamber where they were left for 720 h.

Fig. 3.14 shows the several autoclaves mounted on the rotating shaft.

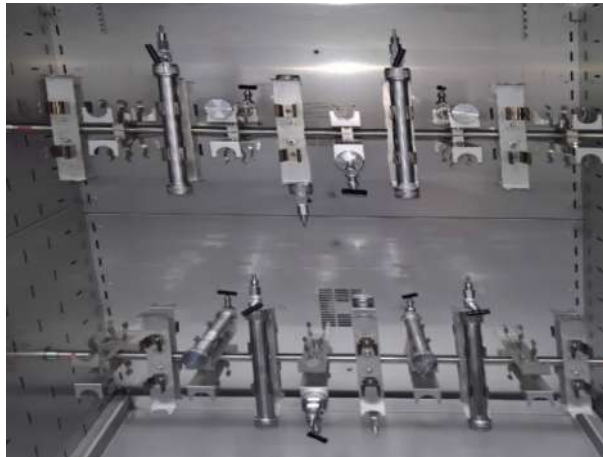


Figure 3.14: Autoclave mounted on the rotating shafts within a heated chamber

4. Results

Results are divided into different sections, one for each type of test performed. The biggest part is about the potentiodynamic measurements because it is the test about all the different material specimens. The immersion test was made only for sample 1.4404 because it is the only one showing uniform corrosion during the potentiodynamic test in an acidic environment and for this reason it was decided to test it in a longer test. The autoclave test was made by Stefan Hönig directly in the OMV research laboratory in Gänserndorf and only the materials 1.4404, 1.4539, 1.4462, 1.4410, Sanicro35 and 2,4819 were tested.

4.1 Potentiodynamic measurement

The principal reason to make the potentiodynamic measurement is to analyse the behavior of stainless steels and nickel alloys as function of temperature, PREN number and pH.

In Fig. 4.1 shows the sum of all the results obtained with this thesis and this proves that by decreasing the pH and/or the PREN number the behavior of shift from the formation of a stable passive layer (green point) to the uniform corrosion (red point) passes through pitting corrosion (yellow point). This figure also shows that the same behaviour occurs when the temperature increases but at higher pH and PREN.

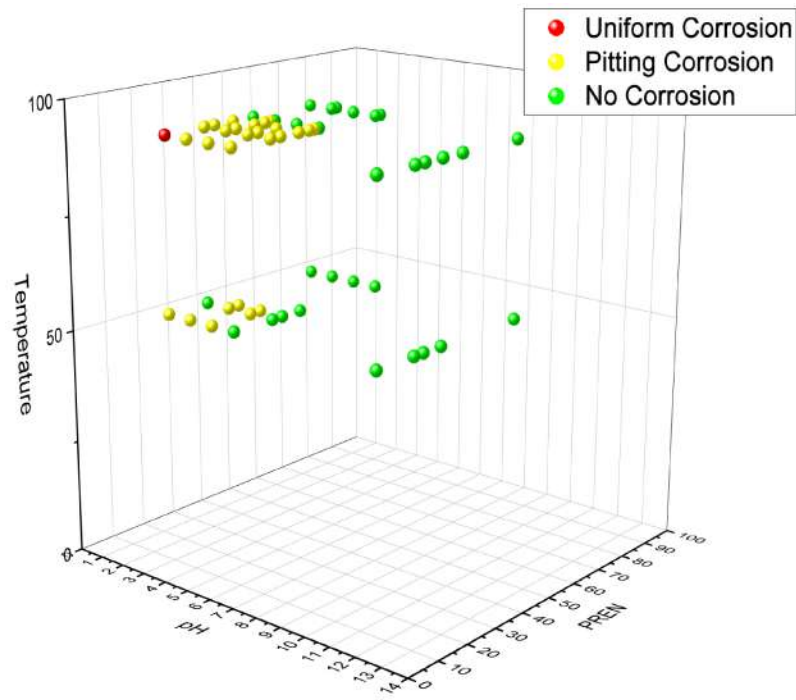


Figure 4.1: Type of result after potentiodynamic tests

The behavior of the materials in different conditions are described and illustrated below. The color in each material in the diagrams represents its PREN number. The higher the PREN number is, the colder the color is (blue/black) while the lower the number is, the hotter the color is (red). The straight line symbolizes the not-welded materials, and the welded materials are represented by the dash dot line. The thickness of the line has a particular meaning in the following diagrams: the thin line represents the samples tested at 50°C whereas the thick line symbolises that the specimen was tested at 90°C.

Fig. 4.2 shows the behavior of the specimens at pH 1.

As shown in the diagram, specimen 1.4404 does not show any passive layer formation because corrosion starts directly after the cathodic zone. Sample 1.4539 has a very small passive layer stability range, but it also shows a very big hysteresis area, which means that in this condition it suffers from pitting corrosion. In addition, the repassivation potential is in the cathodic zone, for this reason it is impossible for the material to have repassivation; this causes a very fast pitting growth. Specimens 1.4462 and 1.4410 have the biggest passive stability zone, both specimens present a hysteresis area but the higher the PREN number is, the smaller the hysteresis is. Both materials

have the repassivation potential on the passive zone. Sanicro35 is the only stainless steel that does not present any hysteresis area, which means that it does not show any corrosion attack in this testing condition. The nickel base alloy 2.4819 is the best material tested in this condition, it has a passive zone closer to the duplex stainless steel but it does not show any hysteresis area, which means that also 2.4819, as Sanicro35, does not show any corrosion attack at pH1 at 90°C with the presence of 1000 mg/l Cl^- in the environment.

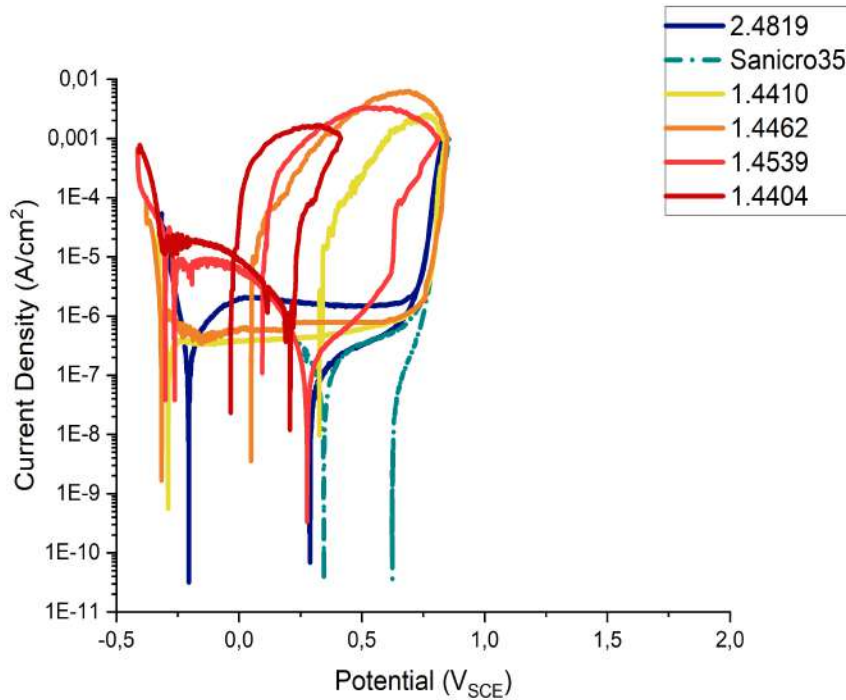
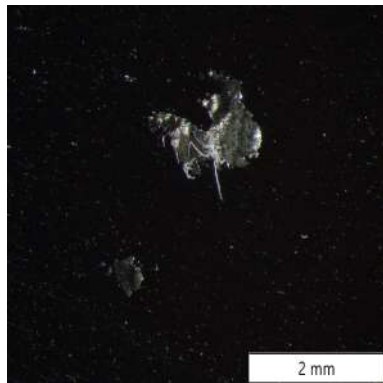


Figure 4.2: Results in the solution 1000 mg/l $\text{Cl}^- + \text{H}_2\text{SO}_4$ at 90°C and pH 1

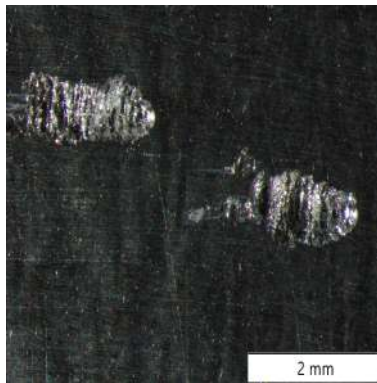
The specimens tested were also investigated with a stereomicroscope. Before that, the specimens were cleaned with 20% of HNO_3 for 10 minutes in an ultrasonic bath and later with deionised water and at the end with ethanol for a few minutes in an ultrasonic bath.

Fig. 4.3 shows the specimens at 40x magnification, after the testing in 1000 mg/l $\text{Cl}^- + \text{H}_2\text{SO}_4$ at 90°C and pH 1. As shown in the Fig. 4.3a, 4.3b, 4.3c and 4.3d stainless steels can show pitting corrosion but increasing the PREN number of steels the pitting dimension decreases. On the contrary, the nickel base alloy does not show any corrosion attack in this very aggressive environment either, as shown in Fig. 4.3f. Sanicro35, as shown in the Fig. 4.3e, is the only steel that does not show any pitting attack. This happens for its very high quantity of alloy elements, that give it a very high

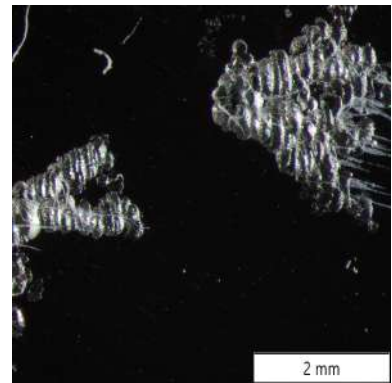
PREN number, over 53.



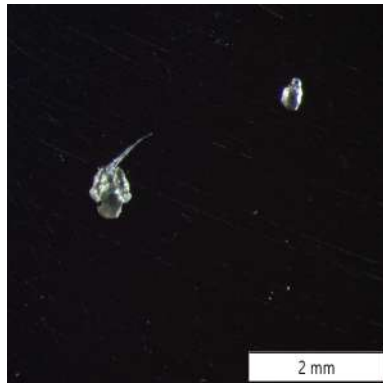
(a) Sample 1.4404 after testing at 40x magnification



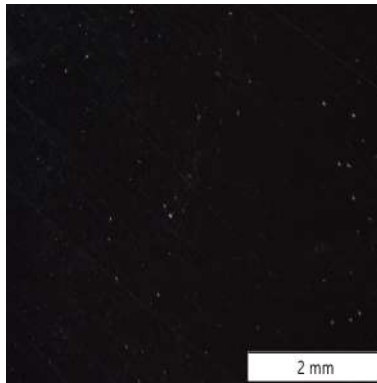
(b) Sample 1.4529 after testing at 40x magnification



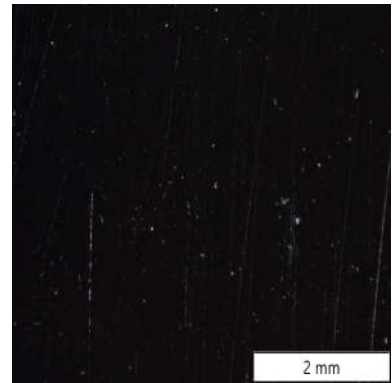
(c) Sample 1.4462 after testing at 40x magnification



(d) Sample 1.4410 after testing at 40x magnification



(e) Sample Sanicro35 after testing at 40x magnification



(f) Sample 2.4819 after testing at 40x magnification

Figure 4.3: Specimens after testing in 1000 mg/l $\text{Cl}^- + \text{H}_2\text{SO}_4$ at 90°C and pH 1

Fig. 4.4 shows the behavior of the different materials at pH 2.

As shown in the diagram, specimens 1.4404 and 1.4539 show a very small passive layer stability range but it also shows a very big hysteresis area, which means that in this condition they suffer from pitting corrosion, and also the repassivation potential is in the cathodic zone. For this reason, it is impossible for the materials to have any repassivation. This causes a pronounced pit growth. Specimens 1.4462 and 1.4410 have the biggest passive stability zone, both specimens present a hysteresis area but the higher the PREN number is, the smaller the hysteresis is, both materials have the repassivation potential in the passive zone. Material 1.4410 shows a very small second passivation zone after 0.8 mV but this passive layer is very weak and for its high current density that second passive layer is not so stable in this condition. Sample P569 shows a first and a second

passive zone like 1.4410 but in this case the current density of the second passive layer is lower. That material shows a small hysteresis area but the repassivation potential is inside the second passive zone. Sanicro35 and sample 1.4562 are the only two stainless steels that do not present any hysteresis area, which means that they do not show any corrosion attack in this testing condition. The nickel base alloys 2.4819 and 2.4605 are the best materials tested in this condition, they have a passive zone closer to the duplex stainless steel but they do not show any hysteresis area, which means these two materials do not show any corrosion attack at pH2 at 90°C with the presence of 1000 mg/l Cl^- in the environment.

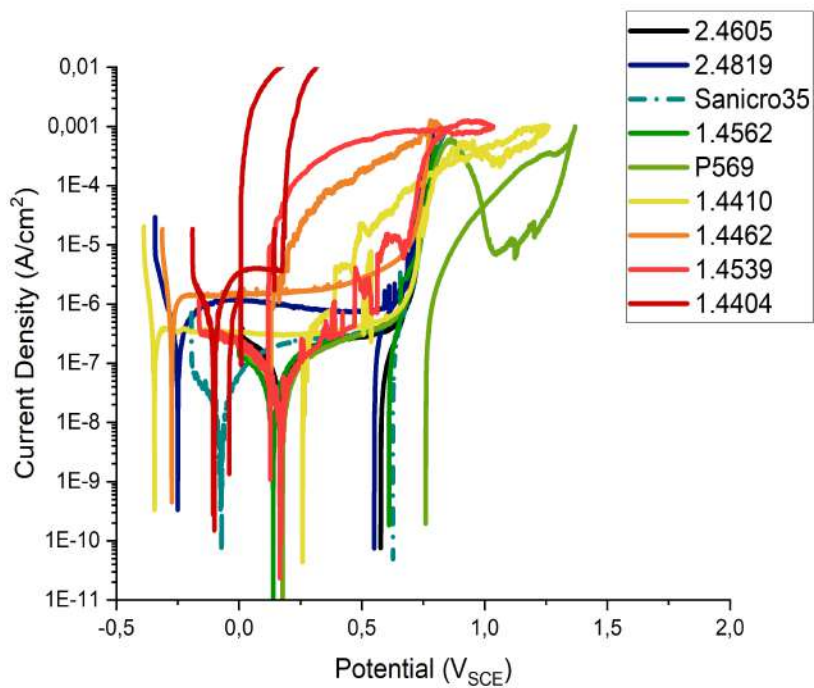
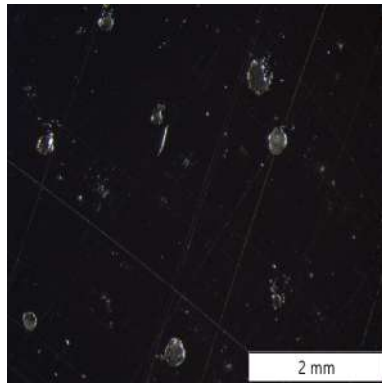


Figure 4.4: Results in the solution 1000 mg/l $\text{Cl}^- + \text{H}_2\text{SO}_4$ at 90°C and pH 2

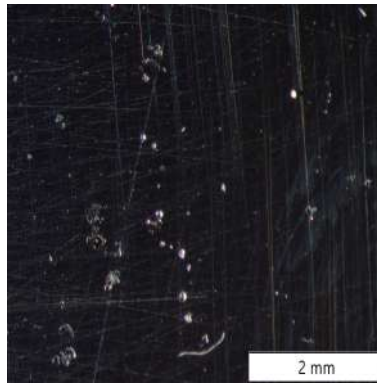
After the potentiodynamic test at pH 2 a group of specimens were selected to be investigated with a stereomicroscope. Before the stereomicroscope, the specimens were cleaned with 20% of HNO_3 for 10 minutes in an ultrasonic bath and after with deionized water and finally with ethanol for a few minutes in an ultrasonic bath as the specimens tested at pH 1.

Fig. 4.5 4.5 shows specimens at 40x magnification, after the testing 1000 mg/l $\text{Cl}^- + \text{H}_2\text{SO}_4$ at 90°C and pH 2. As is showed in the Fig. 4.5a, 4.5b, 4.5c and 4.5d, stainless steels show pitting corrosion but by increasing the PREN number of the steels the pitting dimension decreases up to

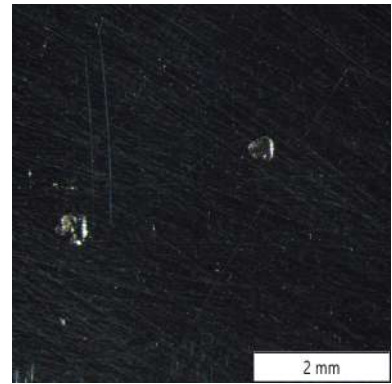
reach Sanicro35, where there is no presence of any pit. On the contrary, the nickel base alloys do not show any corrosion attack as shown by Fig. 4.5e 4.5f.



(a) Sample 1.4404 after testing at 40x magnification



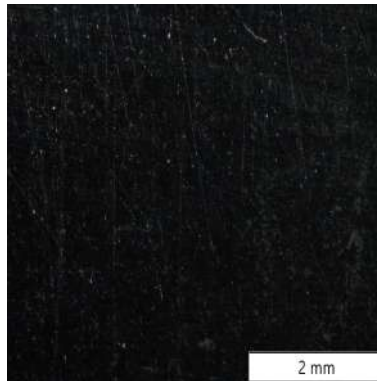
(b) Sample 1.4539 after testing at 40x magnification



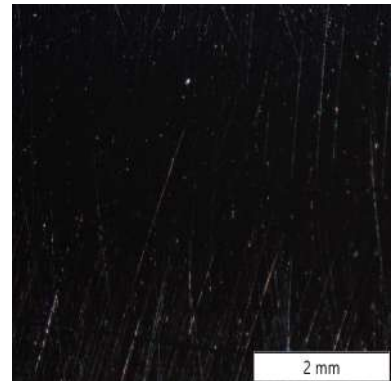
(c) Sample 1.4462 after testing at 40x magnification



(d) Sample P596 after testing at 40x magnification



(e) Sample 2.4819 after testing at 40x magnification



(f) Sample 2.4605 after testing at 40x magnification

Figure 4.5: Specimens after testing in 1000 mg/l $\text{Cl}^- + \text{H}_2\text{SO}_4$ at 90°C and pH 2

Fig. 4.6 shows the behavior at pH 3.

As shown in the diagram, specimens 1.4404 and 1.4539 have a small passive layer stability range but it also shows a very big hysteresis area, which means that in this condition it suffers from pitting corrosion and also the repassivation potential is in the passive zone. Specimens 1.4462 and 1.4410 have the biggest passive stability zone, both specimens present a hysteresis area but the higher the PREN number is, the smaller the hysteresis is, both show a small second passive zone and have the repassivation potential on the first passive zone. Sanicro35 is the only stainless steel that does not present any hysteresis area and also a second passive zone. The nickel base alloy 2.4819 is the best material tested in this condition, it has a passive zone closer to the duplex stainless steel but it does

not show any hysteresis area, which means that specimen 2.4819, like Sanicro35, does not show any corrosion attack at pH3 at 90°C with the presence of 1000 mg/l Cl^- in the environment.

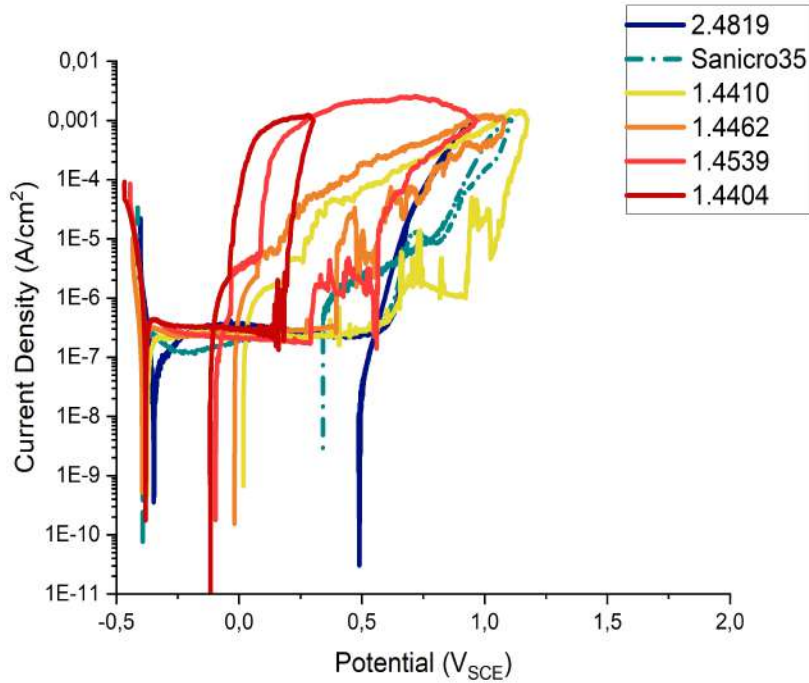
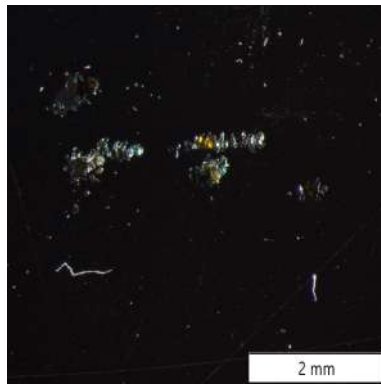


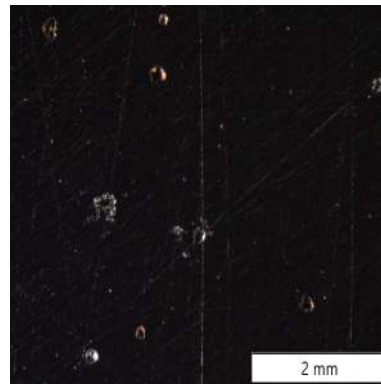
Figure 4.6: Results in the solution 1000 mg/l $\text{Cl}^- + \text{H}_2\text{SO}_4$ at 90°C and pH 3

Also in this case 4 specimens were chosen to be investigated with the stereomicroscope. The specimens were cleaned with 20% of HNO_3 for 10 minutes in an ultrasonic bath and after with ethanol and deionised water for a few minutes in an ultrasonic bath.

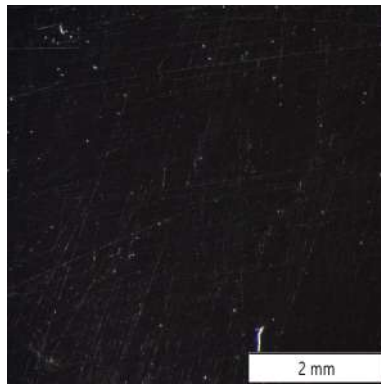
Fig. 4.7 shows the specimens at 40x magnification, after the testing in 1000 mg/l $\text{Cl}^- + \text{H}_2\text{SO}_4$ at 90°C and pH 3. As shown in Fig. 4.7a and 4.7b stainless steels show pitting corrosion but increasing the PREN number of steels the pitting dimension decreases until to reach Sanicro35 (4.7c), where there is no presence of any pit. On the contrary, the nickel base alloy does not show any corrosion attack as shown in Fig. 4.7d.



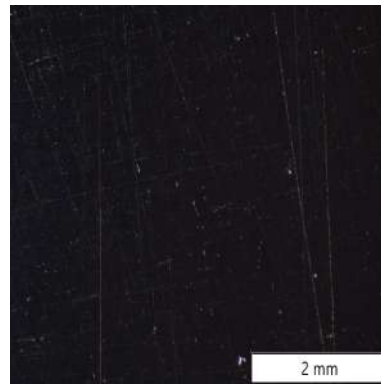
(a) Sample 1.4539 after testing at 40x magnification



(b) Sample 1.4410 after testing at 40x magnification



(c) Sample Sanicro35 after testing at 40x magnification



(d) Sample 2.4819 after testing at 40x magnification

Figure 4.7: Specimens after testing in 1000 mg/l $\text{Cl}^- + \text{H}_2\text{SO}_4$ at 90°C and pH 3

The Fig. 4.8 shows the behavior of the different material at pH 4.

As shown in the diagram, specimens 1.4404 and 1.4539 show a big passive layer stability range but They also show a very big hysteresis area, which means that in this condition they suffer from pitting corrosion but the repassivation potential is in the passive zone. Specimen 1.4462 has a big first passive stability zone and a small second passive. This specimen presents a hysteresis area and it has the repassivation potential on the first passive zone. Samples 1.4410, P569 and 1.4562 show a first and a second passive zone and a hysteresis area but for sample 1.4410 the repassivation potential is in the first passive zone. On the contrary, for the other two samples the repassivation potential is in the second passive zone. Sanicro35 is the only stainless steel that still presents a second passive zone, but it does not present any hysteresis area, which means that it does not show any corrosion attack in this testing condition. The nickel base alloys 2.4819 and 2.4605 have only the first passive

zone, but do not show any hysteresis area, which means that these two materials do not show any corrosion attack at pH4 at 90°C with the presence of 1000 mg/l Cl^- in the environment.

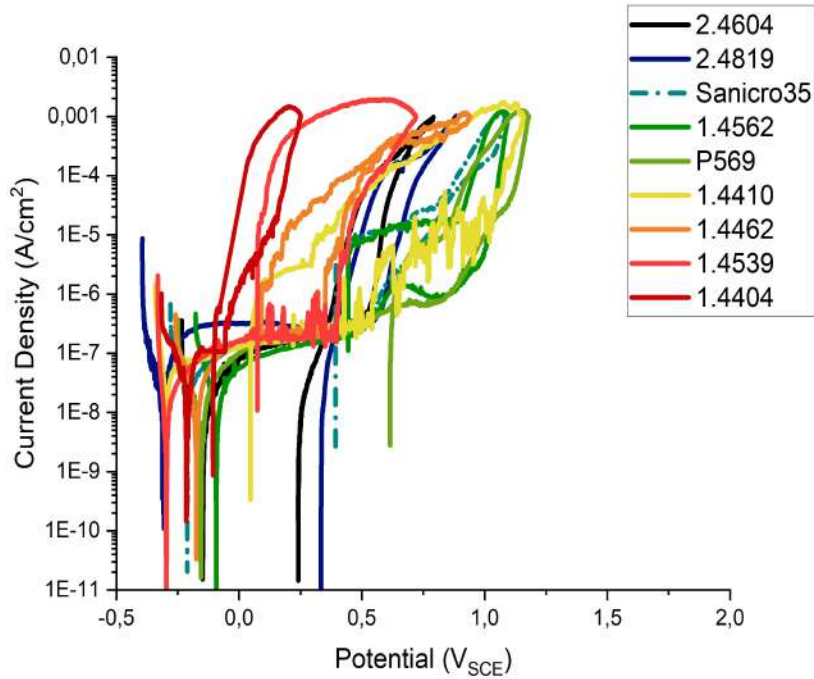
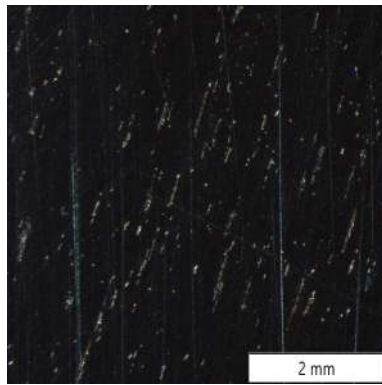


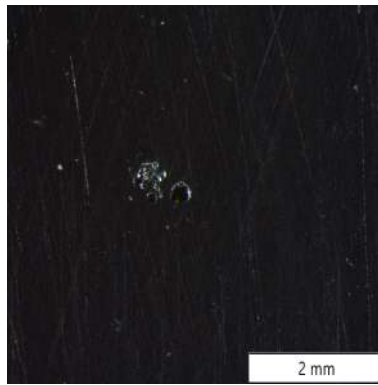
Figure 4.8: Results in the solution 1000 mg/l $\text{Cl}^- + \text{H}_2\text{SO}_4$ at 90°C and pH 4

After the measurement some specimens were cleaned with 20% of HNO_3 for 10 minutes in an ultrasonic bath, with deionised water and at the end with ethanol for a few minutes in an ultrasonic bath. After the cleaning process they were investigated with a stereomicroscope.

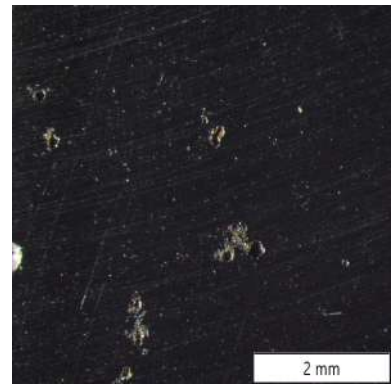
In Fig. 4.9 shows the specimens at 40x magnification, after the test in 1000 mg/l $\text{Cl}^- + \text{H}_2\text{SO}_4$ at 90°C and pH 4. As shown in Fig. 4.9a, 4.9b, 4.9c, 4.9d and 4.9e stainless steels show pitting corrosion but by increasing the PREN number of steels the pitting dimension decreases up to reach Sanicro35, where there is no presence of any pit. On the contrary, the nickel base alloys do not show any corrosion attack as shown by Fig. 4.9f.



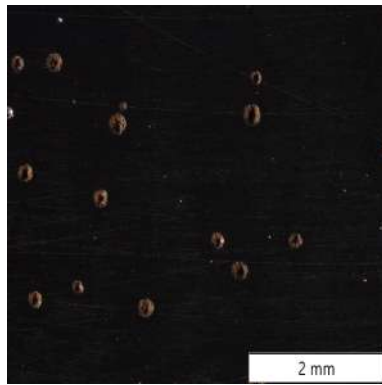
(a) Sample 1.4404 after testing at 40x magnification



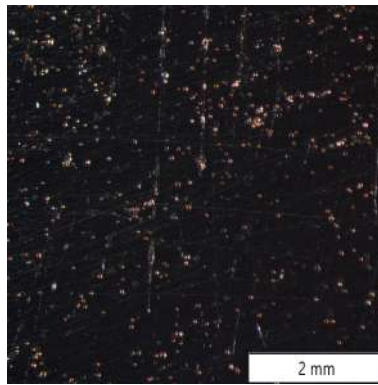
(b) Sample 1.4539 after testing at 40x magnification



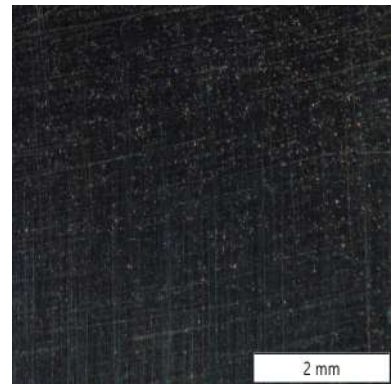
(c) Sample 1.4410 after testing at 40x magnification



(d) Sample P596 after testing at 40x magnification



(e) Sample 1.4562 after testing at 40x magnification



(f) Sample 2.4605 after testing at 40x magnification

Figure 4.9: Specimens after testing in 1000 mg/l $\text{Cl}^- + \text{H}_2\text{SO}_4$ at 90°C and pH 4

Fig. 4.10 shows the behavior of different materials welded and not-welded in Acidic Wash at 90°C. As shown in the diagram, specimens 1.4404 welded and not-welded are the only two with a different behavior because the not-welded sample does not present any hysteresis area while the welded sample shows a very big hysteresis area, which means that the welded is the critical point for this material in this condition. Both specimens 1.4462 welded and not-welded show a second passive zone as the two 1.4404 but in this case the welded and not-welded samples have the same behavior, none of them has a hysteresis area. The nickel base alloy 2.4819 has only the first passive zone but it does not show any hysteresis area.

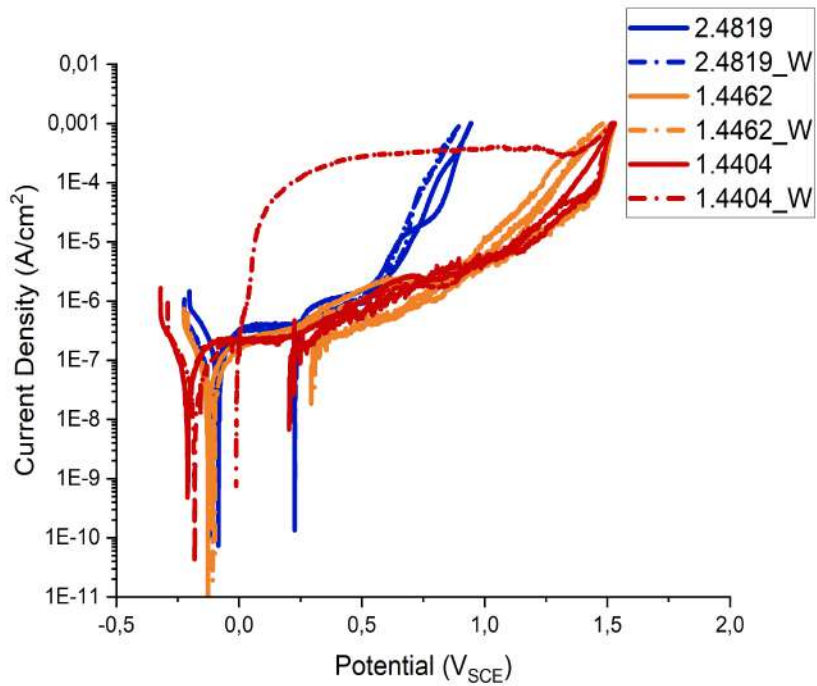


Figure 4.10: Results in the solution Acidic Wash at 90°C and pH 4

Fig. 4.11 shows the behavior of the different materials welded and not-welded, in Acidic Wash at 50°C.

There is no difference of behavior between welded and not-welded specimens, all the specimens do not show any hysteresis area. The latter is the presence of two groups of materials, nickel base alloys and stainless steels. The former group shows only a first passive zone while steels show also a second passive zone. The second passive layer is caused by the passivization of iron, which is present in high quantity in steel but not enough in nickel alloys.

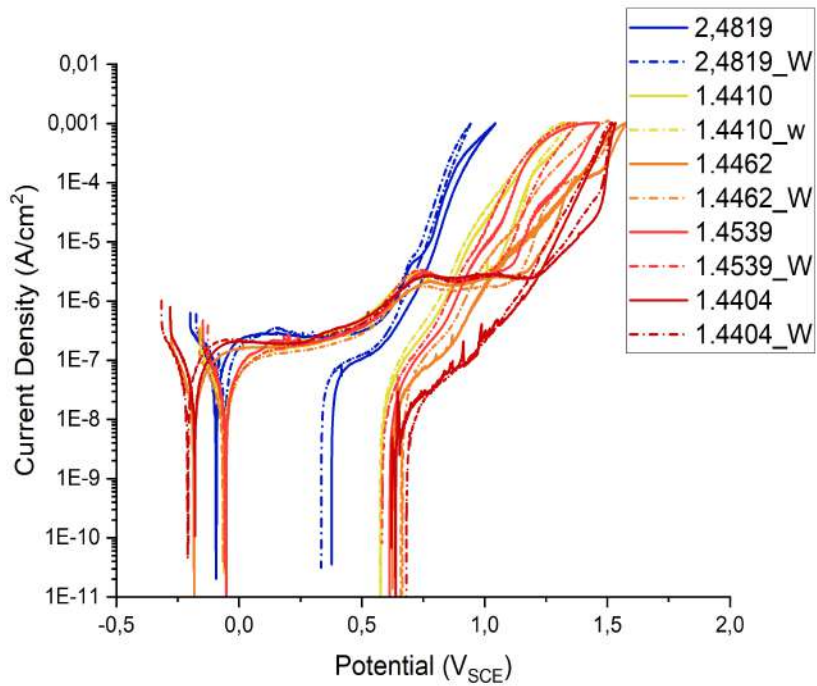


Figure 4.11: Results in the solution Acidic Wash at 50°C and pH 4

The Fig. 4.12 shows the behavior of the different materials in Neutral Wash at 90°C.

As shown in the diagram, specimen 1.4404 presents a first and a second passive zone but this passive layer is very weak and due to its high current density the second passive layer is not so stable in this condition. Specimens 1.4539, 1.4462 and 1.4410 show two big passive zones, one at a lower current density caused by chromium and the second one after 0.7 mV caused by the iron passivization. All stainless steels show a hysteresis area in these conditions. The nickel alloy sample 2.4819 shows only one passive zone but it is the only sample that does not show any hysteresis.

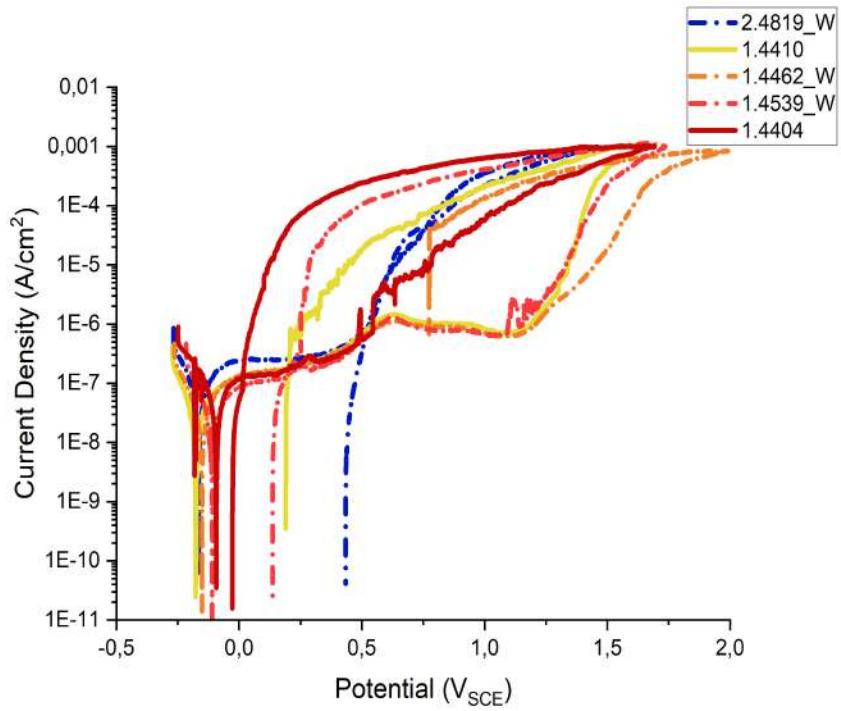


Figure 4.12: Results in the solution Neutral Wash at 90°C and pH 5,5

Fig. 4.13 shows the behavior of different materials welded and not-welded in Neutral Wash at 50°C. This graph shows that in this condition there is no difference of behavior of the specimens 1.4462 welded and not-welded, both have a first and second passive zone with the repassivation potential on the second passivization. Specimens 1.4404, 1.4539 and 1.4410 show a first and second passive zone and all three have the repassivation potential in the first passive zone. All stainless steels show a hysteresis area. On the contrary, in this condition the nickel alloy is the only one that does not show any hysteresis area but it has only the first passive zone.

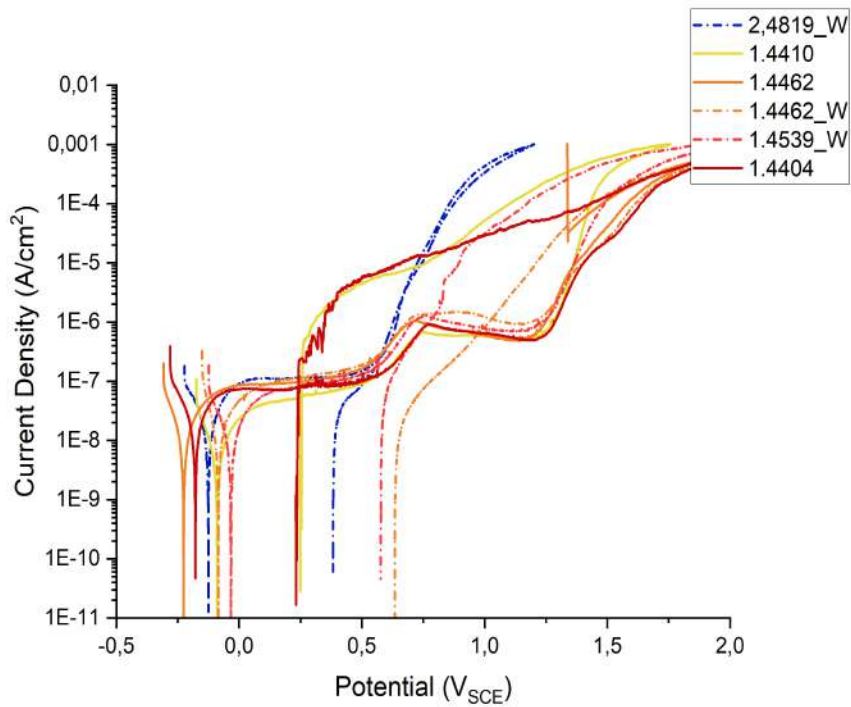


Figure 4.13: Results in the solution Neutral Wash at 50°C and pH 5,5

Fig. 4.14 shows the behavior of the specimens in Caustic Wash.

As shown, none of the materials tested reveals any corrosion attack in this condition. This happened because in alkaline pH the presence of iron is sufficient to have the formation of a passive layer. The only disadvantage of this layer is that it is present at a higher current density than the chromium passive layer.

This is the only condition tested in this thesis where stainless steels show a better behavior than the nickel base alloy. That situation is caused by the low quantity of iron in specimen 2.4819 which makes a thinner passive layer than in steel. This is also shown by Sanicro35, which due to its low quantity of iron and a very high quantity of alloy elements in this condition has a worse behavior than other stainless steels.

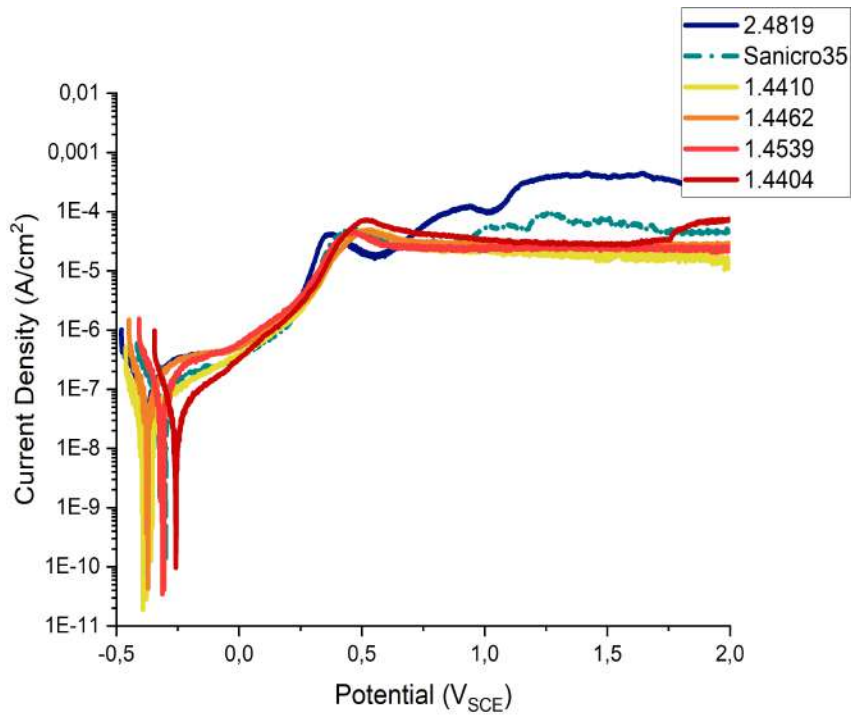
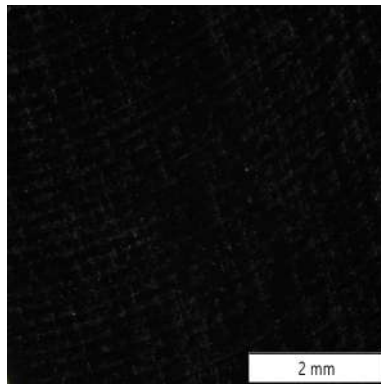


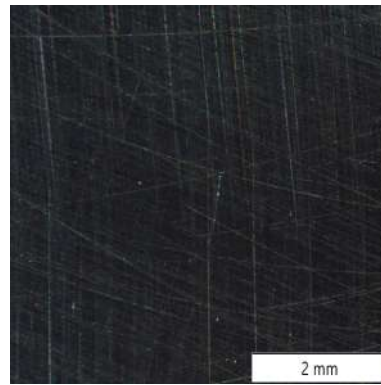
Figure 4.14: Results in the solution Caustic Wash at 90°C and pH 10

Some specimens were selected to be investigated with a stereomicroscope. The specimens were cleaned with ethanol, with 20% of HNO₃ for 10 minutes in an ultrasonic bath, another time with ethanol and finally with deionised water for a few minutes in an ultrasonic bath.

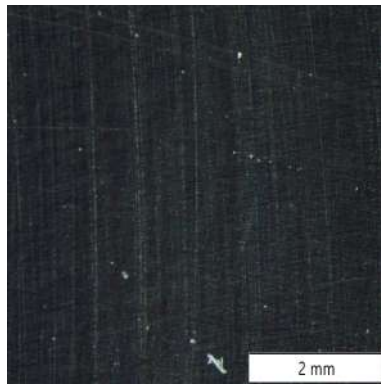
Fig. 4.15 shows the specimens at 40x magnification, after testing in Caustic Wash at 90°C. As is showed in Fig. 4.15a, 4.15b and 4.15c stainless steels do not show any corrosion attack. On the contrary, in the nickel base alloy there is the presence of some corrosion products as shown by Fig. 4.15d.



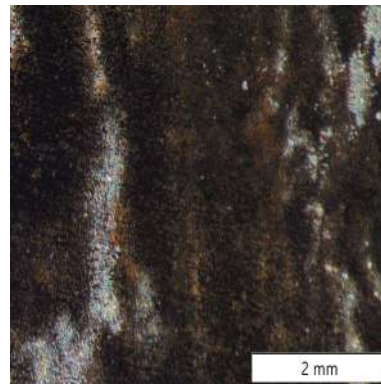
(a) Sample 1.4404 after testing at 40x magnification



(b) Sample 1.4539 after testing at 40x magnification



(c) Sample Sanicro35 after testing at 40x magnification



(d) Sample 2.4819 after testing at 40x magnification

Figure 4.15: Specimens after testing in Caustic Wash at 90°C

4.2 Immersion test

The immersion test showed that specimen 1.4404 is not able to form a passive layer on its surface at 90°C, which is showed by its strong mass loss, illustrated in Fig. 4.16 and for the presence of uniform corrosion shown in Fig. 4.18a.

As shown in the following diagram (Fig. 4.16), there is a relevant mass loss only at pH1, the small mass changes in the other pH are principally caused by the sensibility of the instrument used for the measure. At pH 1 there is a big difference between the result at 50°C and 90°C. This is explained by Fig. 4.17a and 4.18a, because at 90°C there is the presence of uniform corrosion and at 50°C there is only pitting corrosion.

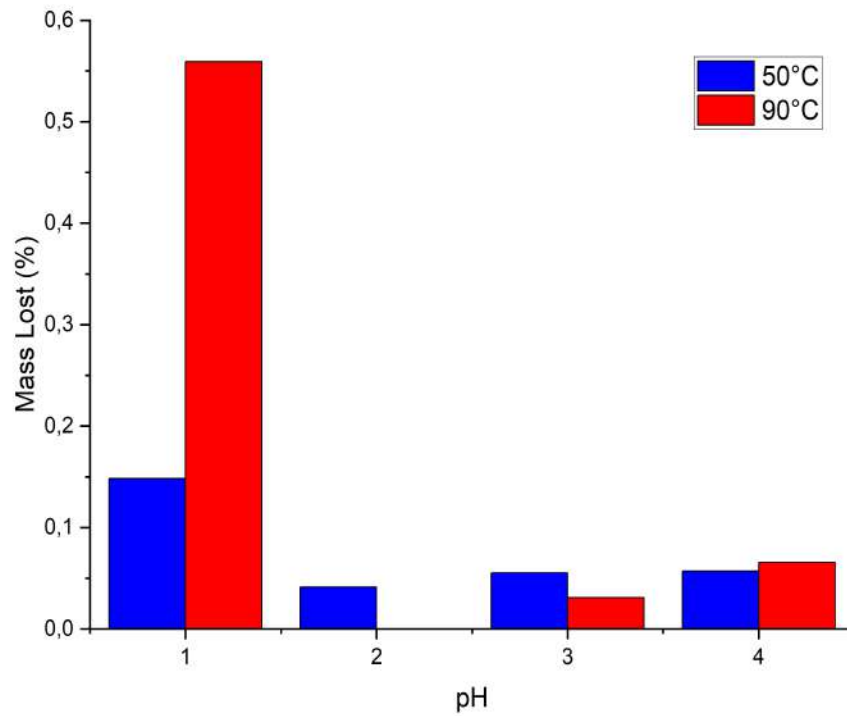


Figure 4.16: Mass lost immersion test

Fig. 4.17 shows the specimens at 63x magnification after the immersion test at 50°C. Specimen 1.4404 suffers from pitting corrosion at pH 1, 2 and 3 as shown in Fig. 4.17a, 4.17b and 4.17c, but at pH 4 there is no visible corrosion attack as shown in Fig. 4.17d.

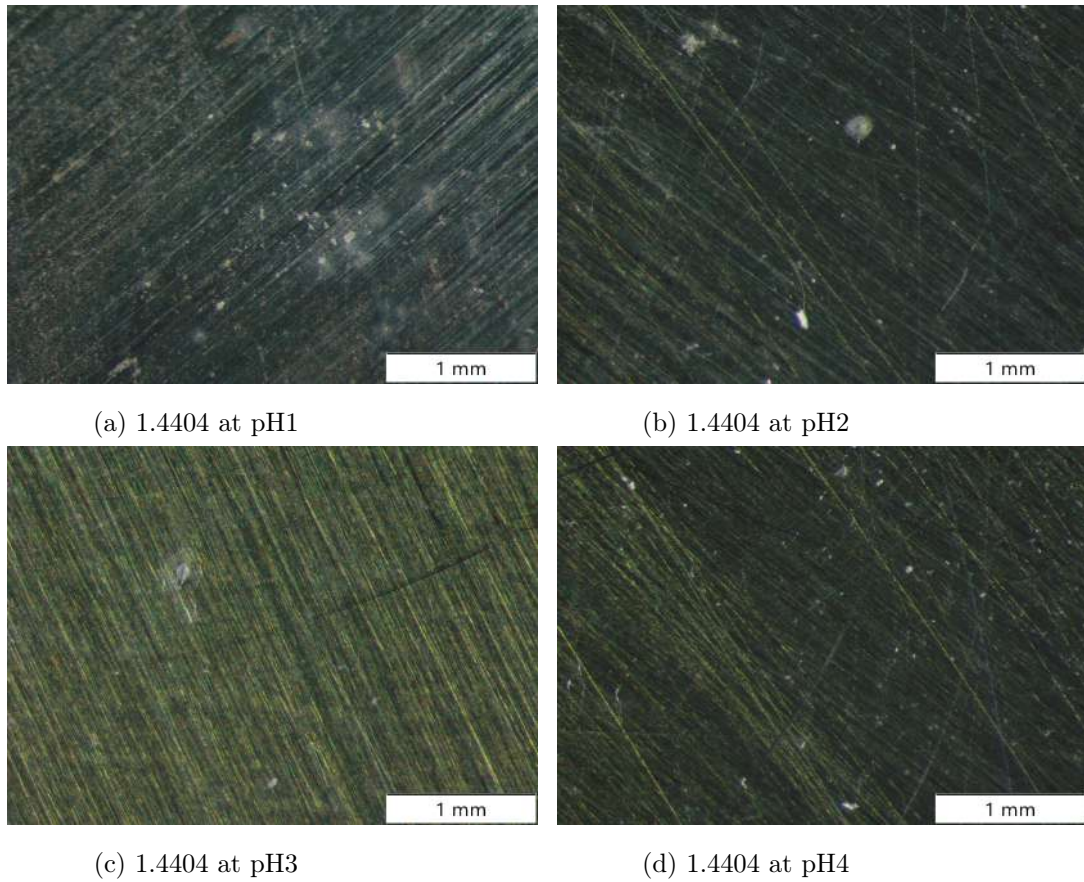


Figure 4.17: Samples 1.4404 63x magnification after the immersion test at 50°C

Fig. 4.18 shows the specimens at 63x magnification after the immersion test at 90°C. As shown in Fig. 4.18a in the solution at pH1, specimen 1.4404 suffers from uniform corrosion, whereas at pH from 2 to 4 it suffers from pitting corrosion as shown in Fig. 4.18b, 4.18c and 4.18d.

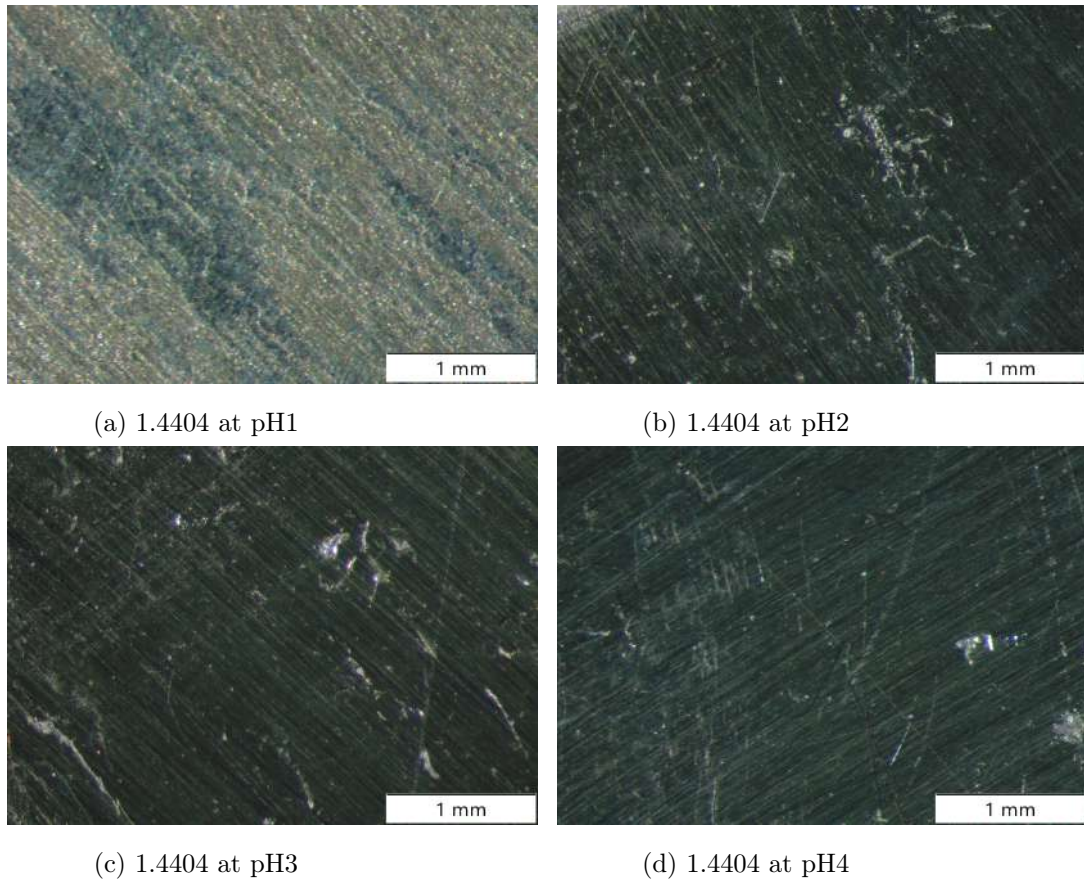


Figure 4.18: Samples 1.4404 63x magnification after the immersion test at 90°C

4.3 Autoclave test

None of the specimens which were loaded at 90% of the yield stress (YS) broke within the condition tested in the autoclaves, as illustrated in Table 4.1 and in Fig. 4.19. In general, no relevant fracture occurred in any of the specimens within 720h, regardless of the pH, temperature, and the condition applied.

Table 4.1: Total results of the autoclave test

Material	Time to Failure (h)				
	Acidic wash	Neutral wash	Caustic wash	H ₂ SO ₄	NaOH
1.4404	>720	>720	>720	>720	>720
1.4539	>720	>720	>720	>720	>720
1.4462	>720	>720	>720	>720	>720
1.441	>720	>720	>720	>720	>720
2.4819	>720	>720	>720	>720	>720
Sanicro35	>720	>720	>720	>720	>720

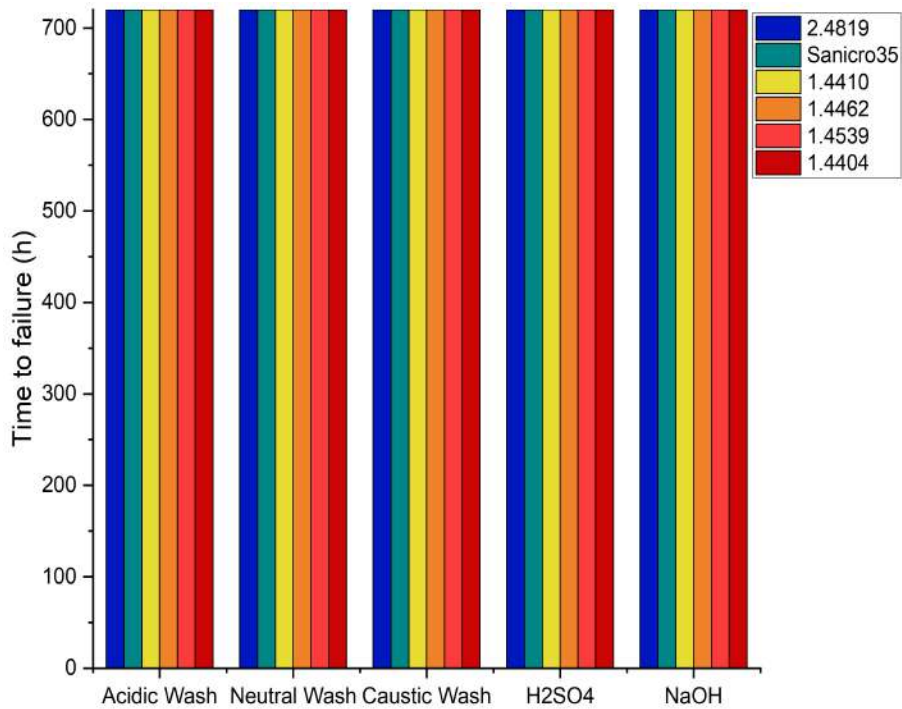


Figure 4.19: Total results of the autoclave test

Besides, no apparent cracks were seen in any unbroken specimens. All the tested specimens were investigated with the stereomicroscope after be cleaned with ethanol and deionised water for a few minutes in an ultrasonic bath.

Fig. 4.20 shows four specimens at 20x magnification, after the autoclave test. As is showed in Fig. 4.20a, 4.20b and 4.20c, different stainless steel do not have any visible corrosion attack after being

loaded at 90% of the YS for 30 days (720h) in different solutions. This is the same for the Nickel alloy as shown in Fig. 4.20d.

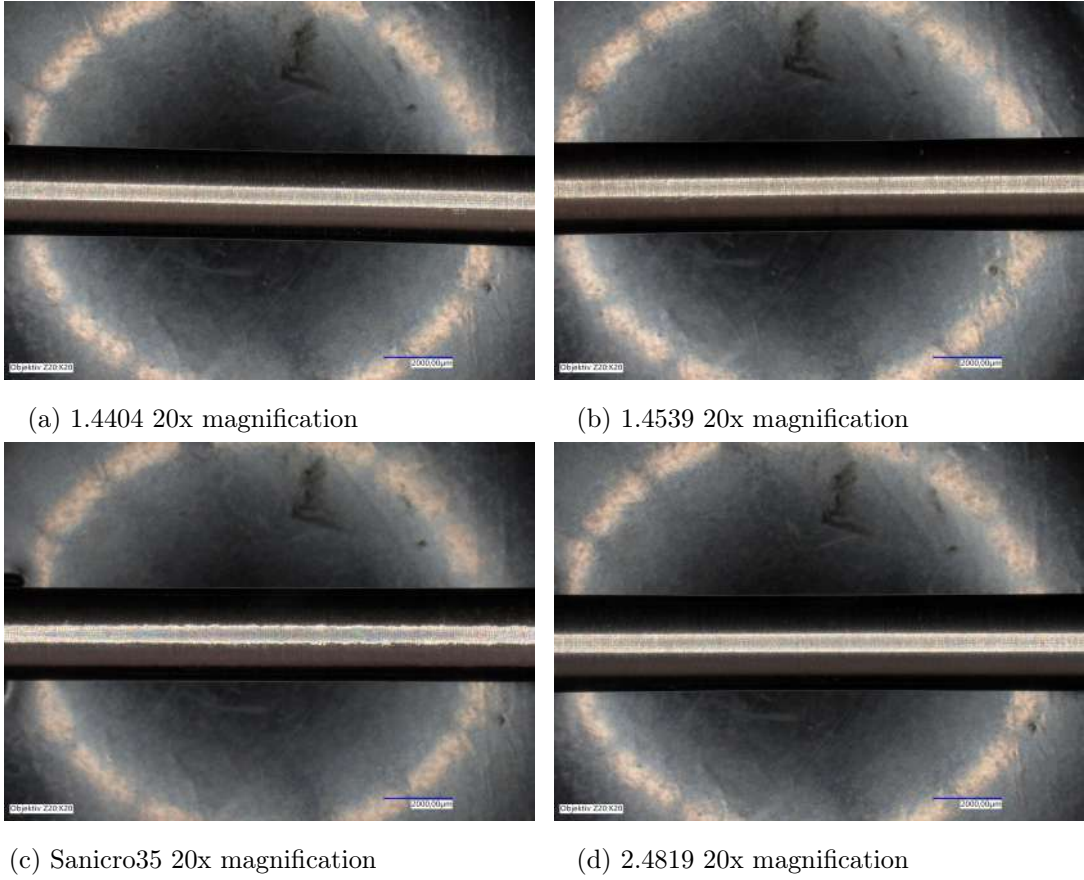


Figure 4.20: Visual appearance of some specimens after the autoclave test

5. Discussion

5.1 Impact of Inhibitor and Chloride content

The presence of inhibitor, as organic compound, decreases the aggressivity of the corrosion environment. In contrary the presence of chloride increases the aggressivity of the environment and caused the pitting corrosion.

At the same pH and temperature of the environment, changing the electrolyte from OMV to artificial acidic wash changes the behaviour of the specimens significantly, as is shown in Fig. 5.1 and Fig. 5.2, where the delivered solution with the presence of inhibitors and low chloride (gold line) show a more stable behaviour than the artificial solution without any inhibitor and with 1000 mg/l of chloride (light blue line).

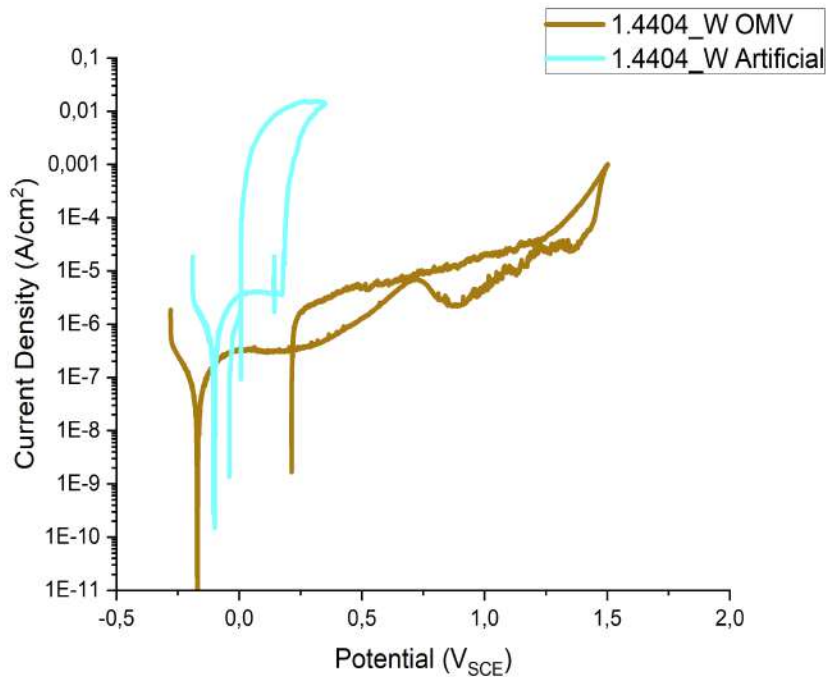


Figure 5.1: Different behavior of the specimens 1.4410 at 90°C at pH 2 between the OMV Acidic Wash and Artificial solution 1000 mg/l $\text{Cl}^- + \text{H}_2\text{SO}_4$

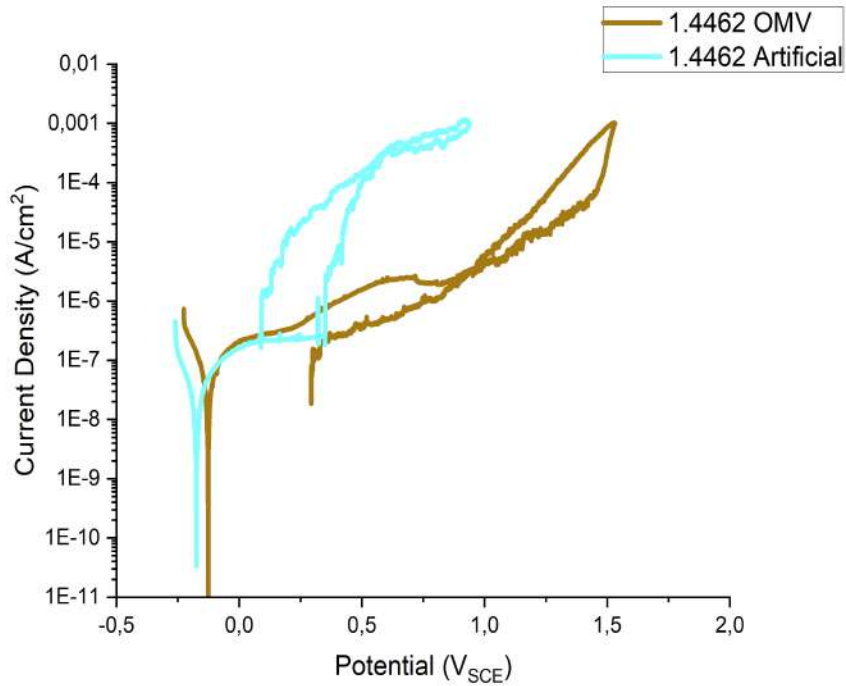


Figure 5.2: Different behavior of the specimens 1.4462 at 90°C at pH 4 between the OMV Acidic Wash and Artificial solution 1000 mg/l $\text{Cl}^- + \text{H}_2\text{SO}_4$

5.2 Impact of Temperature

The tests showed the relation between the behavior of the specimens and the temperature of the corrosive environment.

At the same pH and same chemical composition of the environment, by decreasing the temperature there is a decreasing current density and an increasing stability potential range of the passive layer. The temperature is also a very important parameter to the general behavior of the specimens because, as shown in Fig. 5.3, by changing the temperature there is strengthener from the uniform corrosion (red line) to the formation of a passive layer (blue line). Temperature is very important also for pitting corrosion, the critical pitting temperature (CPT) is the parameter that controls the formation of pitting or not-pitting. If the temperature is lower than the CPT, the aggressive environment is not able to break the passive layer and for this reason no pitting corrosion will be initiated.

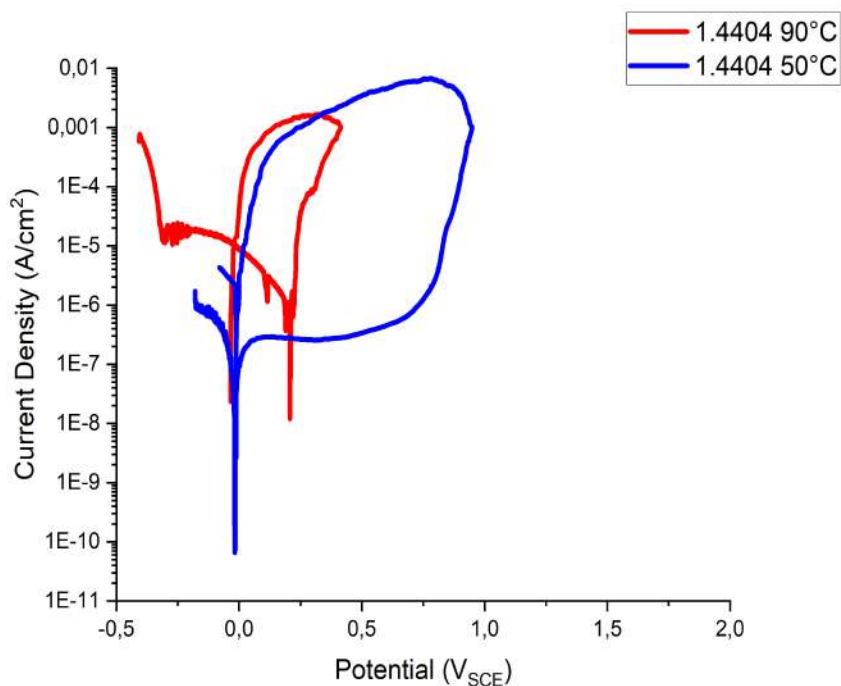


Figure 5.3: Behavior of the specimens 1.4404 at pH 1 at the variation of the temperature

5.3 Impact of pH

The results of the tests for the different materials show that there is a very strong correlation between the behavior of the sample in the environmental condition and the pH of the environment.

Changing the pH from an acidic ($\text{pH} < 6$) to a neutral ($6 < \text{pH} < 8$) and alkaline ($\text{pH} > 8$) environment changes the behavior of the specimen as shown in Fig. 4.10 and 4.14.

Also smaller variations of the pH in the solution can cause a change in the behavior of the materials. By increasing the pH there is a decreasing current density through the passive layer and at the same time it can cause an increasing stability range of the passive layer.

It is also possible for some alloys that a small change of the pH permits the formation of a secondary passive layer. This is all shown in Fig. 5.4 where the shift of the color from magenta to yellow of the I-U curves symbolizes the increase of the pH.

For all these reasons the pH is one of the most important parameters to determinate whether an environment is more or less aggressive than another one. The pH can also determinate the solubility of the corrosion products. This characteristic is shown for every element in the Pourbaix diagram.

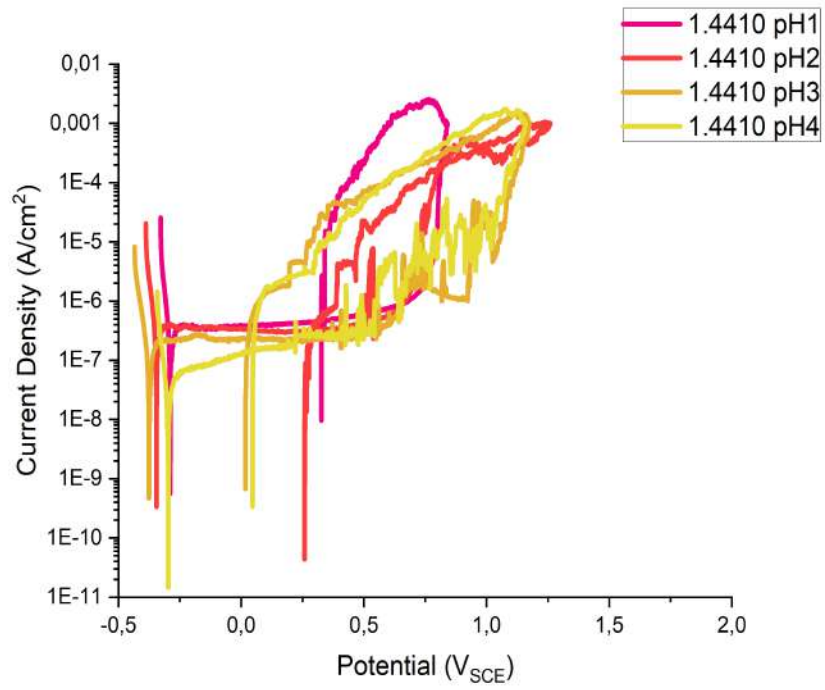


Figure 5.4: Behavior of material 1.4410 at 90°C at different pH values

6. Conclusion

The analysis has shown the different behavior of the different alloys in the different environments. Increasing the PREN number of the alloy there is an increase of corrosion resistance. At the same time decreasing the pH of the environment increases the aggressivity of the solution and the same effect is shown by the increase of the environment temperature.

The stainless steels have a very good resistance in alkaline environments, a good resistance in neutral environments, and bad resistance in acidic environments.

The nickel alloys have a very good resistance in acidic and neutral environments and a good resistance in alkaline environments.

The Sanicro 35 has a very good resistance in alkaline, neutral and acidic environments.

The delivered solutions from the OMV caused a lot of problems during the measurement period, because they were degradable with time and there was the change of the pH value from the moment when the solution arrived, when the test was done and when the test was finished, for this reason it was decided to use artificial solutions with the composition planned by OMV.

All the specimens pass the autoclave test without showing any corrosion attack in all the test solutions.

The other two test gave interesting result: the immersion test showed the corrosion of the austenitic steel 1.4404 at different pH at the open circuit potential for 3 days, and the potentiodynamic measurements showed the behavior of each specimen during variation of test parameters (temperature, pH, chloride content, inhibitor presence).

In detail the immersion test has shown that for the austenitic stainless steel pH 2 is the limit value to have stability of the passive layer at open circuit potential, and below this pH there is a fast depassivation and uniform corrosion.

Potentiodynamic tests have shown that increasing the PREN number of stainless steels increases the corrosion resistance in acidic environment. Until the PREN value of 36 there is a low corrosion resistance also at pH 1, below that value there is uniform corrosion.

Increasing the pH or decreasing the temperature of the solution permits to have a small resistance to uniform corrosion also for stainless steels with a PREN number lower than 36.

In order to have a material with a very high corrosion resistance (uniform and pitting corrosion) at pH 1 using a stainless steel with PREN number higher than 53 or a nickel alloys is required.

From the samples tested in this thesis the austenitic stainless steel 1.4404 tested at pH 1 at 90°C was the only one that has shown uniform corrosion, in opposite the Sanicro 35 is the only stainless steel that do not show any corrosion attack also in acidic solutions, all the other stainless steels tested have shown pitting corrosion in acidic solution at 90°C. A different behavior was determined for the two tested nickel alloy (2.4819 and 2.4605) that have not shown any corrosion attack, uniform or pitting, in any acidic environment.

In alkaline environment the behaviour of the tested specimens was different. All the tested stainless steels have not shown any corrosion attack. This is caused by the stability of the iron hydroxide, that forms as a product of corrosion in alkaline environments, which is a very dense layer on the surface of the steel. In contrast, the tested nickel alloys have shown a lower resistance than the steels because the low quantity of iron in the alloys was not enough to cause the formation of an iron hydroxide passive layer and at the same time the very high pH caused the dissolution of chromium from the surface of nickel alloy and caused pitting corrosion.

From the present thesis and considering the result obtained, the following material recommendations can be given. They are summarised in the Table 6.1.

Table 6.1: Recommendation for choice of material during washing steps in a ReOil process

Temperature	Acidic Wash		Neutral Wash		Alkalinic Wash	
	ReOil	Artificial	ReOil	Artificial	ReOil	Artificial
50	1.4462	1.4410	1.4462	n.i.	1.4404	n.i.
90	1.4462	Sanicro 35	1.4410	n.i.	1.4404	n.i.

n.i. = not investigated

References

- [1] COP26. *Decision CP26*. 2021. URL: https://unfccc.int/sites/default/files/resource/cop26_auv_2f_cover_decision.pdf.
- [2] OMV. *ReOil – Recycling technology for used plastics*. URL: <https://www.omv.com/en/sustainability/climate-protection/reoil>. (accessed: 04.12.2020).
- [3] S. Covino Jr D. Cramer. *Handbook 13B*. ASM International, 2006. ISBN: 0-87170-707-1.
- [4] A. Sedriks. *Corrosion of Stainless Steels*. WILEY-INTERSCIENCE, 1996. ISBN: 0-471-00792-7.
- [5] Y. Yang. “Effect of chromium content on the corrosion resistance of ferritic stainless steels in sulfuric acid solution”. In: *Helvion* 4 (2018). DOI: 10.1016/j.helivon.2018.e00958.
- [6] J.A.L. Dobbelaar, E.C.M. Herman, and J.H.W. “The corrosion behaviour of iron-chromium alloys in 0.5 M sulphuric acid”. In: *Corrosion Science* 33 (1992), pp. 765–778. ISSN: 0010-938X. DOI: [https://doi.org/10.1016/0010-938X\(92\)90109-G](https://doi.org/10.1016/0010-938X(92)90109-G). URL: <https://www.sciencedirect.com/science/article/pii/0010938X9290109G>.
- [7] TMR Stainess. *Practical guidelines for the fabrication of duplex stainless steels*. International Molybdenum Association (IMOA), 2014. ISBN: 978-1-907470-09-7.
- [8] M. Pourbaix. *Atlas of Electrochemical Equilibria in Aqueous Solution*. NACE International, 1974.
- [9] S. H. Mameng. *Localised corrosion and atmospheric corrosion of stainless steels*. KTH Royal Institute of Technology, 2019. ISBN: 978-91-7873-330-9.
- [10] Z. S. Smiałowska. *Pitting and Crevice Corrosion*. NACE International, 2005. ISBN: 1-57590-185-4.
- [11] Tan Sun Y. Ting et al. “Revisiting the effect of molybdenum on pitting resistance of stainless steels”. In: *Tungsten* 3 (2021), pp. 329–337. ISSN: 2661-8036. DOI: 10.1007/s42864-021-00099-1.

- [12] Sherif Alharthi Nabeel, Hany El-Sayed Abdo, and Sherif Z. El-Abedin. “Effect of Nickel Content on the Corrosion Resistance of Iron-Nickel Alloys in Concentrated Hydrochloric Acid Pickling Solutions”. In: *Advances in Materials Science and Engineering* 2017 (June 2017), pp. 1–8. DOI: 10.1155/2017/1893672.
- [13] D. O. Condit. “Potentiodynamic polarization studies of Fe-Ni binary alloys in sulfuric acid solution at 25°C”. In: *Corrosion Science* 12 (1972), pp. 451–462. ISSN: 0010-938X. DOI: [https://doi.org/10.1016/S0010-938X\(72\)80091-X](https://doi.org/10.1016/S0010-938X(72)80091-X). URL: <https://www.sciencedirect.com/science/article/pii/S0010938X7280091X>.
- [14] O. Markus Speidel. “Stress corrosion cracking of stainless steels in NaCl solutions”. In: *Metallurgical Transactions A* 12 (1981), pp. 779–789. ISSN: 1543-1940. DOI: 10.1007/BF02648342.
- [15] P.R. Levey and A. Bennekomt. “The involvement of alloyed nitrogen in the corrosion of stainless steels”. In: *The Journal of The South African Institute of Mining and Metallurgy* 12 (1995), pp. 337–346. ISSN: 0038-223X/3.00.
- [16] Asimenye Muwila. *The Effect of Manganese, Nitrogen and Molybdenum on the Corrosion Resistance of a Low Nickel (<2 wt%) Austenitic Stainless Steel*. Faculty of Engineering, The School of Process and Metallurgical Engineering, University of the Witwatersrand, Johannesburg, 2006.
- [17] S. S. M. Tavares H. M. L. F. de Lima and W. S. Araújo M. Martins. “The effect of copper addition on the corrosion resistance of cast duplex stainless steel”. In: *Journal of Materials Research and Technology* 8 (2019), pp. 2107–2119. ISSN: 2238-7854. DOI: <https://doi.org/10.1016/j.jmrt.2019.01.018>. URL: <https://www.sciencedirect.com/science/article/pii/S2238785418308172>.
- [18] R. L. Snezhnoi A. A. Zhukov. “The iron-carbon system. new developments—III. The iron-diamond phase diagram”. In: *Acta Metallurgica* 23 (1975), pp. 1103–1110. ISSN: 0001-6160. DOI: [https://doi.org/10.1016/0001-6160\(75\)90114-5](https://doi.org/10.1016/0001-6160(75)90114-5). URL: <https://www.sciencedirect.com/science/article/pii/0001616075901145>.
- [19] S. T. Kim S. H. Jeon and Y. S. Park S. Lee. “Effects of sulfur addition on pitting corrosion and machinability behavior of super duplex stainless steel containing rare earth metals: Part 2”. In: *Corrosion Science* 52 (2010), pp. 3537–3547. ISSN: 0010-938X. DOI: <https://doi.org/10.1016/j.corsci.2010.07.002>. URL: <https://www.sciencedirect.com/science/article/pii/S0010938X10003409>.

- [20] Raul Rebak and Crook. “Nickel alloys for corrosive environments”. In: *Advanced Materials and Processes* 157 (2000), pp. 37–42.
- [21] M.G. J. R. Bech F. H. Fontana. “Anodic Polarization Behavior Of Nickel-Chromium Alloys In Sulfuric Acid Solutions”. In: *Corrosion* 21 (Jan. 2013), pp. 277–287. ISSN: 0010-9312. DOI: 10.5006/0010-9312-21.9.277. eprint: <https://meridian.allenpress.com/corrosion/article-pdf/21/9/277/1522673/0010-9312-21\9\277.pdf>. URL: <https://doi.org/10.5006/0010-9312-21.9.277>.
- [22] J.R. Gray Hayes and A.W. Orme J.J. Szmodis. “Influence of Chromium and Molybdenum on the Corrosion of Nickel-Based Alloys”. In: *Corrosion* 62 (June 2006). ISSN: 0010-9312. eprint: <https://onepetro.org/corrosion/article-pdf/2186524/nace-06060491.pdf>.
- [23] Robert J. Mckay. “Nickel and corrosion resisting nickel alloy”. In: *Industrial & Engineering Chemistry* 28 (1936), pp. 1391–1397. DOI: 10.1021/ie50324a012. eprint: <https://doi.org/10.1021/ie50324a012>. URL: <https://doi.org/10.1021/ie50324a012>.
- [24] N.E Hakiki and M.G.S Ferreira. “Semiconducting properties of passive films formed on nickel–base alloys type Alloy 600: influence of the alloying elements”. In: *Electrochimica Acta* 44 (1999), pp. 2473–2481. ISSN: 0013-4686. DOI: [https://doi.org/10.1016/S0013-4686\(98\)00372-7](https://doi.org/10.1016/S0013-4686(98)00372-7). URL: <https://www.sciencedirect.com/science/article/pii/S0013468698003727>.
- [25] Aneta S.Nykiel. “The influence of molybdenum on corrosion resistance of sintered austenitic stainless steels”. In: *Technical Transactions* 4-M (Jan. 2015), pp. 131–142. DOI: 10.4467/2353737XCT.15.344.4865.
- [26] U. Heubner. *Nickel alloys and high-alloy special stainless steels*. Krupp, 1998. ISBN: 3-8169-1588-4.
- [27] L. Monaco M. Sabatini and U. Erb. “Corrosion of nanocrystalline and coarse-grained nickel-iron (Ni-Fe) alloys in neutral and alkaline sulfate environments”. In: *Corrosion Science* 163 (2020), p. 108233. ISSN: 0010-938X. DOI: <https://doi.org/10.1016/j.corsci.2019.108233>. URL: <https://www.sciencedirect.com/science/article/pii/S0010938X19305384>.
- [28] Y. Tian et al. “The effect of nickel on corrosion behaviour of high-strength low alloy steel rebar in simulated concrete pore solution”. In: *Construction and Building Materials* 246 (2020), p. 118462. ISSN: 0950-0618. DOI: <https://doi.org/10.1016/j.conbuildmat.2020.118462>. URL: <https://www.sciencedirect.com/science/article/pii/S0950061820304670>.

- [29] O. Markus Speidel. “Stress corrosion cracking of stainless steels in NaCl solutions”. In: *Metallurgical Transactions A* 12 (1981), pp. 779–789. ISSN: 1543-1940. DOI: 10.1007/BF02648342.
- [30] Y. Wang M.Li T. Yin and H. Gregersen and G. Wang F. Du X. Zou. “Study of biocompatibility of medical grade high nitrogen nickel-free austenitic stainless steel in vitro”. In: *Materials Science and Engineering: C* 43 (2014), pp. 641–648. ISSN: 0928-4931. DOI: <https://doi.org/10.1016/j.msec.2014.06.038>. URL: <https://www.sciencedirect.com/science/article/pii/S0928493114004044>.
- [31] X. R. Nóvoa L. Freire and V. Vivier G. Pena. “On the corrosion mechanism of AISI 204Cu stainless steel in chlorinated alkaline media”. In: *Corrosion Science* 50 (2008), pp. 3205–3212. ISSN: 0010-938X. DOI: <https://doi.org/10.1016/j.corsci.2008.08.029>. URL: <https://www.sciencedirect.com/science/article/pii/S0010938X08003260>.
- [32] P. Houille P. Crook N. Meck. “The Caustic Dealloying of Molybdenum-Bearing Nickel Alloys”. In: *EUROCORR 2005* (2005).

A. Solutions Composition

Table A.1: Total composition of pH 2 solution for the autoclave test

Chemical Species	Chemical Compound	mg/l
F^-	NaF	2
Cl^-	HCl	250
Br^-	NaBr	5
CN^-	KCN	2.7
SO_3^{2-}	$Na_2SO_3 \cdot 9H_2O$	20
SO_4^{2-}	Na_2SO_4	500
S^-	NaS	7
Formate	Formic Acid	13.3
Acetate	Sodium Acetate trihydrate	50
Benzoic Acid	Sodium Benzoate	10
Naphenic Acid	Sodium Palmitate	40
Ammine	Monoethanolamine	400
Pyridin	Pyridin	400
Hydrocarbons	1-Metiletanol	2000
Phenol	Phenol	20

Table A.2: Total composition of pH 13 solution for the autoclave test

Chemical Species	Chemical Compound	mg/l
F^-	NaF	10
Cl^-	HCl	427
Br^-	NaBr	50
CN^-	NaCN	40
SO_3^{2-}	$Na_2SO_3 \cdot 9H_2O$	17
SO_4^{2-}	Na_2SO_4	20
S^-	NaS	100
PO_4^{3-}	NaH_2PO_4	100
NO_3^-	$NaNO_3$	40
Formate	Formic Acid	136
Acetate	Sodium Acetate trihydrate	1000
Benzoic Acid	Sodium Benzoate	400
Naphenic Acid	Sodium Palmitate	1000
Ammine	Monoethanolamine	1250
Hydrocarbons	1-Propanol	5000
Phenol	Phenol	400